FEEDSTOCK LOGISTICS (PART 3 OF 6)

TASK 2. DEVELOP MOISTURE MANAGEMENT STRATEGIES AND MODELS

Authors	ORGANIZATION
John Sessions	Oregon State University OSU
Kevin Boston	Oregon State University OSU
Rene Zamora-Cristales	Oregon State University OSU
Francisca Belart	Oregon State University OSU
Gevan Marrs	Consultant
Glen Murphy	Consultant

(This report is part of a larger collection: Sessions, J., Boston, K., Zamora-Cristales, R., Belart, F., Marrs, G. & Murphy, G. (2017). Feedstock Logistics. NARA Final Reports. Pullman, WA. Northwest Advanced Renewables Alliance (NARA). “Feedstock Logistics” can be retrieved at https://research.libraries.wsu.edu/xmlui/handle/2376/5310)

COMPLETED 2017

TABLE OF CONTENTS

TABLE OF CONTENTS

NARA is led by Washington State University and supported by the Agriculture and Food Research Initiative Competitive Grant no. 2011-68005-30416 from the USDA National Institute of Food and Agriculture.

LIST OF FIGURES

LIST OF TABLES

TABLE NO. TABLE TITLE PAGE NO.

TASK 2. DEVELOP MOISTURE MANAGEMENT STRATEGIES AND MODELS

1. Introduction

Moisture content management is a key requirement to improve forest harvest residue economics for bioenergy production. For liquid fuels derived from fermentation, an obvious gain in reducing moisture content is reduction of transportation cost. A less obvious gain associated with moisture content reduction are the material properties of the dry biomass. For bioenergy using combustion, reduced moisture content can also influence energy value. Wood moisture can be reduced in the forest by transpiration and air-drying. It has already been shown that drying rates, and therefore optimal storage time, will depend on climate conditions, species, storage configuration and initial moisture content (Hakkila, 1989).

Task 2 has four parts. In Section 2 we identify the initial moisture content of residues. In Section 3 we identify the factors that affect moisture reduction and developing a model that can predict moisture content. In Section 4 we develop a decision support system that can be used in managing moisture content. In Section 5 we examine the impact of fresh versus aged forest residues on making liquid fuels. Material for Sections 2-4 are largely developed by Francisca Belart and documented in Belart (2016).

Ben Leshchinsky guided the finite element analysis. Sections 2-4 are also in peer review in three journal manuscripts. Material for Section 5 was developed by Gevan Marrs, Rene Zamora-Cristales, and John Sessions and is in final peer review.

2. Initial Moisture Content of Forest Residues

Several researchers have studied moisture patterns at tree stem levels. Clark and Gibbs (1957) did a detailed study in Eastern Canada in bole wood of different species of birch (*Betula spp*.). They found that the highest moisture content occurs in mid-spring and the lowest in early-fall. They identified two marked stress periods, the first at the end of winter (right before breaking dormancy) and the second in late summer. Highest MC (moisture content) in mid-spring would be due to the breaking of tree dormancy, and then the lowest MC in early-fall would be due to the gradual loss of water during the growing season. In this study, it was also found that species within a same genus closely follow the same MC seasonal pattern. For these species, orientation is also important since during winter and spring the bole is being exposed to direct solar radiation while in summer and fall it is being protected by foliage. These broadleaf tree MC patterns seem to agree with many species studied by Gibbs (1957). However, some families seem to have a MC peak later in the year (by mid-summer) and their transition through winter is less dramatic.

Clark and Gibbs (1957) did some studies in eastern hemlock (*Tsuga canadensis*), balsam fir (*Abies balsamea*), red spruce (*Picea rubens*) and eastern white cedar (*Thuja occidentalis*). They observed that conifers tend to have a more stable MC though the year compared to broadleaves due to their evergreen habit. As for seasonal MC variation, there is no general pattern for these species. Some of them have minima in late spring (eastern hemlock, balsam fir); others in late summer (red spruce and eastern white cedar). However, all seem to have lower MC in early to mid-fall. Most of the variation and moisture content is occurring in sapwood, and in all species, tops are wetter than the lower parts of the bole. This is due to a higher proportion of sapwood in the upper part of the tree. These findings are not fully consistent with Greenidge (1957) who reported that patterns in moisture movement in normal trees differs widely within species, between species and different structural types (i.e. ring porous, diffuse-porous and gymnosperms).

Gingras and Sotomayor (1992) studied MC variation in standing trees, harvested trees and stored logs for over one year. They found that in standing trees MC is higher in soils where water is not secured (trees store more water) and observed that there is an effect on the tree between different geographical areas. Seasonal patterns are similar to what Clark and Gibbs (1957) found (there is not a general pattern; however there is a lower MC in early-fall). They also found that MC falls rapidly within the first five weeks of felling and leaving branches and tops attached to the stem greatly increases overall MC loss.

Beedlow *et al.* (2007) concluded in a study in Douglas-fir that there is little seasonal variation in 100 year-old trees. Different to what Clark and Gibbs (1957) found, they concluded that MC markedly increased during late spring and reached a minimum in fall. They reported these differences from maximum and minimum to be approximately 5% MC.

All of these authors except for Beedlow *et al.* (2007) took sample wood discs and used the oven drying method to determine moisture content. The study performed by Pong *et al.* (1986) described bole wood moisture pattern through tree height. Their study was done in Douglas-fir (*Pseudotsuga menziesii*) and Western hemlock (*Tsuga heterophylla*). Their tree selection was from a randomly stratified sample based on tree DBH (diameter breast height). This is also supported by Maguire *et al.* (1999) whose study concludes that tree diameter is a good predictor of branch size in second growth Douglas-fir. Pong *et al.* (1986) sampled wood discs and cores in different trees with no temporal consideration. They found that highest moisture content occurred at the base of the tree, decreased to a lowest point in the middle third of the tree, and then increased again in the upper stem. Western hemlock was considerably wetter than Douglas-fir at all heights and in both heartwood and sapwood. Results suggested that the moisture profile in green sapwood remains fairly constant with height, and the impact of moisture in green density profiles was much more evident in heartwood than sapwood. This study indicated that higher MC should be expected higher up in the trees.

Markstrom and Hann (1972) studied three species from the Rocky Mountains, including Douglas-fir. They sampled five trees of each species during each four physiological seasons and five additional trees per species during each month of the growing season. They also extended their study for an additional year to verify if there was an effect of annual changes. They found that sapwood MC were the highest during winter freeze-up for all species. They also concluded that both the outer and inner heartwood of Douglas-fir showed no real change in MC throughout the year, but season does have an effect in the sapwood MC.

Parker (1954) studied ponderosa pine (*Pinus ponderosa*) and Douglas-fir stem moisture content through 10 months. His study revealed that Douglas-fir heartwood remains practically constant through the year (~23% water, wet basis [100*weight of water divided by wet weight]), sapwood is wettest in early winter (~55% water, wet basis) and driest in early summer (~50% water, wet basis). Heartwood in ponderosa pine is much wetter than Douglas-fir and follows the same pattern as sapwood through the year. Heartwood and sapwood are wettest in early spring (~53% and 56% water, wet basis respectively) and driest in mid fall (~47% and 52% water, wet basis respectively). He also concluded that needles greatly impact the amount of water loss in the branches and that stem water content apparently depends on the weather.

Variation of branch moisture during the year has been less well studied. To develop branch moisture, we installed test plots in the major climate regions and species. The Pacific Northwest has different climate regions that range from humid coastal in the states of Washington and Oregon, and alpine to semi-arid climate in rain shadow areas of Oregon, Washington and Idaho. This climate diversity provides growing conditions for different tree species, of which three have a major commercial role and sustain the forest sector economy in the region. The most relevant in Washington and Oregon is Douglas-fir (*Pseudotsuga menziesii*) growing along the Coast, central valley and up to 1,520 m elevation (Burns and Honkala, 1990), next in importance is western hemlock (*Tsuga heterophylla*) growing in the humid regions of coastal Oregon and Washington, and finally, ponderosa pine (*Pinus ponderosa*) growing in the arid regions of each state. Only Douglas-fir and hemlock represent more than 74% of timber harvested in Oregon by 2003 (Brandt *et al.*, 2006) and over 69% in Washington in 2014 (DNR, 2014) and is the reason why this study focused on these species and the distinctive climate regions they grow in.

Live branch moisture content (initial moisture content) is currently not available; having this information for the three main commercial species in the Pacific Northwest is useful to determine what levels of moisture can be expected when this material is fresh, and whether the felling season makes a difference. For those reasons, the objective of this study is to determine the seasonal average moisture content for tree branches and their seasonal changes, focusing on Douglas-fir (*Pseudotsuga menziesii*) ponderosa pine (*Pinus ponderosa*) and western hemlock (*Tsuga heterophylla*) as the main commercial forest species in the Pacific Northwest. We focus on the following research questions:

- What is the seasonal average moisture content of fresh branches for the three main commercially relevant Pacific Northwest tree species?
- Are these average moisture contents statistically different between seasons?
- Is there an effect of height on branch moisture content?
- Is there an effect of heartwood on branch moisture content?

2.1. Methodology for Measuring Live Branch Moisture Content

2.1.1 Site Selection

According to the available forest resource that is being currently harvested in the Pacific Northwest and has potential for biomass production, three species and four locations were identified to place research units (Table FL-2.1).

The main requirement for each forest unit was a forest at harvest age or close to harvest age for typical forest landowners in the region.

Table FL-2.1. Research unit location.

Site description	Location	Elevation (m)	Average annual rainfall (mm)	Coordinates
Willamette Valley Douglas-fir	Corvallis, OR	283	1,092	44°39'29.13"N, 123°15'40.30"W
Higher elevation Douglas-fir	Oakridge, OR	871	1,154	43°30'17.80"N, 122°21'04.91"W
Ponderosa pine	Sisters, OR	1,003	330	44°18'37.75"N, 121°36'05.43"W
Western hemlock	Newport, OR	201	1,778	44°47'09.42"N, 124°03'04.67"W

While all research units were close to harvest age, they had differences given the varied management purposes and species. Twelve trees were sampled at each site (Table FL-2.2).

Table FL-2.2. Total height and DBH (diameter at breast height) of twelve sampled trees at each site.

Site description	Age (years)	Total height (m)		DBH (cm)	
		Average	SD	Average	SD
Valley Douglas-fir	40-100*	34.7	5.2	55.6	10.9
Higher elevation Douglas-fir	51	30.5	4.2	38.9	8.1
Ponderosa pine	50-150**	19.6	3.3	38.6	7.6
Western hemlock	45	19.1	3.6	37.1	8.1

*Uneven aged stand estimate, ** Age estimated from stand structure and a report on a similar study (Youngblood *et al.*, 2004)

2.1.2. Sampling Procedure

To obtain branch moisture content, branches in live trees were cut by a tree climber and then immediately sampled in the field. In order to minimize tree-to-tree variation, the same trees were repeatedly sampled through each season. The effect of cutting a few branches would not have a significant effect on the overall tree moisture; trees lose branches naturally through their life cycle (Dr. Kate McCulloh, pers. communication May 2013).

The number of trees to be selected was determined using information from a woody biomass moisture content data base. This data base consisted of moisture content measured in biomass on trucks arriving to a cogeneration plant in Eugene, Oregon. The data was collected from January 2011 to June 2012 corresponding to 3,109 loads and was separated by eastern and western Oregon provenance. This data was the best local information at the time that could be used to make an estimate of the seasonal moisture content averages and variability.

In order to eliminate the microsite variability that would exist if different trees were to be sampled each season, the experiment was performed as a repeated measures design. One thousand simulations were performed to find the appropriate sample size to achieve power greater than 0.80. The test result indicated that having 4 trees was enough to achieve power of 0.99; however, knowing the data not only includes branches and was processed (ground) before sampling, a safety factor of 3 was used to determine the number of trees to be sampled, that is a total of 12 trees per site.

After a buffer zone was defined to avoid selecting edge trees, a tree was chosen systematically approximately every 24 m following a bearing along the unit length. This was done so one or two transects were formed depending on the forest unit shape (Figure FL-2.1).

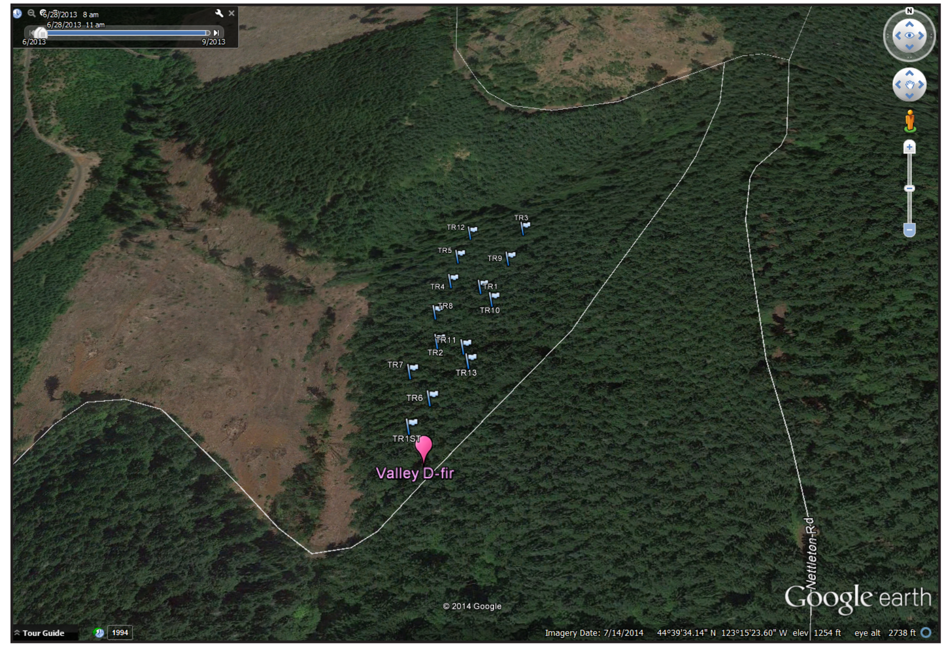

Figure FL-2.1. Tree selection in two transects following North bearing.

The number of branches to be cut per tree was a decision based on a combination of criteria: literature, field experience and cost. We did not have branch moisture content information specific for these forest types that could give us a better lead to determine branch sample size. Temesgen *et al.* (2011) worked on a study to estimate crown biomass through branch measurements. They found that the root mean squared error for biomass estimation was reduced by 43% when sample size was increased from 6 to 12 branches, for that reason we decided selecting 9 branches was a good compromise. However, in practice, many trees do not have enough branches to destructively sample four times and cut 9 branches each time without having a significant effect on the tree. For that reason we decided to take three branches each season and reduce that number if a tree still seems to have too few branches to return four times.

Dead branches were initially planned to be sampled since they are likely to have different moisture content than regular live branches. However, we expect that none of them (or very few) will end in a forest harvest residue pile. Most will shatter when they hit the ground.

Temesgen *et al.* (2011) also found random sampling not to be ideal for biomass estimation and stratified sampling works better. In their sampling, they divided the crown in thirds and randomly selected branches within each section.

Drawing from all this information, the best sampling protocol for our purposes and budget was to randomly choose and cut one branch from each third of the crown. Then, since literature suggests that sapwood and heartwood have different moisture contents, a wood disc was cut every 0.6 m on each branch in order to better capture moisture content as heartwood proportion decreases along the branch (Figure FL-2.2).

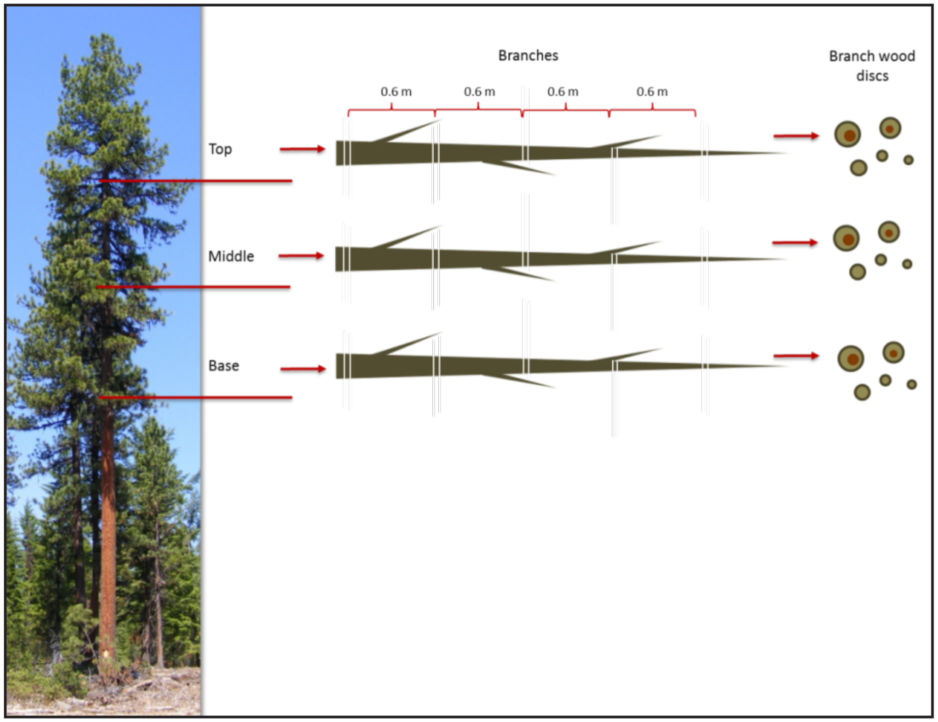

Figure FL-2.2. Branch sampling protocol.

Samples were placed in air tight bags and weighed green right after collection. Later, they were oven dried for 24 hours at 103°C and weighed dry following ASTM standard E871-82 for moisture analysis in particulate wood fuels (ASTM international, 2006). Branch disc diameter under/over bark and sapwood was recorded. Moisture content was determined and reported in this document on a wet basis (weight of water divided by total weight including bark). In addition to the samples, tree total height, branch height on the tree, tree DBH, and branch length was collected in order to investigate any wood moisture content correlation with other measurable characteristics. The branch sampling protocol was repeated on the same 12 trees once per each four seasons during one year between 2013 and 2014.

2.2. Statistical Analysis

Different statistical procedures were used to be able to answer the questions needed to address the objectives of this study.

2.2.1. Average Moisture Content by Species

In order to determine the differences in average moisture content by species, we needed to define a random effects model. Let y_{ij} be the average branch moisture content of tree *j* of species *i*, the model can be described as follows (Eq. 1):

$$y_{ij} = \mu + A_i + B_{ij} \quad (i=1,2,3,4\ ;\ j=1,2,\ldots 12) \qquad \text{(Eq. 1)}$$

Where

μ : Average branch moisture content for the entire population

A_i: Species-specific random effect

B_{ij}: Tree-specific random effect

After performing one-way ANOVA, Levene's test for homogeneous variances (Kuehl, 2000) indicated departures from the equal-variance assumption. For that reason, Welch's test two-sample t-test was used to determine differences in means, and the Bonferroni correction for six procedures applied in order to make the appropriate inferences.

2.2.2. Seasonal Moisture Variation

Since field measurements were performed on the same individuals on four different times of the year, one-way repeated measures ANOVA was used for this longitudinal study. In order to determine seasonal differences, each species/site analysis was made separately to isolate any effect the species may have. That is, a total of four separate analyses were performed. The model for this analysis is described in Eq.2. Let y_{jk} be the average branch moisture content of tree *j* in time (season) *k*,

$$y_{jk} = \mu + C_j + D_k + e_{jk} \quad (j=1,2,\ldots 12\ ;\ k=1,2,3,4) \qquad \text{(Eq. 2)}$$

Where

μ :Average branch moisture content for the entire population

C_j :Individual component for tree *j*

D_k :Effect of time (in this case season of the year)

e_{jk} :Error for tree *j* and season *k*

Since the sphericity assumption was not possible to assess accurately, a Huynh-Feldt correction factor was applied to the probabilities for a conservative estimate. If there was a significant effect of season for a specific species, the procedure followed with pairwise comparisons (pairwise t-tests) to determine which seasons differed with each other.

2.2.3. Branch Height Effect on Moisture Content

In order to establish the relationship between branch height and branch moisture content, a one-way ANOVA was performed to determine if there was an effect of height on moisture content. If there was convincing evidence of an effect, several linear regression models were fitted (linear, polynomial, logarithmic, etc.) following the general model described in Eq. 3. Let *y* be the average branch moisture content of a given tree at height *h*, the model can be described as follows:

$$y_h = \beta_0 + \beta_1 x + e \qquad \text{(Eq. 3)}$$

Where

x :Branch height within the tree

β_0 and β_1 :Model parameters

When the data set was separated by species, the general regression was set as follows (Eq. 4):

$$y_{ih} = \beta_0 + \beta_1 x_i + e \quad (i=1,2,\ldots.12) \qquad \text{(Eq. 4)}$$

Where

y_{ih} :Average branch moisture content of a tree of species *i* at height *h*

x :Branch height of a tree of species *i*

Heartwood effect on branch moisture content

In order to find the relationship between branch heartwood diameter and branch moisture content, a two-sample t-test was performed first to determine if there was an effect of heartwood presence in average moisture content of a branch wood disc. If there was convincing evidence of an effect, several linear regression models were fitted (linear, polynomial, logarithmic, etc.) following the general model described below (Eq. 5).

$$s = \beta_0 + \beta_1 hd + e \qquad \text{(Eq. 5)}$$

Where

s :Average branch wood disk moisture content of a given branch

hd :Heartwood diameter of that given wood disk

Once this relationship was demonstrated, an ANOVA was performed to determine if there was an effect of the heartwood diameter at the branch attachment point (named "first sample") and the average branch moisture content. Once the effect was established as significant, a linear regression model was fitted that would allow prediction of average branch moisture content from the heartwood diameter of the branch at the point of attachment on the tree (Eq. 6).

$$y_d = \beta_0 + \beta_1 hd1 + e \qquad \text{(Eq. 6)}$$

Where

y :Average branch moisture content of a given tree with heartwood diameter

$hd1$:Branch heartwood diameter at point of attachment

When the data set was separated by species, the general regression was set as follows (Eq. 7):

$$y_{id} = \beta_0 + \beta_1 hd1_i + e \quad (i=1,2,\ldots.12) \qquad \text{(Eq. 7)}$$

Where

y_{id} :Average branch moisture content of a tree of species *i* with branch heartwood diameter *d*

$hd1$:Branch heartwood diameter at point of attachment of a tree of species *i*

A randomized subset of 30% of the data was excluded from the regression analyses so it could later be used for validation. All the analyses were performed using R except for the contrasts performed in SPSS.

2.3. Results

2.3.1. Bark Proportion

During four seasons and in four sites, 3,245 wood discs were collected from 759 branches. Branch length ranged from 38 cm in ponderosa pine up to 871 cm in Douglas-fir. Diameter over bark ranged from 5.1 to 109 mm. The highest branch was located at 40 m and the lowest at 2.4 m.

Bark proportion in ponderosa pine samples was highest, followed by Willamette Valley Douglas-fir. Western hemlock presented the lowest proportion. As the branch diameter increases, bark proportion decreases for all species (Figure FL-2.3).

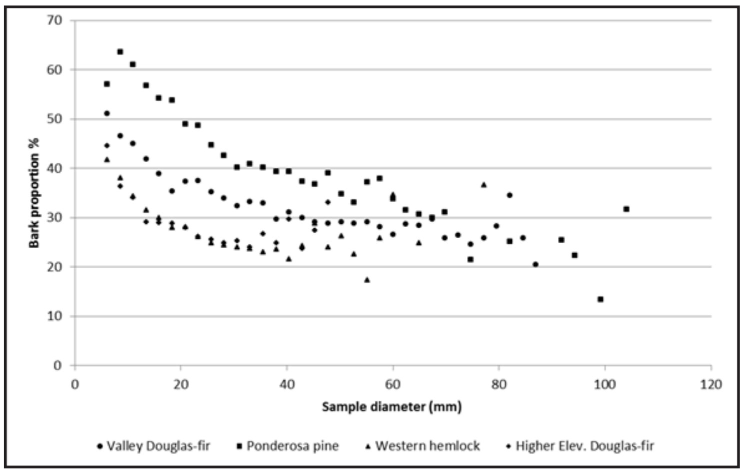

Figure FL-2.3. Branch bark proportion (100* [(ADOB-ADUB)/ADOB]). Where ADOB is the sample cross sectional area over bark and ADUB is the sample cross sectional area under bark.

2.3.2. Average Branch Moisture Content

The first observation after calculating a diameter-weighted tree branch moisture content average is the variability within species and sites. After making an assessment for assumptions, data showed departures from equal-variance, for that reason Welch's test was used to test for differences in means. Only Valley Douglas-fir compared with western hemlock and higher elevation Douglas-fir have significant differences in weighted average moisture content (Welch's two-sample t-test with the Bonferroni correction p-values < 0.001) (Figure FL-2.4). The test was adjusted with Bonferroni for six procedures (number of comparisons of species pairs).

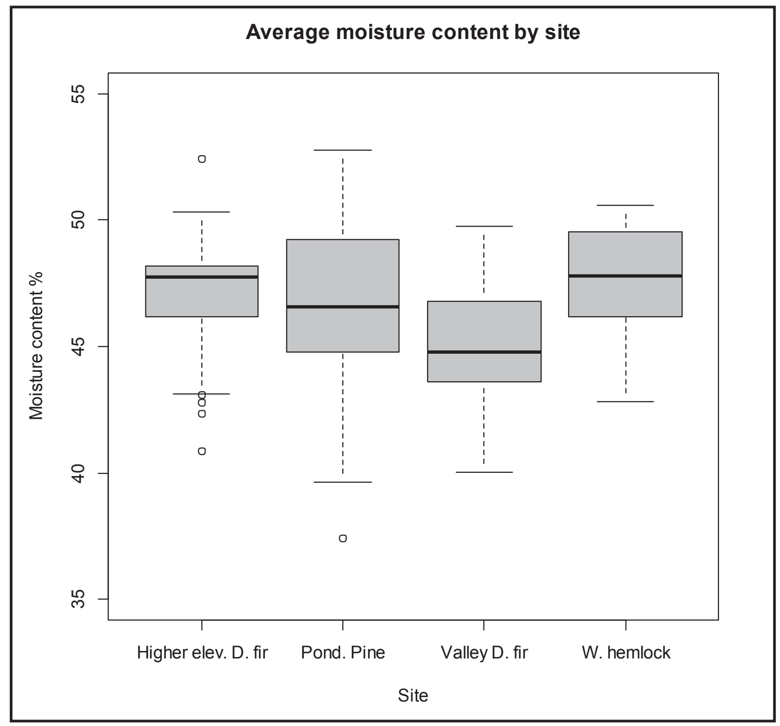

Figure FL-2.4. Branch moisture content weighted average by site.

The boxplots in Figure FL-2.5 show high moisture content fluctuations within ponderosa pine trees and stability in western hemlock.

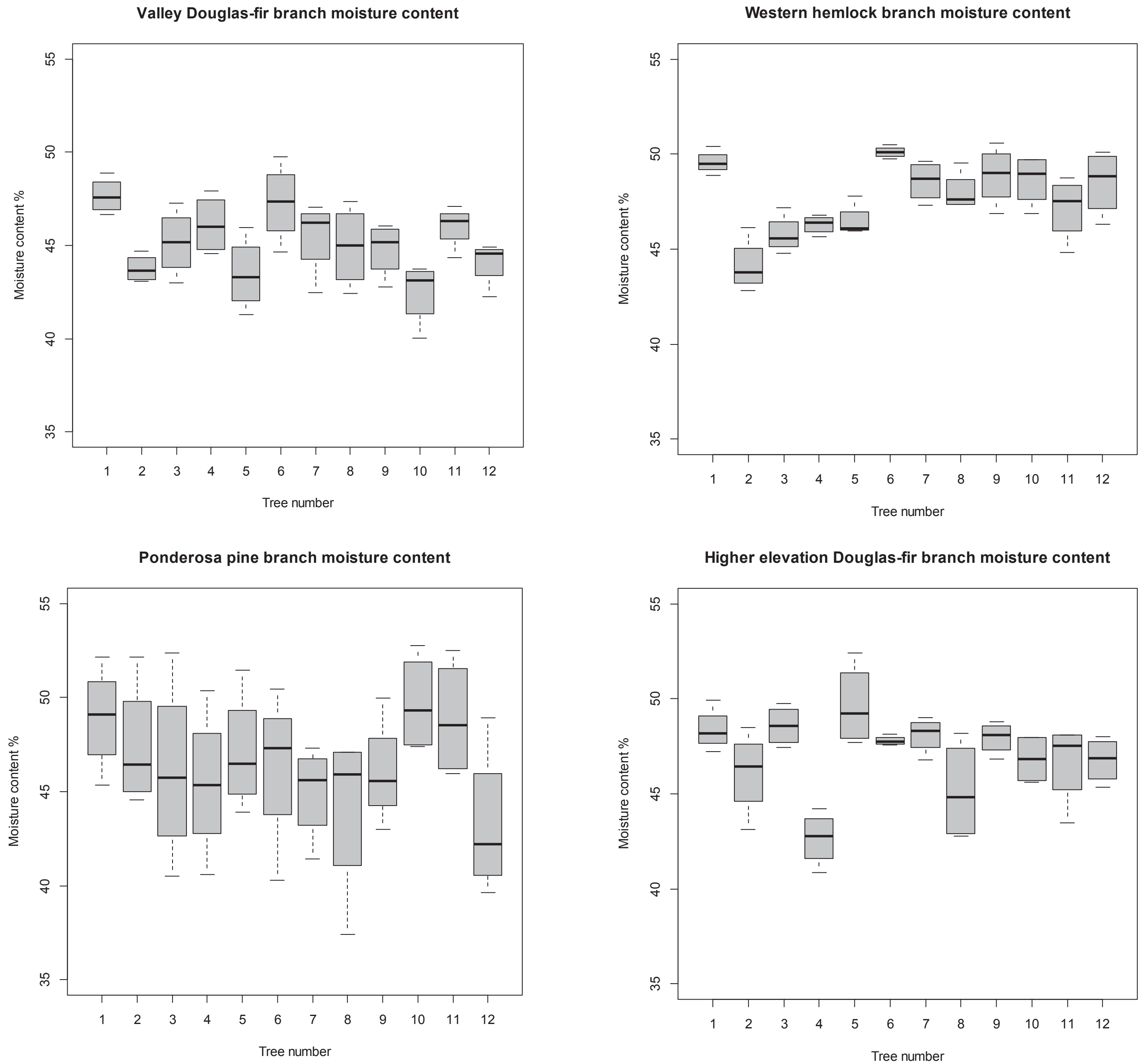

Figure FL-2.5. Tree average branch moisture content, independent of season.

In general, most trees consistently had higher moisture content in the upper third of the crown and lower moisture content in the lower third of the crown, independent from season (Figure FL-2.6).

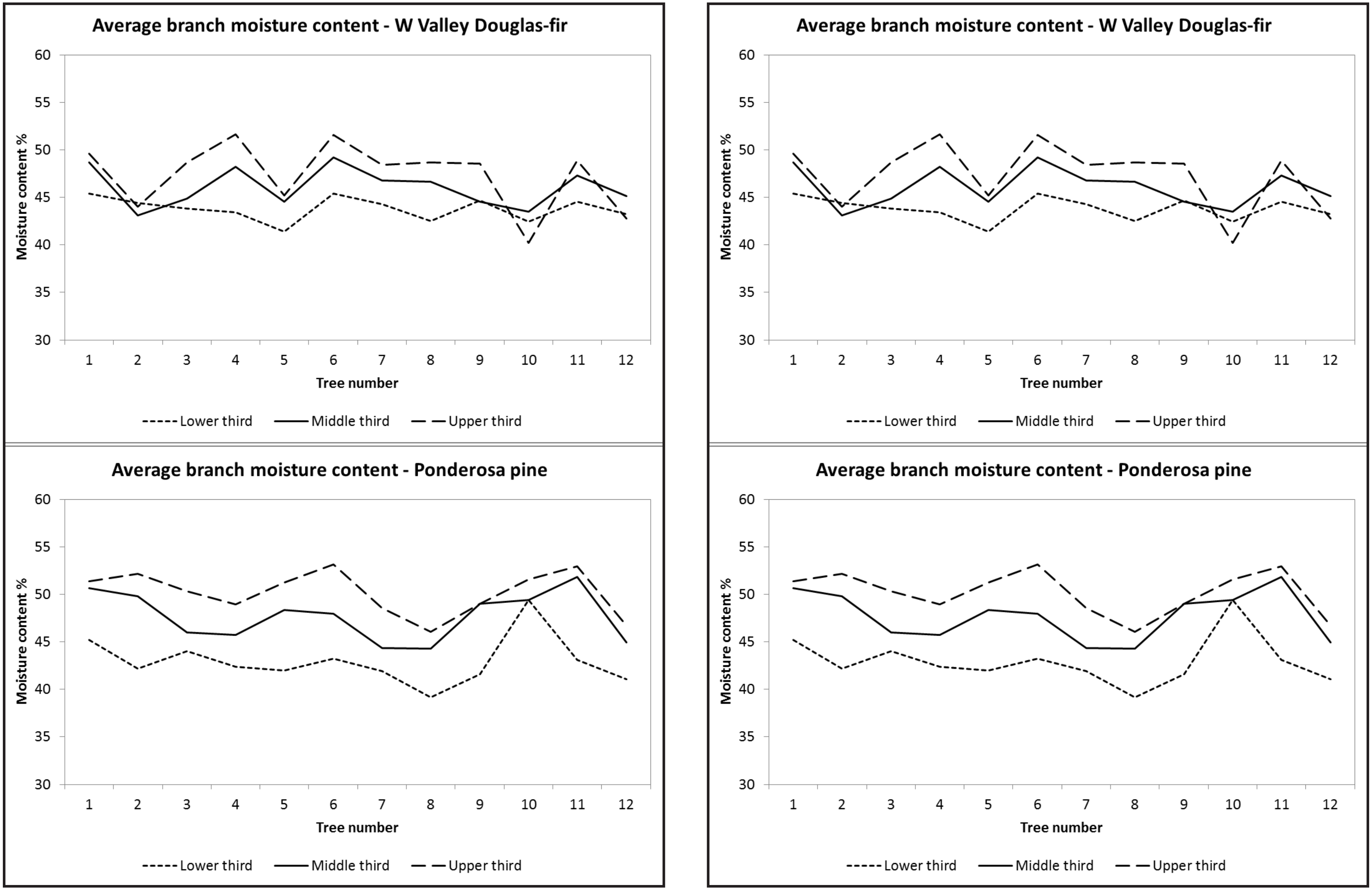

Figure FL-2.6. Average branch moisture content by crown level, independent of season.

When branch average moisture content is examined by season, the lowest moisture contents occur during summer (43 %) and highest during fall or winter (50 %) depending on the species. There is not a clear pattern to identify differences (Table FL-2.3) without additional statistical analysis.

Table FL-2.3. 95% confidence intervals for weighted average seasonal branch moisture content (%) by site.

Site	Fall	Winter	Spring	Summer
Valley Douglas-fir	46 ± 1	45 ± 1	46 ± 1	43 ± 1
Ponderosa pine	47 ± 1	50 ± 1	45 ± 1	43 ± 1
Western hemlock	47 ± 1	48 ± 1	48 ± 1	47 ± 1
Higher elevation Douglas-fir	46 ± 1	48 ± 1	47 ± 1	47 ± 1

2.4. Seasonal Moisture Variation

In order to address the seasonal differences in mean branch moisture content, the best approach was to perform one-way repeated measures ANOVA for each of the species separately. Species were defined a-priori in order to determine whether the seasonal effect is different depending on the regional climate.

Since Mauchly's test is not appropriate to assess the sphericity assumption, all p-values are reported with the Huynh-Feldt correction for conservative probability estimation. At a significance level of $\alpha= 0.05$, results indicate that there is a significant effect of season in ponderosa pine and Valley Douglas-fir branch moisture content (one-way repeated measures ANOVA, H-F $p < 0.0001$). Western hemlock shows a suggestive but inconclusive effect of season (One-way repeated measures ANOVA H-F p =0.036) and higher elevation Douglas-fir indicates no effect of season (one-way repeated measures ANOVA H-F p=0.097).

Valley Douglas-fir and ponderosa pine seem to have the most noticeable moisture content differences between seasons (Figure FL-2.7), both showing the lowest moisture contents during summer. Most species seem to increase branch moisture content after summer.

Since the main effect of season was significant for three species, post hoc pairwise tests were performed. After taking into account the repeated measures, for Valley Douglas-fir, probabilities show that the difference in mean branch moisture content is statistically significant between summer and every other season (pairwise t-test p-values < 0.01), with summer being the season with the lowest mean moisture content. Tests in ponderosa pine indicate significant differences in mean branch moisture content between winter and every other season (pairwise t-test p-value < 0.01), with winter being the season with highest mean branch moisture content. Additionally, for the same species, there was a statistically significant mean branch moisture content difference between fall and summer (pairwise t-test p-value < 0.01) (Table FL-2.4). After performing pairwise comparisons in western hemlock, there was no evidence of difference in mean branch moisture content between seasons (pairwise t-test p-values > 0.50).

Table FL-2.4. Pairwise comparisons for difference in seasonal means.

	Valley Douglas-fir			Ponderosa pine		
	Confidence Interval			Confidence Interval		
Season	lower	upper	p-value	lower	upper	p-value
Spring-Fall	-1.13	1.71	1.00	-4.55	1.22	0.55
Summer-Fall	-3.67	-1.02	0.001*	-5.39	-2.46	< 0.001*
Winter-Fall	-1.98	1.74	1.00	1.55	5.44	0.001*
Summer-Spring	-3.88	-1.38	< 0.00*	-5.66	1.15	0.34
Winter-Spring	-2.15	1.33	1.00	2.70	7.62	< 0.001*
Winter-Summer	0.75	3.69	0.003*	5.00	9.83	< 0.001*

Analyses of variance for linear, quadratic and cubic contrasts were calculated (Table 5). For ponderosa pine (Table FL-2.5(a)) tests indicate a significant linear, quadratic and cubic trend of mean branch moisture content over the year (starting fall). Valley Douglas-fir tests (Table FL-2.5(b)) identified a significant quadratic and cubic trend of mean branch moisture content over the year.

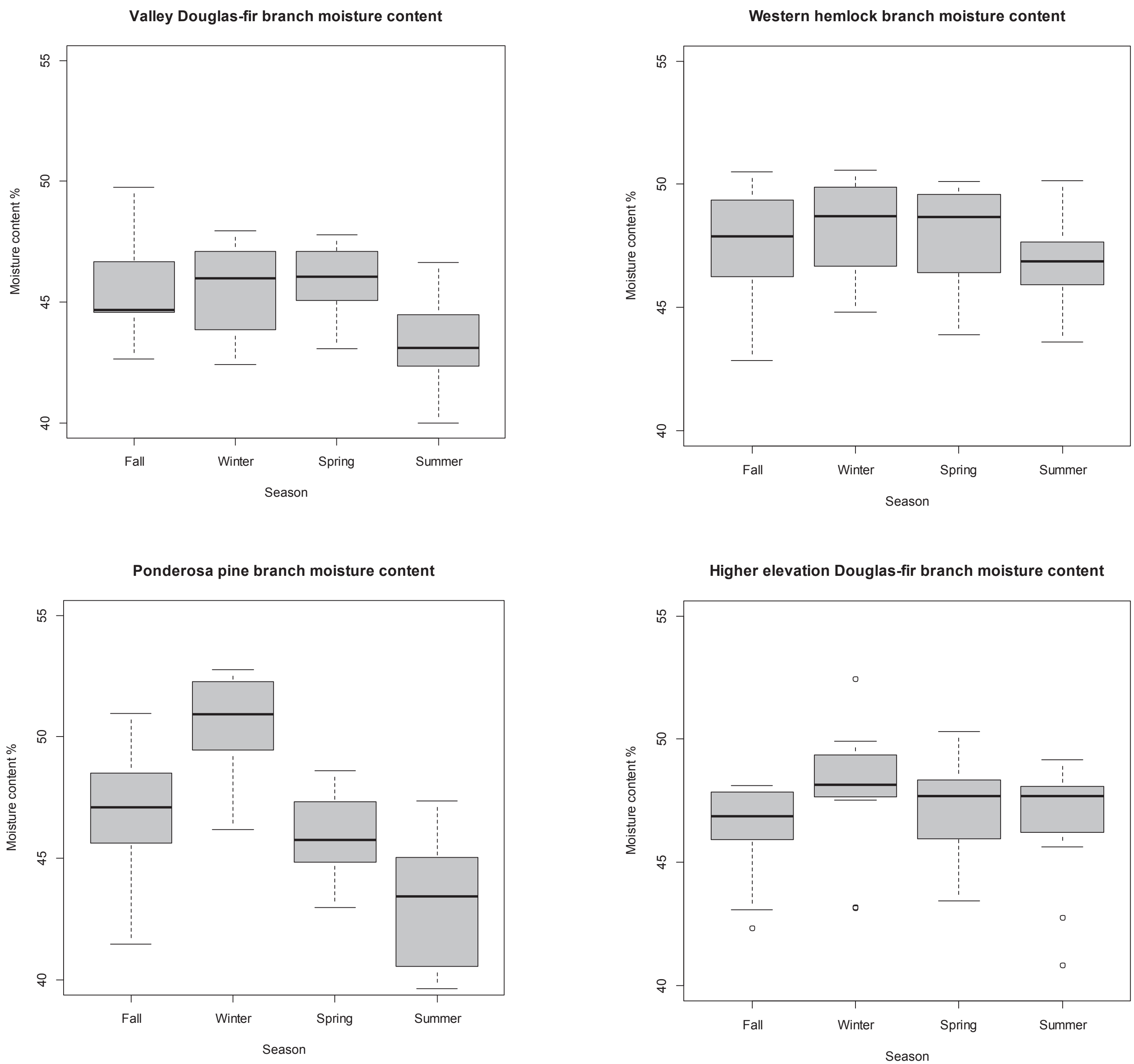

Figure FL-2.7. Average branch moisture content by season.

Table FL-2.5. ANOVA tests of within-subjects contrasts.

a) Ponderosa pine

Source	Seasons	Type III SS	df	MS	F	p-value
Seasons	Linear	225.8	1	225.8	73.3	0.000
	Quadratic	99.2	1	99.2	16.0	0.002
	Cubic	26.1	1	26.1	14.4	0.002
Error (seasons)	Linear	33.9	11	3.1		
	Quadratic	68.3	11	6.2		
	Cubic	18.7	11	1.7		

b) Valley Douglas-fir

Source	Seasons	Type III SS	df	MS	F	p-value
Seasons	Linear	0.7	1	0.7	0.5	0.502
	Quadratic	18.9	1	18.9	14.9	0.003
	Cubic	33.2	1	33.2	26.6	0.000
Error (seasons)	Linear	17.1	11	1.5		
	Quadratic	14.0	11	1.3		
	Cubic	13.7	11	1.2		

2.5. Branch Height Effect on Moisture Content

Since branch height is considered a good predictor for moisture content, an analysis was made in order to determine and define this relationship. An analysis of variance test provides convincing evidence (two-way ANOVA p-value <0.0001) of an effect of branch height on mean branch moisture content. Therefore, a regression analysis was made using branch height as an independent variable and mean branch moisture content (weighted average of all samples within the branch) as dependent for all species and seasons.

After fitting different types of curves, the best fit was a natural log function (R^2 = 0.73), (Figure FL-2.8(a)). The validation data set had consider scatter (Figure FL-2.8(b).

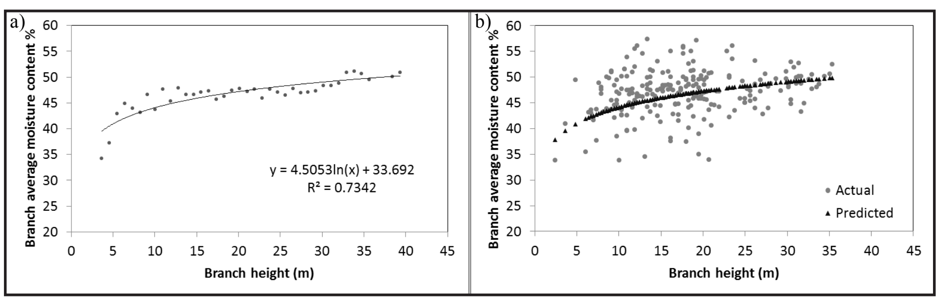

Figure FL-2.8. a) General equation for average branch moisture content estimation by height, b) Actual versus predicted values for the validation subset.

When the data set was analyzed by species, the coefficient of determination increased for all species when compared with the general equation. These specific equations might be a better option if aiming to predict average branch moisture content on these specific sites (Table FL-2.6).

Table FL-2.6. Prediction equations for branch moisture content estimation.

Site	Regression equation	R^2
General	$mc = 4.50\ln(h) + 33.694$	0.73
Valley Douglas-fir	$mc = 9.27\ln(h) + 15.93$	0.82
Ponderosa pine	$mc = 7.04\ln(h) + 28.49$	0.74
Western hemlock	$mc = 5.19\ln(h) + 34.337$	0.75
Higher elevation Douglas-fir	$mc = 7.72\ln(h) + 23.90$	0.84
h = branch height (m)		

2.6. Heartwood Effect on Branch Moisture Content

Another factor considered while gathering data was heartwood diameter. The ponderosa pine data set was excluded from this analysis since it was not possible to distinguish heartwood visually and it could not be measured on the samples.

The graph (Figure FL-2.9) suggests a difference between moisture content of samples containing heartwood. Apparently, its presence results in a reduction in mean moisture content, ranging between 25 and 50%. The range in moisture for samples without heartwood is wider, given that samples without heartwood are 85% of the total number of samples, with a mean centered at 50%.

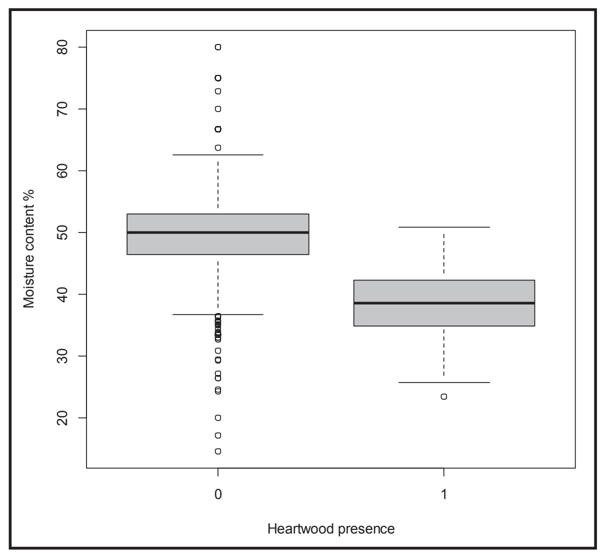

Figure FL-2.9. Effect of heartwood presence in sample moisture content: 0=not present, 1= present.

When performing ANOVA, the test provides strong evidence (two sample t-test p-value <0.0001) of an effect of sample heartwood diameter and sample moisture content. Therefore, a regression model was fitted using branch samples, independent from species and collection season. By fitting a second degree polynomial function to samples with heartwood presence, the coefficient of determination is $R^2 = 0.90$ (see Appendix A in this report) which means that heartwood diameter in the sample, explains over 90% of the sample's moisture content. As the amount of heartwood increases, moisture content decreases (Figure FL-2.10).

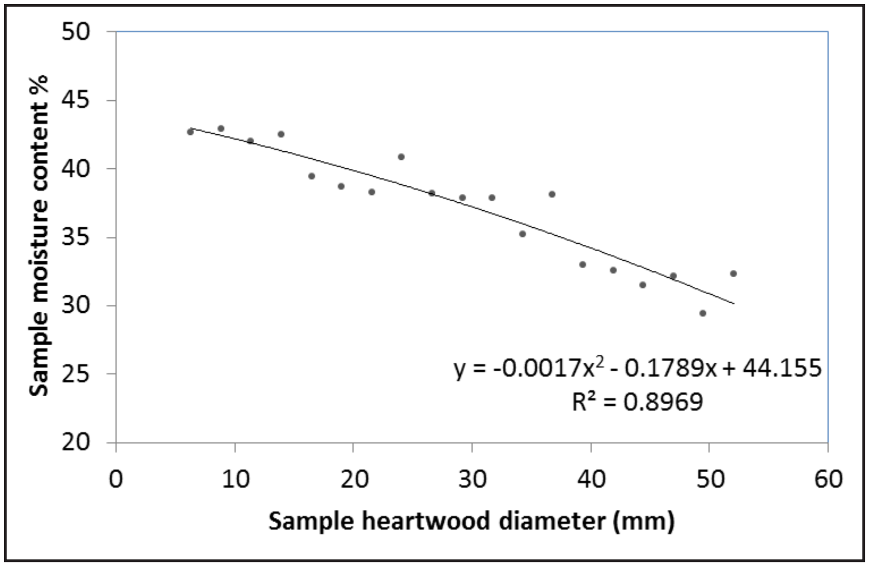

Figure FL-2.10. Sample moisture content by heartwood diameter.

Since having to take samples over the entire extent of the branch in order to predict its moisture content might be time consuming, the possibility of finding a relationship between the branch moisture content and heartwood diameter of the sample taken closest to its attachment point was explored. This would allow making an estimation of the overall branch moisture content by measuring the heartwood diameter at the base of the branch.

This analysis was made ignoring the season and species in order to obtain a general equation for the three species group. Analysis of variance provides convincing evidence (two-way ANOVA p-value <0.001) of an effect of first sample heartwood diameter and branch mean moisture content (see Appendix B of this report). When a regression analysis was performed, the best fit was obtained with a linear function ($R^2 = 0.74$) (Figure FL-2.11). The sample closest to its attachment point is identified as "first sample". Branch average moisture content decreases as the amount of heartwood in the first sample increases (Figure FL-2.11(a)). Model validation is shown in Figure FL-2.11 (b)), the graph was constructed by using the validation data set.

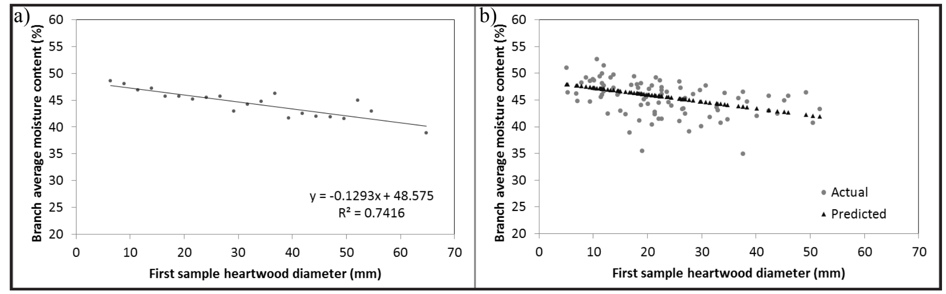

Figure FL-2.11. a) General equation for average branch moisture content estimation by first sample heartwood diameter, b) Actual versus predicted values for the validation subset. First sample is sample closest to the branch attachment point.

When the data set is analyzed by species, the regression models have lower coefficients of determination. However, they all are greater than 50% significance (Table FL-2.7).

Table FL-2.7. Prediction equations for branch moisture content estimation.

Site	Regression equation	R^2
General – 3 species	mc = -0.129*hd* + 48.57	0.74
Valley Douglas-fir	mc = -0.112*hd* + 47.93	0.67
Western hemlock	mc = -0.4061*hd* + 53.41	0.74
Dry Douglas-fir	mc = -0.2831*hd* + 51.31	0.66
hd = first sample heartwood diameter (mm)		

2.7. Discussion

Higher bark proportion in ponderosa pine and Willamette Valley Douglas-fir was to be expected; Miles and Smith (2009) reported that ponderosa pine has a higher bark proportion in the bole compared with the other two species in this study, and ponderosa pine is a species known to have thick bark due to fire adaptation. Willamette Valley Douglas-fir could have a thicker bark because of its larger tree size. Kohnle *et al.* (2012) showed that double bark thickness is correlated with tree size for various Douglas-fir provenances. Even though bark moisture content was not determined in this study, Hakkila (1989) indicates that bark has a higher branch moisture content compared with wood in the summer; consequently, higher branch moisture content in these species in the summer season could be related to higher bark moisture content.

General branch average moisture content for each species and geographic location was calculated. After testing for differences in mean moisture content between species, only Douglas-fir growing in the Willamette Valley shows significant differences when compared with higher elevation Douglas-fir and western hemlock.

This suggests that differences are related to site conditions rather than species. This is consistent with what was found by Gingras and Sotomayor (1992). Furthermore, at the tree level, the higher variability in average moisture content found in ponderosa pine in contrast with more stable western hemlock could explain the same phenomenon. The same authors concluded that MC is higher in trees where water supply is not secured; this is most likely the case of ponderosa pine in the high desert during winter (Figure FL-2.7).

Data shows that higher moisture contents are found in higher branches in the tree and lower moisture contents in the branches of the lower portions of the tree, this trend was found in 96% of the trees sampled and is consistent with what was found for bole wood by Clark and Gibbs (1957) and Pong *et al.* (1986). The average moisture content variability within different seasons is not large, corroborating findings of Clark and Gibbs (1957), Beedlow *et al.* (2007) and Gingras and Sotomayor (1992). However, two species were found to have statistically significant differences in average moisture contents between seasons. Douglas-fir growing in the Willamette Valley contains significantly lower moisture content in summer compared with all other seasons; this difference ranges from -3.9% to -0.8% (95% CI for difference). This result agrees with what was found by Beedlow *et al.* (2007) for Douglas-fir bole wood, where differences in moisture content were less than 5% MC.

In ponderosa pine, significant differences in mean MC were found between winter and every other season, with winter being the season with highest moisture content. Differences range from 1.6% to 9.8% (95% CI for difference), summer being the season with the largest difference. Additionally, there were significant differences between summer and fall ranging from -5.4% to -2.5% (95% CI for difference). These differences could indicate rapid water replenishment with the first fall rain events.

In general, these results do not agree with lowest moisture contents reached by bole wood in the fall as found by Clark and Gibbs (1957) and Beedlow *et al.* (2007). It has been reported by several authors (Dobbs and Scott (1971), Waring and Running (1978), Loustau *et al.* (1996), Phillips *et al.* (2003), Cermák *et al.* (2007)) that bole sapwood serves as a water reservoir. In trees that are subject to drought it could be that they adapt to keep amounts of water storage during most of the growing season until summer drought when they can no longer replenish it until first fall rains. Waring and Running (1978) observed that bole sapwood MC decreases in old growth Douglas-fir during the growing season reaching a minimum of 50% in mid-August. Additionally, Cermák and Nadezhdina (1998) found that for adult Norway spruce, bole sapwood was maximally hydrated in early spring and dehydrated substantially as summer drought approached.

Contrast analysis indicates strong evidence of quadratic and cubic trends over time (seasons) starting in spring, this confirms the gradual increase and then decrease of branch MC throughout the year.

Tree height and heartwood effects in moisture content are well described in the literature. After testing for main effects, both variables have a significant effect on MC and can be effectively used to predict branch moisture content independently. This is, because they are related to each other. Branches located closer to the tree top have a smaller proportion of heartwood than branches located at lower crown levels. Therefore, they have higher moisture contents. Species-specific regression equations have a correlation up to 0.84 using only the branch height to predict its average moisture content. Using the heartwood diameter at the branch attachment point does not increase the coefficient of determination compared with branch height (R^2 =0.74, for general species equation).

2.8. Conclusions for Initial Moisture Content

Seasonal branch moisture content was determined for four major commercial forests areas in the Pacific Northwest. This information is valuable to determine the starting moisture content of a significant portion of forest harvest residues prior to their in-forest storage depending on the harvesting season, forest species and location. Literature reports Douglas-fir bole sapwood moisture content at 53%, heartwood at 27%, ponderosa pine at 60% and 29% respectively (Bowyer *et al.* 2003). Becerra (2012) reports Douglas-fir small log moisture contents of 33% and 55% in summer and winter, respectively, and 51% and 66% moisture contents for western hemlock and ponderosa pine in the winter, respectively. Hakkila (1989) reports 54% for pine and 44% for spruce branches. In our study, only ponderosa pine averaged 50 ± 1% during the winter, all other site averages are below this MC although a few individual branches exceeded 55%. Residues with MC higher than 50% (wet basis) reported at cogeneration plants is probably due to re-wetting of the material, the inclusion of needles/leaves in the moisture content calculation and different species mix. White fir is a common species in the Pacific Northwest that can contain up to 62% MC in the sapwood (Glass and Zelinka, 2010).

Higher initial moisture content can be expected in ponderosa pine residues during the winter. MC can be from 1.6% to 9.8% higher compared with other seasons. For Douglas-fir, initial moisture content can be expected to be lowest when water supply is limited during summer drought. MC can be from 0.8% to 3.9% lower when compared with other seasons. Western hemlock and Douglas-fir growing with a secured water supply do not present significant differences in MC.

Branch height and heartwood content have a strong correlation with branch average MC. Branch height explains up to 74% of branch moisture content by a simple regression. These equations can be used as a non-destructive method to estimate live branch moisture content. Using a sampling destructive method to measure heartwood diameter does not improve the coefficient of determination, making the branch height the simplest and most accurate predictor to estimate average branch moisture content in this study.

The scope of inference for this study is limited to the species and region where samples were taken. It cannot be generalized for other species. Further research could be performed by additionally measuring soil water supply and its effect on branch moisture content.

3. Modeling In-forest Stored Harvest Residue Moisture

Numerous researchers have focused on ways of measuring and predicting wood moisture content in order to find the best field management practices that increase the economic value of small logs or forest harvest residues for bio-energy production. Most have focused on small logs and predicting models include methods such as heuristic fitting and multiple regression. Finite element analysis (FEA) is a method that provides the possibility of determining drying rates while offering the flexibility of changing the way in which these residues are stored, their shape and location, material properties and drying seasons within others. FEA was used to develop drying rates for four different climate regions in Oregon including, Willamette Valley (Douglas-fir), higher elevation Douglas-fir, Coast (western hemlock) and eastern Oregon (ponderosa pine).

Moisture content of forest harvest residue has potential for in-situ drying with knowledge of ambient conditions. It responds to exposure to different environmental factors such as temperature, relative humidity, precipitation and air flow (Hakkila, 1989). Although ambient conditions cannot be controlled, other management factors can be altered in context of environmental conditions to expedite the drying process. Wood is usually stacked to increase air flow and facilitate drying (Simpson and Wang, 2003). In agriculture, hay is left to dry in windrows and several studies have been performed to determine the effects of ambient conditions and conditioning in their drying (Thompson, 1981; Smith *et al.,*1988; Savoie and Beauregard, 1990). However, there is limited literature that describes evaluation of the drying process for forest harvest residue, either experimentally or numerically.

Some studies have addressed the effect of storage time in forest harvest residue moisture content. Gautam *et al.* (2012) determined moisture content and fuel quality in the summer for piled residue of different ages (1, 2, 3 years old). Baxter (2009) determined changes in moisture for piled residue over ten months using digital meters. Routa *et al.* (2015) determined residue moisture content changes over 35-85 weeks using constant weight monitoring. Afzal *et al*. (2010) determined piled residue internal moisture content with destructive methods in three-month intervals over one year.

Gjerdrum and Salin (2009) built a drying model for poles using weather data and pole dimensions. Sikanen *et al.* (2012) developed biomass drying models for whole trees based on heuristics fitting and local weather in Finland. Kim (2012) developed drying models in Oregon for Douglas-fir and hybrid poplar small logs based on precipitation, evapotranspiration and piece size using linear mixed effects multiple regression models. These authors confirm the relationship between weather and drying rates in wood. However, none of them has focused on the use of physics to make moisture predictions or has focused in forest residues.

Since real-time monitoring and instrumentation of residue piles is not practical at a large scale, modeling physical changes driving residue drying serves as a better means of evaluating drying of residue under field conditions. One potential approach towards evaluating coupled physical processes under transient conditions is through application of Finite Element Analysis (FEA), which is used to solve sets of differential equations for a given continuum, boundary conditions and constitutive properties, discretized through a finite mesh of interconnected elements and nodes. The FEA framework is frequently used to evaluate a variety of physical behaviors exposed to change, including structural analysis, thermodynamics, diffusion, electrical conduction, and drying behavior of wood under controlled conditions (Ferguson and Turner, 1996; Hozjan and Svensson, 2011, Kováks *et al.*, 2010; El Gamal *et al.*, 2013; Marchant, 1976; Irudayaraj *et al.*, 1992). The equations governing each element are solved through a system of equations that can give an approximation of the body behavior as a whole (Fagan, 1992).

Ambient drying is a complex problem that involves various interdependent physics relationships, primarily including heat transfer, diffusion and laminar flow (movement of air and moisture surrounding a continuum), but can also include solar radiation and in some cases, turbulent flow (Curcio *et al.,* 2008). Heat transfer occurs by three different mechanisms: radiation, convection and conduction (Monteith and Unsworth, 2008). In the model presented, convection and conduction are considered to describe heat transfer between surrounding air and the residue pile. Both depend on the temperature gradient between the pile and air, and area normal to the direction of heat flow. Convection will also depend on the convective heat transfer coefficient of the surrounding fluid (air/water) and conduction, in both, air and pile thermal conductivity (Welty *et al.*, 2008). Diffusion describes the movement of species between media dependent on concentrations; in this case, the diffusion of moisture between the surrounding air and residue pile, which is most often described by Fick's law, demonstrating the relationship between the flux of diffusing species and the concentration gradient (Welty *et al.*, 2008). Therefore, diffusion will depend on concentration gradient and diffusivity coefficients. For wood, diffusivity will depend on its moisture content since the water contained in cell lumens can escape at a different rate compared to water bound to the cell walls (Baronas *et al.*, 2001). This water is chemically bonded, and it occurs when moisture content is below the fiber saturation point (Bowyer *et al.*, 2003). Diffusion and heat transfer are also driven by fluid momentum transfer, which manifests in this case by the movement of moist air at the surface of the pile (boundary layer). The behavior of this layer depends on fluid properties (in this case air) such as viscosity, density, pressure and velocity and the momentum transfer associated with shear stresses (Monteith and Unsworth, 2008). Often, the presented material properties are related and transient, typically varying with temperature and moisture content, necessitating a numerical analysis that can account for not only changing ambient conditions, but also changing material properties with time, requirements satisfied with FEA.

FEA provides the flexibility of changing drying season and duration, shape, size, location, porosity, moisture distribution within forest harvest residue piles, etc. These advantages cannot be achieved with the current methods and is the rationale for researching this methodology.

This project focuses on implementation of a FEA model that can aid in predicting moisture changes in piled forest harvest residues for given weather variables, informing opportunities to optimize drying of in-forest stored harvest residue. Data collected from a series of field experiments informed a series of baseline FEA models, enabling evaluation of drying sensitivity to various parameters. The results of these models provide further insight into pile drying behavior for given construction and ambient conditions, which can directly utilize data from a given weather station.

3.1. Field Monitoring of Residue Piles

In order to capture the primary regional climates and productive forest types of the Pacific Northwest, four monitoring units were set throughout the state of Oregon, located near Depoe Bay, Corvallis, Dexter, and La Grande, representing Coastal Western Hemlock forest, low-elevation Douglas-fir forest, high-elevation Douglas-fir forest and arid ponderosa pine forest, respectively (Table FL-2.8). Each of these units contained three residue piles built specifically to monitor environmental variables and internal drying behavior of the residue. Residue piles were constructed within one month of tree harvest in order to maintain green moisture content as an initial condition, with the exception of the low elevation Valley Douglas fir unit (VDL), which was constructed two months after harvest due to operation constraints. At pile construction, thirty wood samples were randomly cut (of all different diameters) from material that was going to be used to build each pile in order to determine initial moisture content. For clarification purposes, these samples are named "S" samples though the document.

Table FL-2.8. Site description for each unit.

Index	Site	Main species	Location	Elevation (m)	Average precipitation (mm)
CWH	Coast	Western hemlock	Depoe bay, OR	122	1,779
VDL	Valley	Douglas fir	Corvallis, OR	235	1,029
VDH	Valley-East	Douglas fir	Dexter, OR	984	1,384
EPP	East	Ponderosa pine	La Grande, OR	1,158	457

Pile construction followed a consistent instrumentation framework. Construction of each pile occurred in three stages. First, a 12 x 12 m base pad of approximately 0.9 m in height was constructed with three evenly spaced (3 m) conduit of different lengths (9, 6 and 3 m) placed at the top of the constructed layer (Figure FL-2.12) and equipped with 0.30 m long mesh protectors at their ends (Figure FL-2.13). After the conduit placement, another layer of harvest residue with a rectangular base of 9 x 9 m and 0.9 m in height was carefully placed on top, subsequently placing two more pieces of conduit of different lengths (6 and 3 m) on top. Finally, the pile of harvest residue was capped with a final residue layer, reaching a final height of 3.5 m. Once the conduit was located in the pile, a Polyvinyl Chloride (PVC) pipe (7.6 cm in diameter) of the same conduit lengths was used to introduce samples coupled with a temperature and relative humidity sensor in the pile (Figure FL-2.13). These are referred to as "P" samples though the document. Each P sample was approximately 30 cm long and 3.8-4.3 cm in diameter, consisting of a branch or tree top taken from the same pile material. For protection, sensor cables ran through the PVC pipe, providing real-time data to HOBO® Micro Station data loggers. Sensors were programmed to collect temperature and relative humidity readings every 3 minutes and report an hourly average. The mesh at the end of the pipe served as a protective measure while still enabling exposure to internal ambient conditions of the pile.

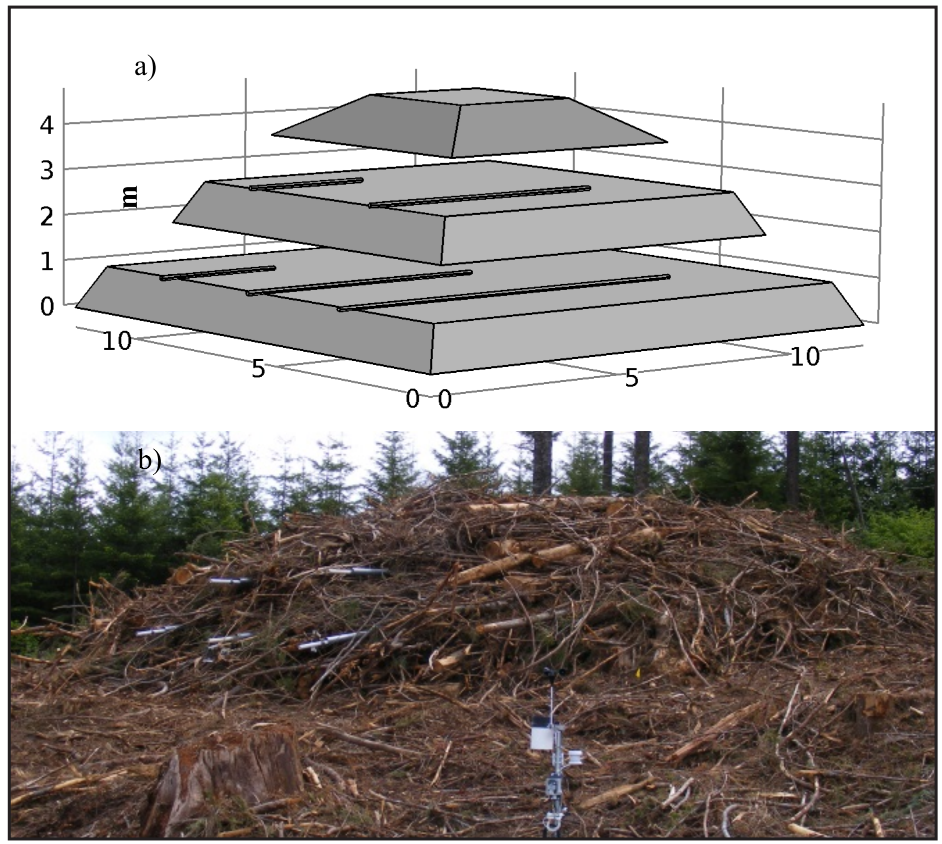

Figure FL-2.12. a) Schematic of conduit placement in each pile; b) Conduit placement on a pile in the field.

Figure FL-2.13. a) Left, electrical conduit with screen; b) Right, sample and temp/RH sensor attached to PVC.

To comply with rules in Oregon, site preparation for reforestation needs to begin one year after harvest operations on a clear cut (Oregon Department of Forestry, 2014), meaning that forest harvest residue would not remain in the field for longer than twelve months unless it does not constitute a fire hazard and does not interfere with the reforestation operation. For that reason, field data collection was limited to one year. Weather stations and pile sensors recorded data hourly for the twelve month monitoring period while P samples were retrieved from the pile and weighed monthly with a scientific scale (0.5 g accuracy) in order to determine their green weight during storage (the monitoring schedule is shown on Table FL-2.9). After data collection was finished, these P samples were oven-dried to determine their dry weight and calculate the moisture content changes through the year. Weather stations installed next to each pile were monitoring precipitation, wind, temperature and relative humidity. Finally, when piles were deconstructed, ten more S samples of different diameters were randomly cut at four height levels of the piles (40 per pile) in order to determine final moisture content throughout the pile.

Table FL-2.9. Schedule of testing sites and sampling*.

	2014								2015											
Site	M	J	J	A	S	O	N	D	J	F	M	A	M	J	J	A	S	O	N	D
VDH	S,P	P	P	P	P	P	P	P	P	P	P	P	P,S							
VDL				S,P	P	P	P	P	P	P	P	P	P	P	P	P,S				
CWH						S,P	P	P	P	P	P	P	P	P	P	P	P	P,S		
EPP								S,P	P	P	P	P	P	P	P	P	P	P	P	P,S

* P wood samples are permanently weighed with constant dimensions, and S samples cut at the beginning and end of each trial covering all ranges of diameters.

3.2. Finite Element Models

Finite element analysis (FEA) was applied in order to evaluate the physical process of the instrumented, drying residue piles. Discrete evaluation of individual pieces of harvest residue, although a better representation of actual pile conditions, is difficult to model due to the uncertainty regarding the pile's porous matrix, distribution of material conditions, boundary conditions and associated computational expense, therefore continuum modeling of porous media was employed as a viable approach towards estimating pile behavior. Accounting for porosity within the continuum within FEA enables reasonable evaluation of transient physical behavior for a pile matrix without computational expense of modeling discrete branches or residue. The domain representing a given pile from field monitoring was designed as a half-ellipsoid with approximate 12 m in width and 3 m in height, surrounded by a box that was 10 m, 10 m, and 30 m in height, width and depth, respectively (Figure FL-2.14). The box dimensions were selected from a sensitivity analysis that demonstrated boundary effects for negligible on the given pile while maintaining computational efficiency. Assigned to the given pile domain was an isotropic, homogenous material representative of the porous matrix (properties are shown in Table FL-2.10), which applied properties presented in prior literature (e.g. Bowyer *et al.*, 2003; Hardy, 1996; Simpson and TenWolde, 1999; Monteith and Unsworth, 2008; TenWolde *et al.,* 1988; Nield and Bejan, 1998; Welty *et al.*, 2008). Wood and air material properties were weighted proportional to porosity according to Nield and Bejan (1998) in order to obtain a better representation of the residue pile. The fluid properties of air were assigned to the surrounding box to represent ambient conditions.

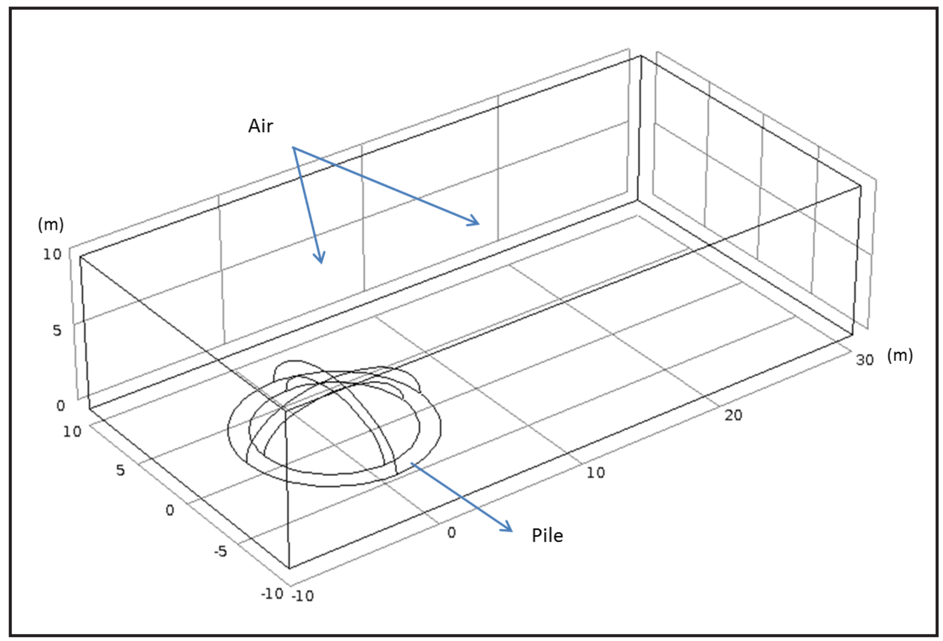

Figure FL-2.14. Diagram of pile and air domains in Comsol.

In order to evaluate transient conditions within a given domain and material properties, meshing, initial conditions and boundary conditions were assigned. The material properties for the four sites are provided in Table FL-2.10**.** A finer mesh was applied to the pile since a higher level of precision is needed in that domain and a coarser mesh applied to the air, both domains were meshed using tetrahedral elements (0.46 m average element size). Since air is not a domain of interest, computational time can be saved by using a coarser mesh, especially around the edges. This analysis accuracy can be refined in areas of interest by increasing element density (reducing element size) where more precision is needed (Cook *et al.*, 2001). Each physics module (heat transfer, laminar flow, convection and diffusion) represents a set of governing differential equations that are coupled through various analytical approaches (Figure FL-2.15); notably, the Arrhenius equation which determines diffusion through activation energy, the universal gas constant and temperature (Welty *et al.*, 2008).

Water is present in wood in two forms, free water and bound water. For this reason, the diffusion process occurs in two ways: free water may leave the cell lumens as water vapor and bound water is transferred cell by cell through their walls (Baronas *et al.*, 2001). This water is chemically bonded to the cells, a process that requires more energy for the water to be released. According to Baronas *et al.* (2001), the diffusion coefficient depends on wood porosity, the bound water diffusion coefficient D_b, and the water vapor diffusion coefficient D_v.

The authors define the vapor diffusion as follows (Eq. 8):

$$D_v = \frac{1.29x10^{-13}(1+1.54u)p_S T_K^{1.5}}{(T_k+254.18)} \cdot \frac{d\varphi}{du} \qquad \text{(Eq. 8)}$$

Where

u :Moisture content

T_k :Temperature in (°)

φ :Relative humidity (%)

p_s :Saturated vapor pressure (Pa), defined as (Eq. 9):

$$p_s = 3{,}390e^{(-1.74+0.0759T_c-0.000424T_c^2+2.44x10^{-6}T_c^3)} \qquad \text{(Eq. 9)}$$

Where

T_c: Temperature in C (°)

The derivative of air relative humidity with respect to wood moisture content was calculated from sorption isotherms adapted by Simpson (1973) for wood after curve fitting and testing the Hailwood and Horrobin theory for hygroscopic materials. According to Baronas *et al.* (2001) the diffusion coefficient for bound water (D_b) can be defined with the Arrhenius equation to determine the diffusion rate based on a material activation energy, air temperature in and gas constant (8,314.3 kmol K). However, little information exists about relative diffusion rates for piles, which are a porous medium containing porous wood (small voids) and air (large voids), therefore, an effective diffusion rate was determined iteratively based on weighted, relative diffusion rates of wood and air based on wood diffusivity values reported by Nadler *et al.* (1985). In the specific case of the ponderosa pine site (EPP), diffusion rate was set to zero during the winter freeze; it is assumed that there is no water movement during that period. That assumption was corroborated by constant moisture content of the P samples located inside the pile during that time.

Table FL-2.10. Material properties for the four sites. Material properties for the Western Oregon sites were assumed to be identical due to species composition.

		Site			
		VDL, VDH, CWH		EPP	
	Air	Wood (solid)	Pile (porous matrix)	Wood (solid)	Pile (porous matrix)
Porosity	1	0.67[1]	0.70[2]	0.72	0.70[2]
Bulk density (kg/m^3)	1	500[3]	150	420[3]	127
Thermal conductivity (W/m K)	0.025[4]	0.11[5]	0.05[6]	0.07[5]	0.04[6]
Heat capacity (J/kg K)	1,000[7]	1,250[3]	1,075[6]	1,250[3]	1,075[6]

[1]Based on 1,520 (kg/m^3) cell wall density (Bowyer *et al.*, 2003), [2]Hardy (1996), [3]Simpson and TenWolde (1999), [4]Monteith and Unsworth (2008), [5]TenWolde *et al.* (1988) Wilkes equation, [6]Nield and Bejan (1998), [7]Welty *et al.* (2008)

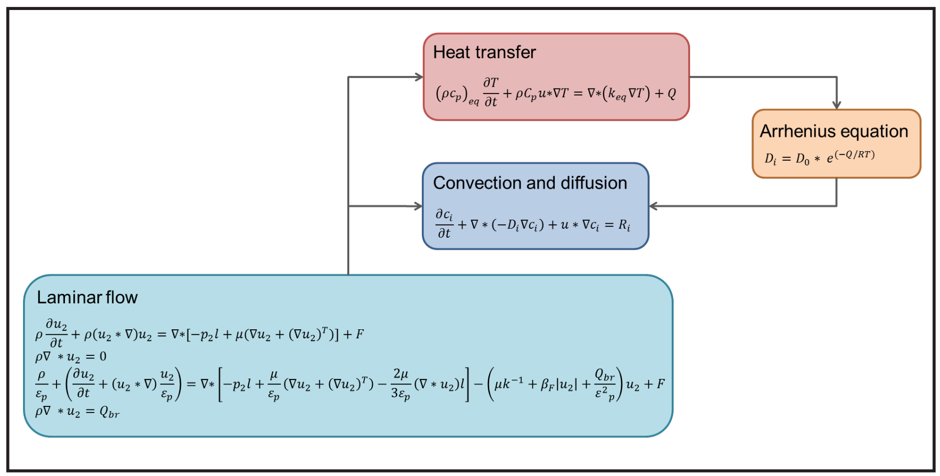

Figure FL-2.15. Diagram of physics modules and their association.

3.3. Input of Environmental Conditions

Weather stations measured environmental variables through a period of one year. To model these environmental factors, mathematical functions were created to approximate weather conditions, including wind, temperature, precipitation and relative humidity for direct entry as boundary conditions for the FEA model. The time-dependent relationships for each site are presented in Figure FL-2.16.

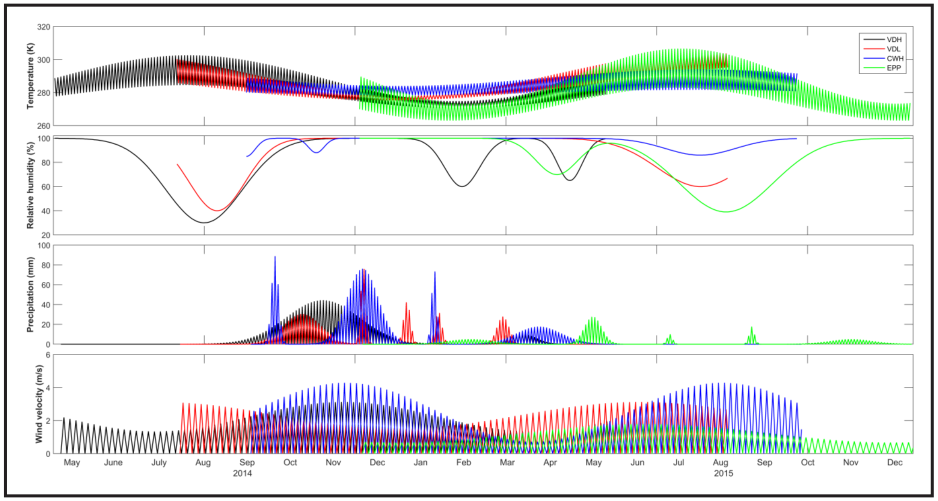

Figure FL-2.16. Functions for environmental variables on each site over their period of measurement.

These functions present an approximation of the data collected in the field starting in the month of May 2014 and ending in December 2015. Solar radiation was not considered in this model as boundary heating could occur, realizing a rise in external pile temperatures and marginal rise in internal pile temperatures. It was, however, omitted from this analysis for computational efficiency and a focus on the diffusion of moisture through diffusive processes greatly influenced by movement of air.

3.4. Boundary Conditions and Initial Conditions

Finite element models require initial conditions to define a representation of conditions before changes occur, specified as values on each domain. Boundary conditions are defined on boundaries of domains, representative of known values that govern the calculated differential equations within the bounded domains. Initial conditions are based off of experimental data and similar modelling techniques presented in literature (Sandoval *et al.,* 2011; Curcio *et al.,* 2008; El Gamal *et al*., 2013). Initial conditions for each test pile are presented in Table FL-2.11.

Table FL-2.11. Initial conditions for each site.

Site	MC_{wb}* (%)	Pile and air temperature (K)	Wind velocity (m/s)
VDH	40	277.6	0
VDL	21	293.7	0
CWH	39	288.15	0
EPP	57	274.3	0
* wb = wet basis			

Specific boundary conditions are shown in Figure FL-2.17. Wind velocity was zero at ground level due to drag, at the inlet was a wind function (m/s) describing the wind fluctuations over time (shown in Figure FL-2.16) and in the outlet, the reference atmospheric pressure (1atm) to solve for wind velocity. Temperature was set as boundary condition in most walls to represent changes in temperature through the year. There was no heat transfer on the ground since soil temperature was not measured. Equilibrium moisture content was set as a boundary condition in inlet, top and side walls so the wood in the pile would reach equilibrium depending on changing temperature and relative humidity.

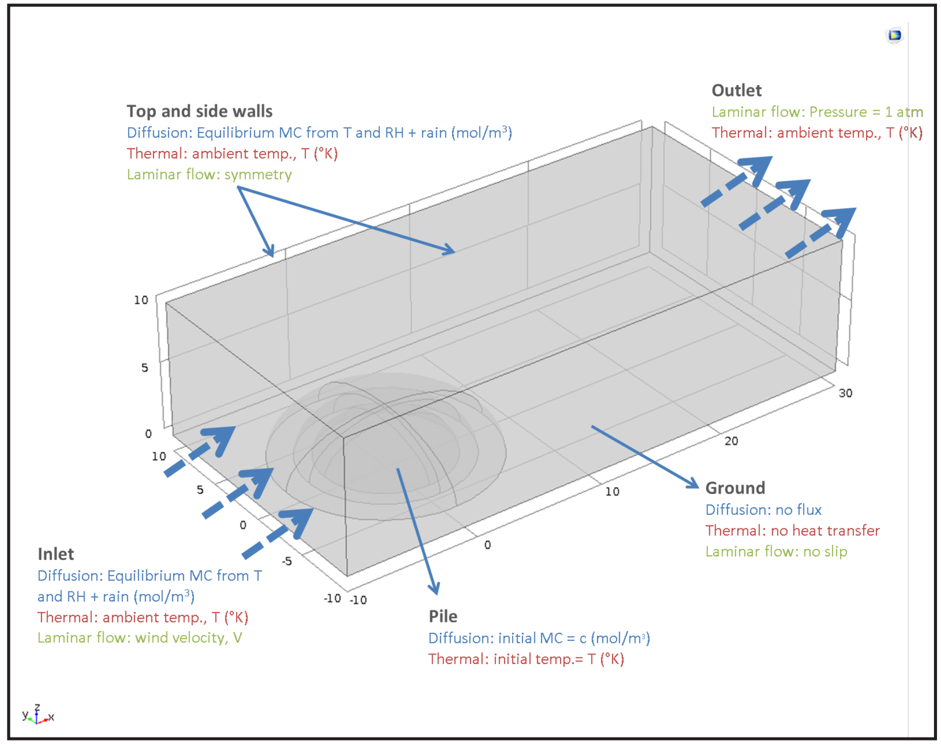

Figure FL-2.17. Boundary conditions for pile, ground and surrounding air.

3.5. Solver

For this study, a commercially available Finite Element Analysis solver (Comsol Multiphysics® v5.1 with the Heat Transfer, Laminar Flow and Chemical Reaction engineering modules) was used. After the input of appropriate properties and physics, a transient analysis was performed for given time increments, the maximum of which was 43,200 seconds (12 hours to capture both day and night conditions), subsequently analyzed in a post-processing regime. In order to simulate the pile drying for one year (31,536,000 s), approximately one and a half to 20 hours of computing time was necessary on an Intel Core 2 PC (Windows 7 Enterprise, 3 GHz, 8 GB RAM).

3.6. Sensitivity Analysis

Many pile parameters can affect drying rates – in this study, pile shape, porosity, volume and starting drying season were observed. The first study presents the effects of shape, using a semi-ellipsoid as a baseline geometry representative of field conditions and both a cone and continuous berm shape of equivalent volumes for comparison (238 m^3). Besides changing the shape, the element size changed with the different geometries after the meshing process. Ranging from a minimum of 0.06 to 0.52 m maximum for the half ellipsoid, 0.10 to 0.91 m for the cone, and 0.11 to 1.06 m for the berm.

Porosity (the volume of voids compared to the total volume of a porous matrix) was observed as a parameter that could affect drying rate. Porosity can vary for a given pile, therefore three reasonable values within a 10% range were chosen for the second study: 70, 80 and 90%. Additionally, half-ellipsoid piles of half (119 m^3) or double (476 m^3) the baseline volume (238 m^3) were evaluated for drying rates was defined as a third study. And finally, the effects of delaying the drying start time was evaluated. The baseline model starting time was delayed 3 and 6 months from the original starting date to assess its effect on drying. Starting month for VDH was May 2014, for VDL August 2014, for CWH October 2014 and for EPP December 2014. The different studies that were implemented are summarized in Table FL-2.12.

Table FL-2.12. Model summary for sensitivity analysis.

Model	Site	Shape	Volume	Porosity	Start time (mo)
1	VDH	Half ellipsoid	Field (control)	0.7	0
2	VDH	Cone	Field (control)	0.7	0
3	VDH	Berm	Field (control)	0.7	0
4	VDH	Half ellipsoid	Half of field	0.7	0
5	VDH	Half ellipsoid	Double of field	0.7	0
6	VDH	Half ellipsoid	Field (control)	0.8	0
7	VDH	Half ellipsoid	Field (control)	0.9	0
8	VDH	Half ellipsoid	Field (control)	0.7	+3
9	VDH	Half ellipsoid	Field (control)	0.7	+6
10	VDL	Half ellipsoid	Field (control)	0.7	0
11	VDL	Cone	Field (control)	0.7	0
12	VDL	Berm	Field (control)	0.7	0
13	VDL	Half ellipsoid	Half of field	0.7	0
14	VDL	Half ellipsoid	Double of field	0.7	0
15	VDL	Half ellipsoid	Field (control)	0.8	0
16	VDL	Half ellipsoid	Field (control)	0.9	0
17	VDL	Half ellipsoid	Field (control)	0.7	+3
18	VDL	Half ellipsoid	Field (control)	0.7	+6
19	CWH	Half ellipsoid	Field (control)	0.7	0
20	CWH	Cone	Field (control)	0.7	0
21	CWH	Berm	Field (control)	0.7	0
22	CWH	Half ellipsoid	Half of field	0.7	0
23	CWH	Half ellipsoid	Double of field	0.7	0
24	CWH	Half ellipsoid	Field (control)	0.8	0
25	CWH	Half ellipsoid	Field (control)	0.9	0
26	CWH	Half ellipsoid	Field (control)	0.7	+3
27	CWH	Half ellipsoid	Field (control)	0.7	+6
28	EPP	Half ellipsoid	Field (control)	0.7	0
29	EPP	Cone	Field (control)	0.7	0
30	EPP	Berm	Field (control)	0.7	0
31	EPP	Half ellipsoid	Half of field	0.7	0
32	EPP	Half ellipsoid	Double of field	0.7	0
33	EPP	Half ellipsoid	Field (control)	0.8	0
34	EPP	Half ellipsoid	Field (control)	0.9	0
35	EPP	Half ellipsoid	Field (control)	0.7	+3
36	EPP	Half ellipsoid	Field (control)	0.7	+6

3.7. Model Scaling

Because the residue pile consists of material of different sizes, species, and because the soil activity and water accumulation affecting the lowest portion of the pile is not modeled, the S samples taken at the beginning and end of the trial were used to scale the models at those two points in time. The scaling was achieved by reducing the diffusion rate by 10 or 20 depending on the site. The shape and the rest of the model parameters remained constant. The rationale for these scaling factors is the fact that larger pieces of wood will dry at a slower rate compared to smaller pieces. Properties that were changed to scale the models are presented in Table FL-2.13. In order to distinguish these models from the originals, they will be referred as "pile model".

Table FL-2.13. Model scaling parameters.

Site	VDH	VDL	CWH	EPP
Initial moisture content$_{wb}$ (%)	34	21	39	54
Final moisture content	27	19	36	39
Diffusion rate m^2/s	2e-8	2e-8	1e-10	4e-8

3.8. Results

The monthly average moisture content obtained with the models was compared with the actual average moisture contents acquired in the field on each corresponding month (P samples). Both averages follow a similar trend through the year (Figure FL-2.18). The greatest disparity can be seen at the EPP site.

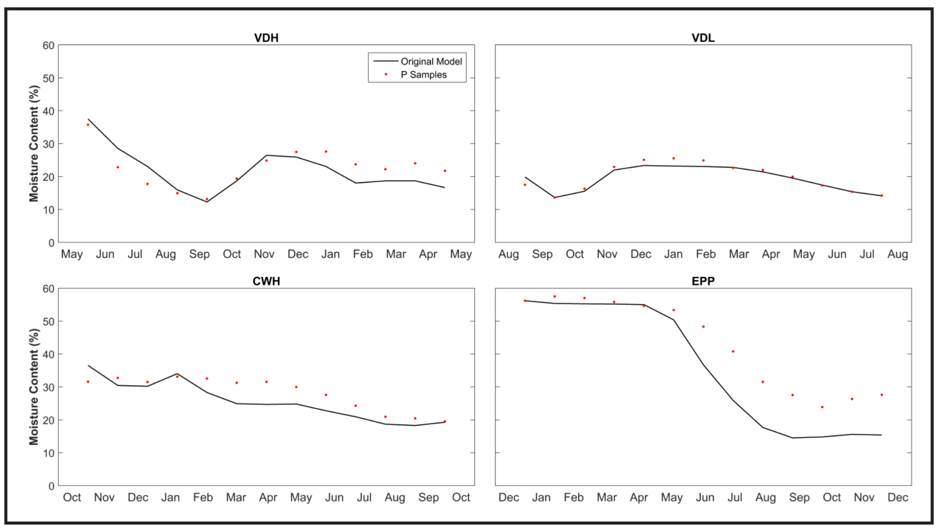

Figure FL-2.18. Modeled average moisture content (wet basis) versus field P samples.

Three statistical tests were performed to verify the agreement between the modeled moisture contents and data obtained in the field, a Wilcoxon signed rank test, a Kendall tau and Spearman's rho correlation tests. At a 0.05 significance level, the modeled and field P sample average moisture content for the two Douglas-fir sites have an identical distribution (VDL and VDH Wilcoxon SR, p-value >0.10). The other two site models (EPP and CWH) have a non-identical distribution when compared with field data. When correlation was tested, all sites present a statistically significant association between the model moisture content averages and field averages. The p-values shown in Table FL-2.14 for Spearman's rho and Kendall's tau indicate that we can reject the null hypothesis that variables are uncorrelated at a 0.05 level. Spearman's rho indicates correlations over 0.70 for all sites (Table FL-2.14). This parameter is more sensitive to differences compared with Kendall's tau since it compares the squared differences between pairs of data. A detail of the test outputs can be found on the Appendix C in this report.

Table FL-2.14. Model correlation and significance tests.

Site	Wilcoxon SR test	Spearman's rho		Kendall's tau	
	p-value	Correlation	p-value	Correlation	p-value
VDH	0.4143	0.73	<2.2e-16	0.56	1.8e-6
VDL	0.1272	0.98	<2.2e-16	0.92	1.4e-7
CWH	0.0215	0.90	<2.2e-16	0.77	7.0e-5
EPP	0.0007	0.96	6.3e-3	0.87	6.7e-3

After the model was scaled in order to represent the overall pile moisture content, drying rates over time follow the same pattern as the base models. However, drying and re-wetting occurs at a slower rate. For that reason, the pile dries to a lesser extent over time and moisture content is more stable throughout the year. The two points of comparison with S samples (pile initial-final moisture content) are represented in Figure FL-2.19.

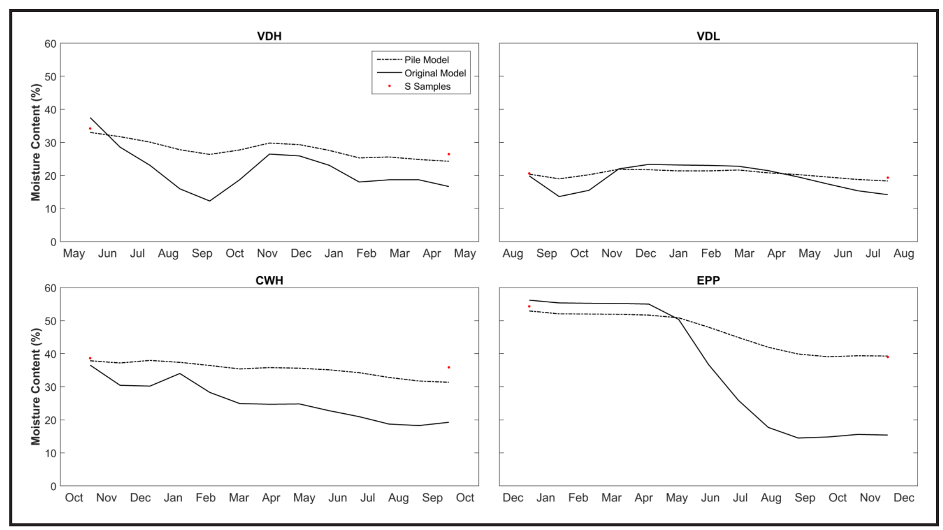

Figure FL-2.19. Modeled average moisture content (wet based) versus field S samples.

3.9. Sensitivity Analysis

3.9.1. Shape

For the original model, upon comparison of the 10-day moisture content averages of the control pile (half ellipsoid, 0.7 porosity and volume 238 m^3) with the cone pile, differences in MC over time are very subtle with the exception of the EPP site, likely due to similar shape and length (6 m radius). However, the berm pile shows a marked difference (20 m length), especially in the drier and rainy months at the Douglas-fir sites. In the VDL site, the difference can be up to 12% higher MC in the winter and 7% lower in the summer (Figure FL-2.20).

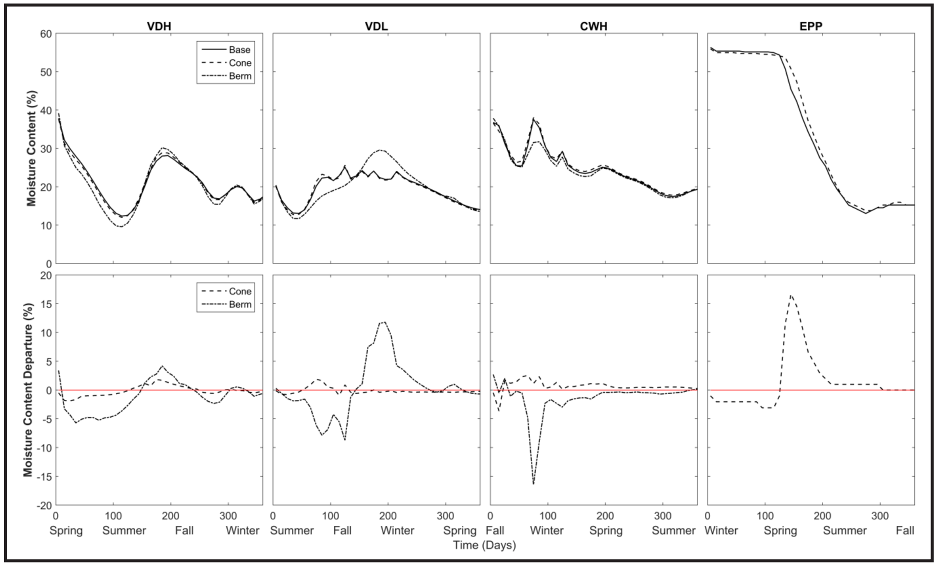

Figure FL-2.20. Shape effect in moisture content (wet basis) for each site.

When the model is scaled to pile averages (S samples), the effect of shape has the same trend as the original model (Figure FL-2.21), which is implicit due to simple changing of the diffusion rate. For example, when compared to the baseline shape, moisture content can be reduced by 3% during the dry season and re-wet up to 5% moisture content during the rainy months in the Valley Douglas-fir site.

3.9.2. Volume

Volume is the parameter that affects drying rate of the piles the most. Material on a pile of the same shape and half the volume would have an average moisture content that was approximately 4 to 12% lower during the dry season and almost 9% higher during the wet months depending on the site location and species (Figure FL-2.22). When the pile volume doubled, average moisture content can remain as high as 26% higher (EPP site) during dry months and oppositely, decrease

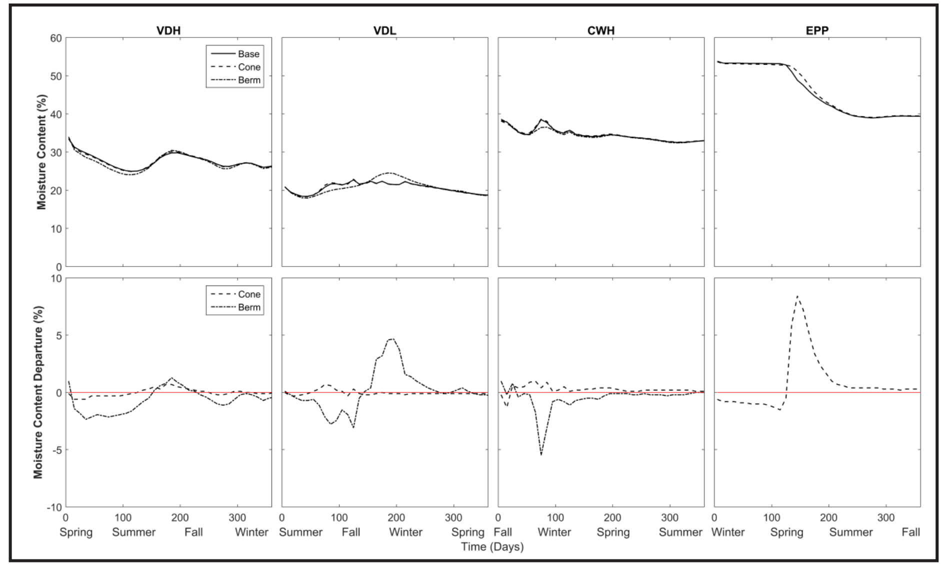

Figure FL-2.21. Shape effect in moisture content (wet basis) for each site, pile model.

during the rainy season when compared with the baseline volume. The effect of pile volume is still the greatest within the sensitivity analysis when the models is scaled, but also realize diminished changes in moisture content (Figure FL-2.23).

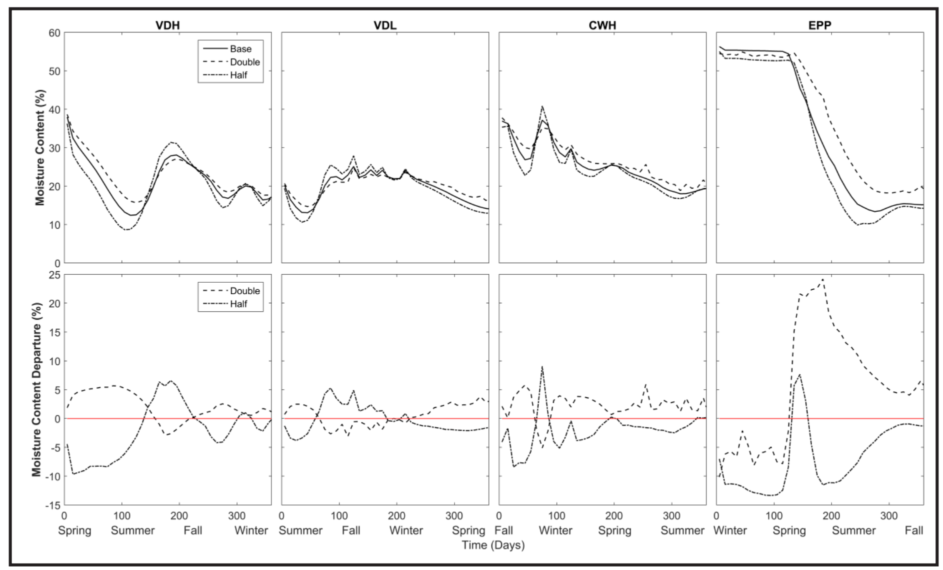

Figure FL-2.22. Effect of pile volume in moisture content for each site.

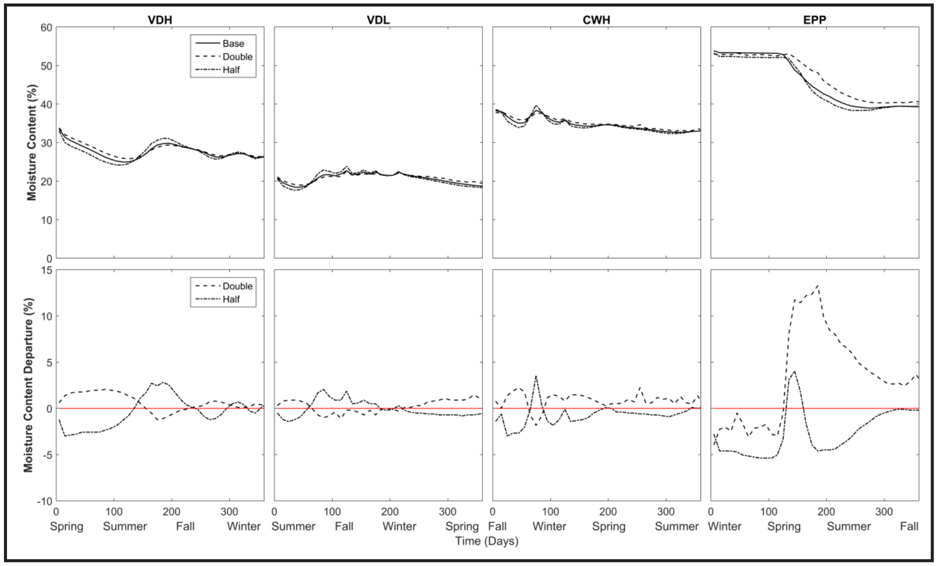

Figure FL-2.23. Effect of pile volume in moisture content for each site, pile model.

3.9.3. *Porosity*

Porosity accentuates the effects of ambient conditions on pile behavior. With increasing porosity, the effects of drying and wetting become exaggerated within the residue pile (Figure FL-2.24). Average moisture content can be reduced by almost by 5% at any given time for the EPP site when porosity is increased by 0.2 (from 0.7 to 0.9) and increased by 19% during the rainy season when porosity is increased by 0.1 (from 0.7 to 0.8).

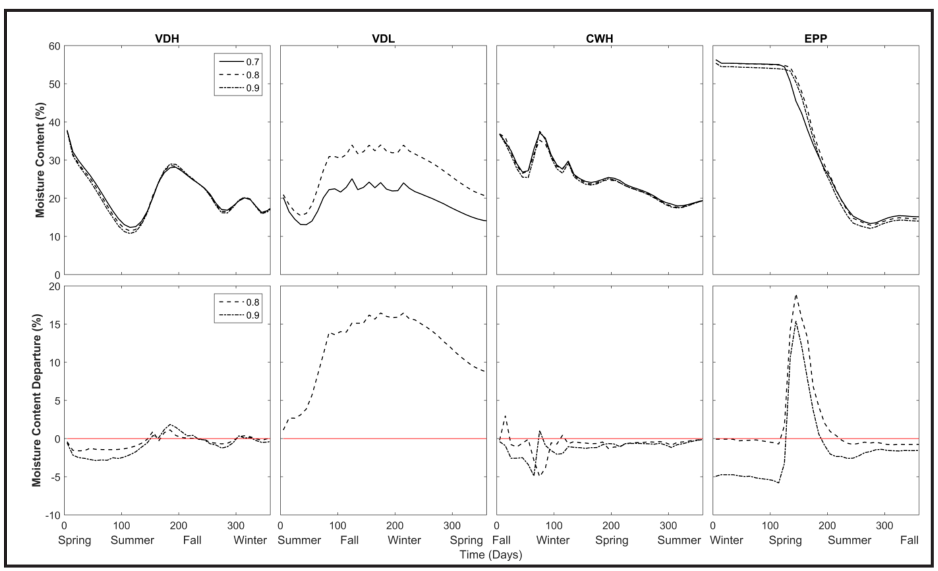

Figure FL-2.24. Effect of pile porosity in moisture content for each site.

In the scaled model, the effect of porosity is marginal in the VDH and CWH sites and significantly smaller in the other two sites when compared with the original model. The greatest effects occur at the ponderosa pine site, were the pile re-wets up to 9% more in a pile with a porosity of 0.8 compared with the baseline (porosity of 0.7) during the spring rains (Figure FL-2.25).

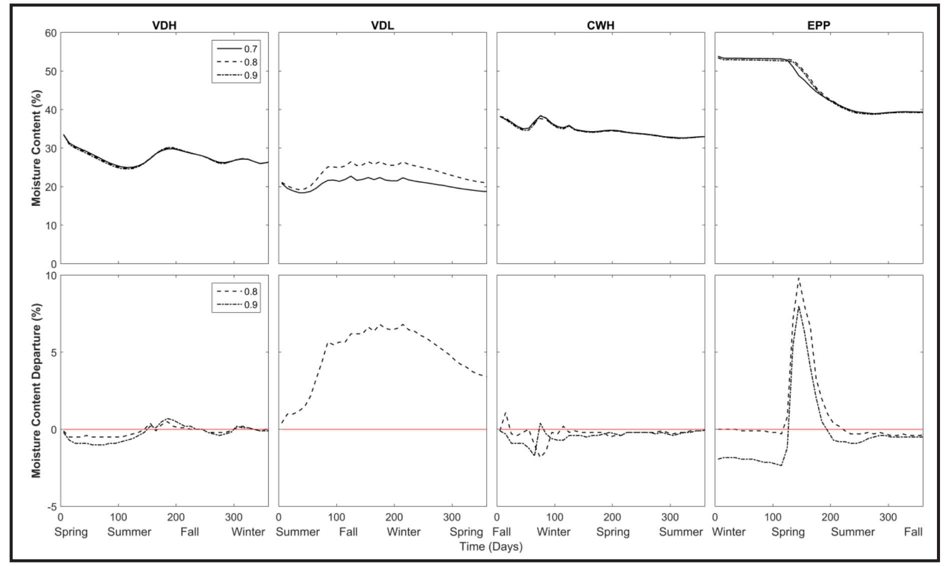

Figure FL-2.25. Effect of pile porosity in moisture content for each site, pile model.

3.9.4. *Time*

Even when the starting moisture content of the residue material that comprises a given pile remains constant, the drying rate changes depending on the starting point in which the material is stored in the forest. For example, in the Valley-East Douglas-fir site, it takes 52 days for the material to reach average moisture content below 20% (wet basis) when drying starts in spring. If the same material is harvested and stored three months later, it would take only 8 days to reach that moisture content. Finally, if it delayed another three months (6 months total), the residues would reach the same moisture content in 73 days. As expected, when drying starts during the dry and warm months, the residue will approach lower moisture contents faster, reaching equilibrium with environmental conditions more expediently (Figure FL-2.26).

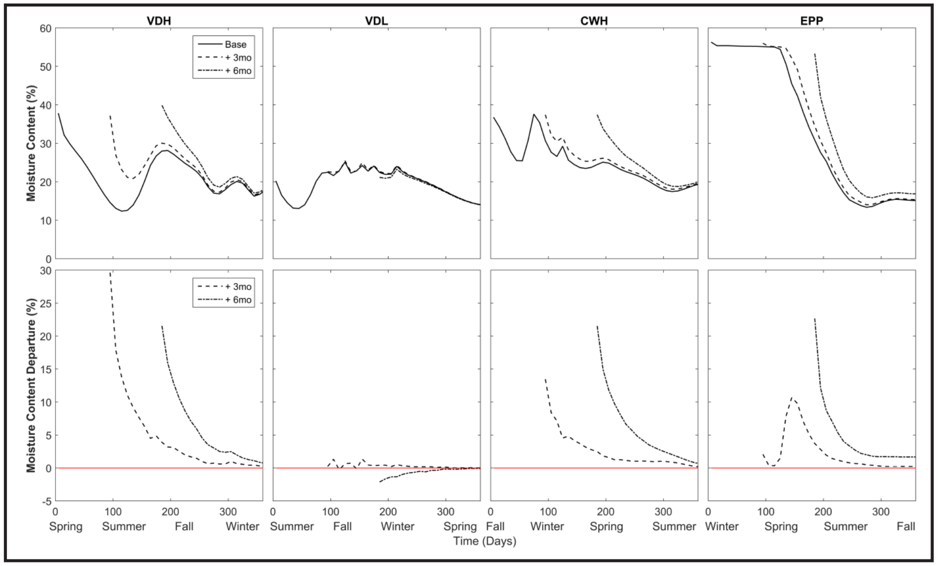

Figure FL-2.26. Effect of drying time in moisture content for each site.

Similar to other parameters, the scaled model has a smaller impact with time changes. For the Valley Douglas-fir site, the effect is marginal. However, for the EPP site, it takes 196 days for the average moisture content to reach levels below 43% (wet basis) if drying starts in winter, 115 days in spring and only 33 days in summer (Figure FL-2.27).

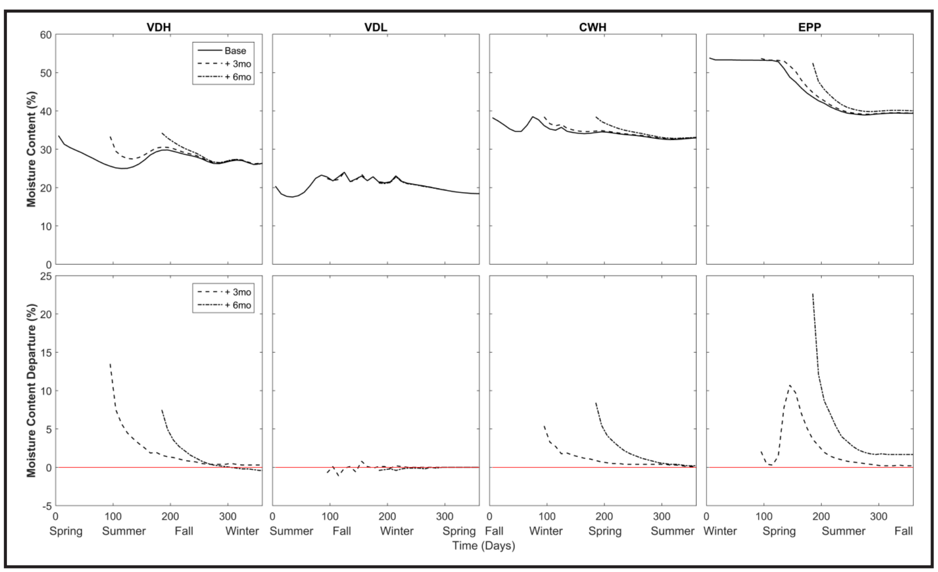

Figure FL-2.27. Effect of drying time in moisture content for each site for scaled models.

3.10. Discussion

The presented series of models offered reasonable agreement with field drying rates, confirmed by statistical tests compared with field data (Table FL-2.13). This sets a framework to define and compare different means of in-situ residue drying for specific ambient conditions. Although it is difficult to represent all potential conditions, the impact of parameters critical to drying may be evaluated. For all sites, residue piles dry fast during the first months, finding particular dependence on the time of harvest, often reaching a minimum in September-October. The ponderosa pine site (EPP) has almost no drying during the first months, since there is no diffusion during the winter deep freeze. Rain, along with lower temperatures and higher relative humidity allow the material to re-moisten during the wet rainy season.

After the model was scaled with S samples, results showed the same trends compared to the base original models, with lower drying rates. Material of larger sizes dries at a slower rate. For these models, there is little drying in both Valley Douglas-fir and Coast western hemlock after one year of field storage. Some possible reasons are that the Douglas-fir began with dry material, likely muting the observed drying effects. The CWH unit was continuously under the effect of marine moist air and could be the explanation for stability of the material's moisture content. The greatest drop in moisture content is observed in the EPP unit; this could be caused because of the material being very wet at the start of the trial and the likely lag of freezing preventing diffusion of moisture, particularly underneath a layer of snow.

As expected, berm or windrow geometry works best to expedite the drying process due to large relative surface area and exposure to ambient conditions and convection. This shape has 60% larger surface area directly exposed to wind, which is probably the main cause for the differences. Residue moisture content is reduced between 2 and 5% compared with a half ellipsoid of the same volume during the dry season. However, the same advantageous conditions for drying may also expedite rewetting in the winter probably because more surface area is directly exposed to rain. The cone shape behaves similarly to the half-ellipsoid for all sites likely due to a generally similar shape in relative surface area.

Volume is the parameter that most affects drying. When the pile volume is halved, moisture content can be reduced by 2 to 5% during the dry months, and increased by 3-4% during the wet season in comparison to baseline volume. When the volume is doubled, moisture content can increase from 1 to 13% depending on the site. These changes are probably driven by the same principles that affect the different pile shapes. A pile with smaller volume allows more air flow through the interior of the pile permitting more efficient drying. At the same time, there is less coverage from the rain allowing more moisture to reach the material inside the pile. A larger pile has the opposite effect; more material is protected from wind and rain.

Porosity is a pile property that is difficult to change in a practical sense, but may have impacts on the rates of drying or wetting for given ambient conditions. Increasing the porosity has a greater effect on sites such as the Valley Douglas-fir site (VDL) and east ponderosa pine (EPP), where more voids may increase sensitivity to weather conditions for the presented baseline model (porosity of 0.7).

The time of harvest has notable effects on residue drying times as the gradient in moisture or temperature for a given time of year may expedite or slow drying. For example, in the case of the ponderosa pine site (EPP), it can take one sixth of the time it takes for the residue to reach 43% moisture content when drying starts in summer versus winter. During summer, higher temperature and lower relative humidity reduce the wood equilibrium moisture content and there is little or no re-wetting of the material.

3.11. Conclusions for Slash Pile Modeling

Finite element models were developed for four sites representing the main climatic regions in Oregon and their respective commercialized forest species. These models are able to sufficiently predict piled forest residue drying rates with weather data input such as precipitation, wind, ambient temperature and relative humidity. Conclusions include:

- Piled residue moisture content responds to the environmental conditions greatly. The selection of pile shape or size can be beneficial or detrimental towards the rate of drying depending on ambient conditions, namely precipitation.
- A berm (windrow) presents the best option for expedient drying due to its large surface area. Drying is the fastest in this shape during dry summer months; however, the pile also re-wets the fastest during wet, winter months.
- It is best to reduce pile volume if storage will occur through summer and increase size if it will occur through winter. The reason behind this is the same as for the shape, a smaller pile will have more airflow but it will also become wetter in the rainy season when compared to a larger pile.
- Significant reduction in drying times can be achieved if the material is cut and left to dry during the dry, warm summer months. This reduction can be up to 1/3 of the time versus starting the process in the winter.
- This methodology is a tool that has the flexibility to be able to change parameters and conditions in which the harvest residues are stored. For that reason, it opens several possibilities for future research.

The models were made with local data and inferences are generally specific to these locations. However, the main concepts and sensitivity of pile drying parameters still present a general understanding for drying conditions in many different climates.

4. Decision Support for Moisture Management of Harvest Residues

The need for improving the cost effectiveness of forest harvest residue utilization for bioenergy production has been widely recognized. There have been a number of studies showing that reducing residue moisture content presents advantages for transportation and energy content. However, previous studies have not focused on the relative advantages of in-forest drying depending on different logging systems or, in the case of cogeneration, energy-based demand. Drying curves have been developed for harvest residue generated from two main Pacific Northwest logging systems for a case study in Oregon using mixed integer programming to optimize the volume delivery to a hypothetical cogeneration plant with a generating capacity of 6 MW-hr.

In the Pacific Northwest there are two primary logging systems for clear cut harvesting. One is cable logging on steep terrain (slope greater than 40%) and the second is ground-based logging in flat terrain. Cable logging generally consists of manual felling and whole tree yarding along a suspended cableway. When trees arrive at the landing they are delimbed, bucked into logs, and the harvest residues are left in large piles at the landing. Ground-based logging consists of either manual or mechanized felling, delimbing, bucking into logs at the felling site and then yarded to the landing with either a shovel (excavator base loader), skidder or forwarder; leaving harvest residues scattered over the forest unit. Alternatively, at ground-based harvest units, trees are felled by mechanized felling and forwarded by shovel to the roadside landing, during which many of the branches and tops break off due to repeated handling.

A harvest residue operation generally involves a grinder positioned at a landing or at roadside. The grinder is loaded by an excavator and as it grinds the material, a trailer is loaded through a conveyor belt. Trucks used to transport this material have lightweight chip trailers that can be 9.8, 11.6, 12.8, 13.7 and up to 15.2 m long. This operation can be challenging as these trucks need roads with larger curve radii, large turn-arounds, and have much lower gradeability than log trucks when empty (Zamora-Cristales *et al.*, 2013). The use of all wheel drive (6 x 6) truck tractors are used by some contractors to improve gradeability and remotely steered trailer wheels are used to improve trailer tracking and reduce required turn-around area.

Since forest residues are a minor part of the above ground biomass, equipment mobilization costs for collection and comminution can be significant (Figure FL-2.28). To account for mobilization costs by harvesting system, we recognize distinct harvest units and model mobilization to each harvest unit. We discuss this in more detail later.

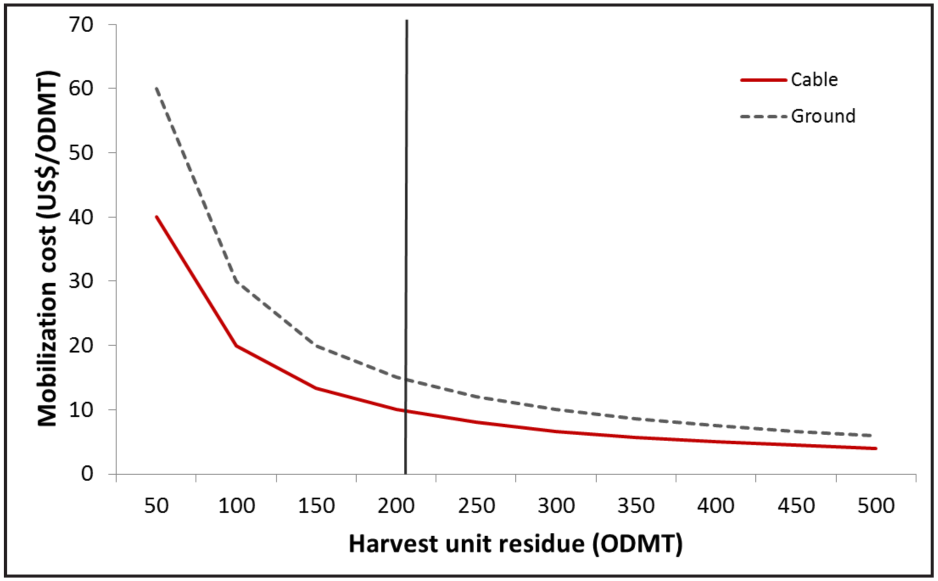

Figure FL-2.28. Exmple of relationship between mobilization cost ($2000 for cable and $3,000 for ground-based units) and total harvested biomass that was removed at that mobilization.

The effect of forest harvest residue moisture content in the economics of pricing, collection and transport has been frequently recognized by researchers (Sessions et al., 2013; Acuna et al., 2012; Ghaffariyan, Acuna and Brown, 2013). High moisture content impacts the volume of residues that can be transported due to the weight restriction on roads and highways (Zamora-Cristales and Sessions, 2015). This causes the truck to reach its weight capacity before reaching its volume capacity due to the extra weight of water, thus making transportation inefficient and uneconomical. On the other hand, when residues are very dry the truck becomes volume limited, caused by lower bulk density of ground material (Sessions et al., 2013). Forest harvest residues start at high moisture content when fresh. Then, they rapidly lose moisture until wood reaches equilibrium with the environment (Simpson and TenWolde, 1999). Storing the material in the forest unit can be beneficial for drying, depending on the season in which they are collected and whether they are stored piled or scattered over the forest unit (Belart, 2016).

Finite element analysis (FEA) is a numerical technique to solve complex problems involving differential equations (Fagan, 1992). A finite element model can be constructed to predict forest residue drying rates over time using ambient condition variables such as temperature, relative humidity, wind velocity and rain in which the residues are being stored (Belart, 2016). FEA works by integrating the physics phenomena such as heat transfer, laminar flow, diffusion and several assumptions such as material, fluid and thermal properties of the components (wood, water and air). This tool allows the prediction of harvest residue moisture changes over time (Belart, 2016).

Routa et al. (2015) determined residue moisture content changes over 35-85 weeks using constant weight monitoring in stacked wood. Sikanen et al. (2012) developed biomass drying models for whole trees based on heuristics fitting and local weather in Finland. Kim (2012) developed drying models in Oregon for Douglas-fir and hybrid poplar small logs based on precipitation, evapotranspiration and piece size using linear mixed effects multiple regression models. Both authors confirm the relationship between weather and drying rates in wood. However, none has focused on the use of physics to make moisture predictions or has specifically focused in forest residues and the different drying rates depending on logging system operations. Acuna et al. (2012) developed a tool to optimize biomass logistics and determine optimal storage for three different supply chains, including forest residues. They highlight the importance of managing moisture as a way to improve the economics of the biomass supply chain. This study is based on ground-based logging where forest harvest residues are forwarded to roadside. Lower moisture content has an important advantage from the energy content point of view. Power generating plants need fewer residues in order to generate the same amount of power if they are dry. Other studies have recognized the importance of moisture content, but have specified the moisture content exogenously. For example, Ghaffariyan et al. (2013) provide bounds on the amount of water that can be delivered to the plant for a set energy demand. Many companies pay for feedstock on a dry tonne basis, and at least one varies payment per dry tonne based on moisture content. In this study, the delivered feedstock moisture content is a variable to be determined in joint consideration of transport and power generation requirements by an entity that both owns forest land and a power generating facility.

Because drying rates and costs differ between the two main logging systems it is important to understand the difference in economic value of harvest residue from those two different sources; one piled green at the landing, generally in large piles, which dries slowly and the other not piled, or in smaller piles in the field, which dries quickly. A data set of clear-cut harvest units over Linn and Marion Counties (Oregon) was used to formulate an optimization problem to minimize cost of harvest residue delivered to a hypothetical co-generation plant. The problem was set from the perspective of an integrated operation were plant and land owner are the same. In order to address our questions, the specific objectives of this study are the following:

- Determine drying rates for up to two years for forest harvest residues generated from cable and ground logging systems in the area.
- Determine the optimal harvest residue delivery to a hypothetical co-generation plant located in Lyons, Oregon.
- Determine production costs of residue generated from cable and ground logging systems.

- Determine the cost effectiveness of expressing the plant demand as a function of moisture content of delivered residues.

4.1. Methodology

Data was provided by the Oregon Department of Forestry J. Clark and J. Butteris (personal communication, 2016) and consisted of approximately 944 Ha of regeneration harvests (clear-cuts) within Marion and Linn counties in Oregon. These 138 units were harvested between 2003 and 2015 totaling 81,500 MBF, were 87% of the total gross BF was Douglas-fir. The average yield for the harvest units was 86 MBF/Ha, and 35% of the forest units were yarded with a cable system. The date of each truck load delivery was provided and used as a start date in which the harvest residues become available for processing and transport or in-forest storage. Additionally, spatial data was provided, including road networks that allowed distance calculation to a hypothetical co-generation plant located in Lyons, OR. Harvest volume was provided in MBF, and to calculate the amount of generated harvest residue, a factor of 0.82 ODMT/MBF was used (Lord, 2009). All the material was treated as if it was Douglas-fir, and all units with a residue volume below 68 ODMT (approximately four truckloads) were excluded from the analysis to reduce the amount of variables in the model.

Two mathematical models were developed. Both are mixed integer programming problems with the objective of minimizing the sum of fixed and variable cost of delivered forest harvest residue to a co-generation plant over a 24-month period. The hypothetical cogeneration facility is located in Lyons, Oregon with a generating capacity of 6 MW per hour. The first model, referred to as the baseline scenario, assumes a constant biomass to energy conversion. The second model, referred to as the energy-based demand model, assumes a variable biomass to energy conversion based upon the moisture content of the delivered material

4.1.1 Baseline Scenario

The costs are due to both, fixed components (equipment mobilization) requiring binary variables, and variable components (material transport) that are represented as continuous variables. The fixed cost is charged once when equipment is mobilized to the harvest unit to grind residues, as a result of residue volume flow to the plant. Variable cost is the sum of collection (if unit is harvested with a ground-based system), comminution and transportation costs per ODMT of harvest residue produced. The objective function (Eq. 10) was set as follows:

$$Min \sum_{ij} VCost_{ij} * Volume_{ij} + \sum_{ij} FCost_i * MOB_{ij} \ , \forall \, i,j \in \mathbb{N} \qquad \text{(Eq 10.)}$$

Where, i = unit (1,2, 3,….117) j = period (1, 2, 3, …. 24)

Since the volume of residue in each harvest unit is limited and the plant needs to have a continuous supply of forest residues to operate, two constraints need to be in place to ensure these requirements have been met.

The wood demand is based on a common rule of thumb of 1 dry ton (0.91 ODMT) per MW-hr (US DOE, 2011; eXtension, 2011; Shelly, 2010) and is typical of biomass with moisture content of 40-55%, but actual yield will depend on system efficiency (US DOE, 2011). The consumption of the plant was estimated at 43 105 ODMT/yr based on 330 days of operation, 24 hours per day during the year. This plant would be supplied on a 63% by forest harvest residues and the remaining 37% from bark and other industrial residues.

The data set included volume harvested from 2003 to 2015, leaving a smaller amount of harvest residues available at the beginning of the study period. This, because material that would have been harvested in previous years would have been available for later use. In order to fill this data gap, four months of average forest residue (6168 ODMT) was made available for the first four periods as a "dummy" unit.

$$\sum_i Volume_{ij} = Demand_j \ , \forall \, i,j \in \mathbb{N} \qquad \text{(Eq 11.)}$$

$$\sum_j Volume_{ij} \leq Capacity_i \ , \forall \, i,j \in \mathbb{N} \qquad \text{(Eq. 12)}$$

Eq 11. specifies the demand of the co-generation plant and Eq 12. limits the harvest residue capacity from each harvest unit. Additionally, another constraint (Eq. 13) is specified to ensure that the mobilization cost will be included in the objective function in the period the harvest unit is accessed to retrieve harvest residues.

$$M * MOB_{ij} - Volume_{ij} \geq 0, \forall \, i,j \in \mathbb{N} \, , MOB_{ij} \in \mathbb{Z}_2 \qquad \text{(Eq.13)}$$

Since none of the units have enough volume to keep the equipment working for longer than a month, a constraint (Eq. 14) was needed to make sure the residue is processed and delivered in only one period.

$$\sum_j MOB_{ij} \leq 1 \ , \forall \, i,j \in \mathbb{N} \qquad \text{(Eq. 14)}$$

Finally, a minimum volume of 200 ODMT in the harvest unit is required to move in the equipment and operate. This constraint was set to avoid having equipment stay in a unit for a very small volume to avoid another move-in cost that would be charged if there is residue delivery in the same unit on inconsecutive months.

$$Volume_{ij} - M * W_{ij} \leq 0, \forall \, i,j \in \mathbb{N} \, , W_{ij} \in \mathbb{Z}_2 \qquad \text{(Eq. 15)}$$

$$Volume_{ij} - 200 * W_{ij} \geq 0, \forall \, i,j \in \mathbb{N} \, , W_{ij} \in \mathbb{Z}_2 \qquad \text{(Eq. 16)}$$

The constants are described in Table FL-2.15. The decision variables of this problem are:

- $Volume_{ij}$ Continuous variable, volume of forest residue processed and transported to plant from unit *i* in period *j* (ODMT)
- MOB_{ij} Binary variable [0,1] triggering mobilization cost when material is processed and transported to plant from unit *i* in period *j.*
- W_{ij} Binary variable [0,1] to ensure there is a minimum volume flow on unit *i* in period *j.*

Table FL-2.15. Constants of the mathematical formulation.

$VCost_{ij}$	$TCost_{ij} + GCost_{ij} + CCost_{ij}$
$TCost_{ij}$	Transportation cost from unit *i* to plant in period *j* (US$/ODMT)
$GCost_{ij}$	Grinding cost unit *i* in period *j* (US$/ODMT)
$CCost_{ij}$	Collection cost unit *i* in period *j* (US$/ODMT)
$FCost_i$	Fixed cost (mobilization cost) of equipment to unit *i* (US$)
$Capacity_i$	Available forest harvest residue volume in unit *i* (ODMT)
$Demand_j$	Plant forest harvest residue in period *j* (ODMT)

4.1.2. Energy-based demand

A co-generation plant would need a different amount of feedstock to generate power depending on its moisture content. Heat energy rates per wood mass burned in a boiler were developed assuming 33% conversion of the net boiler output to electricity and recoverable Btu per green lb from Ince (1979) and fit with a polynomial function (Figure FL-2.29).

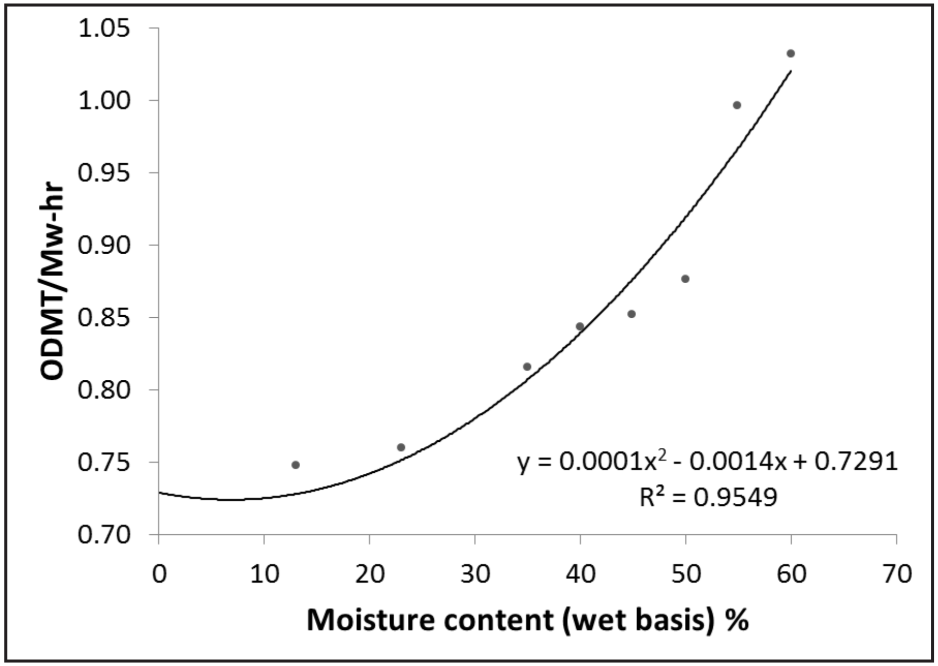

Figure FL-2.29. Rate of wood (ODMT) per MW-hr needed at the energy plant depending on wood moisture content.

In order to implement this energy-based residue demand, the mathematical formulation of the problem had to be modified. The first part was to calculate the energy content of the residue on each unit at each point in time (Eq. 17).

$$0.0001 * 100 * mc_{ij}^2 - 0.0014 * 100 * mc_{ij} + 0.7291 = Energy_{ij} \; \forall \, i, j \in \mathbb{N} \quad \text{(Eq 17.)}$$

Where mc_{ij} is the moisture content (wet basis) of harvest residue of unit *i* in period *j* and $Energy_{ij}$ is the amount of energy MWh-ODMT of unit *i* in period *j*. Finally, the original demand equation (Eq 11.) needs to be modified to make the amount of ODMT demanded at each period vary, depending on the average moisture content of the delivered material. Then $Demand_j$ is the sum of energy demanded in period j in MW-h/month.

$$\sum_i Volume_{ij} * Energy_{ij} = Demand_j \; , \forall \, i, j \in \mathbb{N} \quad \text{(Eq 18.)}$$

4.2. Solver

For this study, a commercially available optimization model solver (Lingo® v16.0.28) was used. This solver allows importing volume and cost data to the Lingo platform from Microsoft Excel and the mathematical formulation can be written in Lingo language. The amount of solving time will depend on the difference between the current best integer and current best partial integer solution that the user wants to achieve. This difference is known as the gap. Approximately 2 minutes of computing time was necessary on an Intel Core 2 PC (Windows 7 Enterprise, 3 GHz, 8 GB RAM) to produce less than a 1% gap with both models. In other words, the solutions were within 1% of the optimal solution.

4.3. Moisture Content

Finite element models to predict forest residue drying rates for four climate regions in Oregon were generated and calibrated with field samples, Belart (2016). Those models focused on piled residue and calibrated with data collected in the field; however, moisture content data was also collected for scattered residue using samples of the same dimensions as the ones in the piles (30 cm long, approximately 3.8-4.3 cm in diameter).

Since the geographic location and species provided in the harvest data-set are similar to the Valley-East Douglas-fir unit used to build and calibrate that FEA model, the Valley East Douglas-fir unit was used to determine the drying rates for the piled residue of the study area. In addition, the same model with a flat pile was used to estimate the drying rates for scattered residues. After running an initial model, it was calibrated with data obtained in the field. The piled residue geometry was a half ellipsoid of 12 m wide and 3 m high and the scattered residue a half ellipsoid 12m wide and 0.5 m high.

The original FEA models were set to run for only one year. However, since we wanted to have the residue available for one full year for each unit, independent from the harvesting date, the models were set to run for two years, starting at different months. The same weather data was used for the second year, assuming both years would have the same weather pattern. Since the starting date for storage provided in the data set is the date in which the loaded trucks were delivered, a 50% moisture content was considered as the initial moisture on each month (Belart, 2016). Each model component was specified with material properties found in the literature (Table FL-2.16). Ghaffaryian et al. (2003) assume material loss and deterioration over time. Losses can result from changes in specific gravity as wood decomposes and the loss of biomass components such as needles separating from the branches. Nurmi (2014) studied pine and birch whole tree storage and concluded that significant losses in dry mass of pine only occurred after more than one year of storage. Significant losses in dry mass of birch occurred after only one drying season. For our anticipated storage times we assume no mass loss of wood. Harvest residue samples cut after 23 and 48 weeks of storage in piles primarily of Douglas-fir in western Oregon showed no significant differences between the mean specific gravity of samples obtained at those different times (t-test p-value = 0.2677). We assume needles separate from the residues either in storage or during handling and comminution. Needle fall increases the value of the harvest residue as a fuel and benefit nutrient retention in the harvest unit.

Table FL-2.16. Material properties.

	Air	Wood	Pile
Porosity	1	0.67[1]	0.70[2]
Bulk density (kg/m^3)	1	500[3]	150
Thermal conductivity (W/m K)	0.025[4]	0.11[5]	0.05[6]
Heat capacity (J/kg K)	1 000[7]	1 250[3]	1 075[6]

[1]Based on 1,520 (kg/m^3) cell wall density (Bowyer et al., 2003), [2]Hardy (1996), [3]Simpson and TenWolde (1999), [4]Monteith and Unsworth (2008), [5]TenWolde et al. (1988) Wilkes equation, [6]Nield and Bejan (1998), [7]Welty et al. (2008)

4.4. Costs

For the purpose of this exercise, the cable logging comminution operation consists of a horizontal grinder, an excavator loading the grinder and a 13.7m chip trailer for transportation. Both the grinder and excavator need to be mobilized with one lowboy trip each. The ground-based logging collection and comminution operation consists of a horizontal grinder, an excavator loading the grinder, two forwarders and a loader loading the forwarders. The productivity and cost effectiveness for this system was evaluated by Zamora-Cristales and Sessions (2016). The grinder and two excavator-loaders need to be mobilized with three lowboys; it was assumed that the forwarders were close enough to the operation that could be self-mobilized. The mobilization cost was estimated in US $1 000 per piece of equipment (Table FL-2.17).

Grinding cost was obtained from Marrs et al. (2015) at 21 US$/ODMT at 60% utilization and 3.54 US$/gal for diesel and average productivity of 32 ODMT/PMH. Transportation cost was calculated based on a 13.7 m trailer with a volumetric capacity of 99 m^3, a maximum payload of 25 metric tons and a ground material dry bulk density of 160 kg/m^3 (Zamora-Cristales and Sessions, 2015). These calculations are based under the assumption that the trailers can access all the units.

As the moisture content of the material changes over time, the truck load was limited by either weight (when wet) or volume (when dry). Transportation hourly cost was calculated based on 8% of the time on dirt road, 15% on gravel road and 77% highway and different costs for travel loaded and unloaded. Additionally, 3.2 US$/ODMT for an unloaded truck waiting for one hour in order to keep the grinder utilization high was added since typically the grinder needs to wait for trucks to turn around or the road standard does not allow transit for more than one vehicle at a time. Since we assume that all trucks can access all units, a rear steered axle trailer was used to transport residues from cable units at a higher cost, and a standard trailer for ground-based units. The total truck cost is then US$103/hr for the standard trailers (Marrs et al., 2015) and US$126/hr for the steerable rear trailers (Zamora-Cristales et al. 2015) with an average speed assumed at 48.3 Km/hr. B. Daugherty (personal communication, 2016) is currently documenting self-steering trailer mobility.

Table FL-2.17. Cost summary per logging system.

System	Mobilization (US$)	Comminution (US$/ODMT)	Collection (US$/ODMT)	Truck waiting (US$/ODMT)	Transportation (US$/hr)
Cable	2 000	21	0	3.2	126
Ground	3 000	21	24	3.2	103

Collection cost was considered to be zero when the harvest units were yarded with a cable system and 24 US$/ODMT on ground-based units (Zamora-Cristales and Sessions, 2016) using two forwarders and one loader with a harvest residue average distance to roadside of 156 m (Zamora-Cristales and Sessions, 2016). Distance from each harvest unit to the cogeneration plant was calculated from the centroid of each timber sale with the harvest units to Lyons, Oregon using ArcGIS.

4.5. Drying Curves

Forest harvest residue dries rapidly during the first weeks in the harvest unit and then reaches equilibrium with ambient conditions. This is similar to what Pettersson and Nordfjell (2007) found; their harvest residue MC fell from 50 to 29% in only three weeks. Scattered residue left after a ground-based logging operation in this particular harvest unit (assumed typical of Valley East Douglas-fir) can reach moisture contents as low as 10% (wet basis) during the summer months, and can re-moisten up to 30% (wet basis) during the winter (Figure FL-2.30).

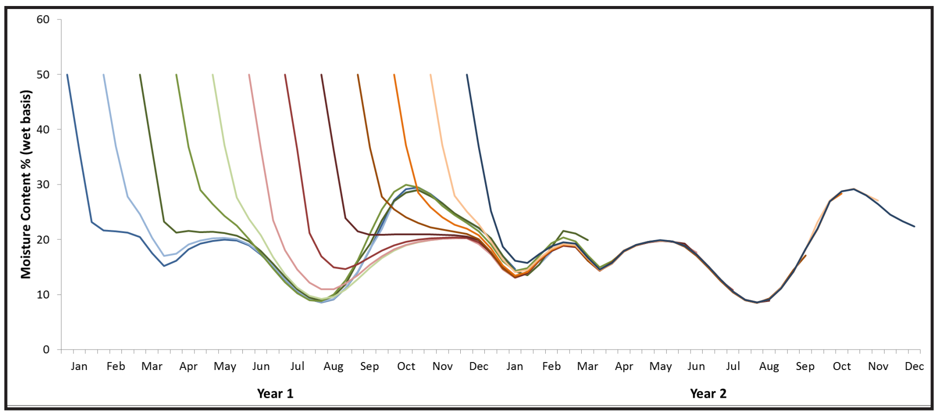

Figure FL-2.30. Drying curves for Douglas-fir scattered residue based on modeling of Valley East Douglas-fir empirical data.

When residue is left piled at the landing on a cable logging operation, it does not reach as low moisture content as if it was scattered. Also, the piled residues gain moisture during the winter, although the piled residue has less moisture fluctuation over time compared to scattered residue (Figure FL-2.31).

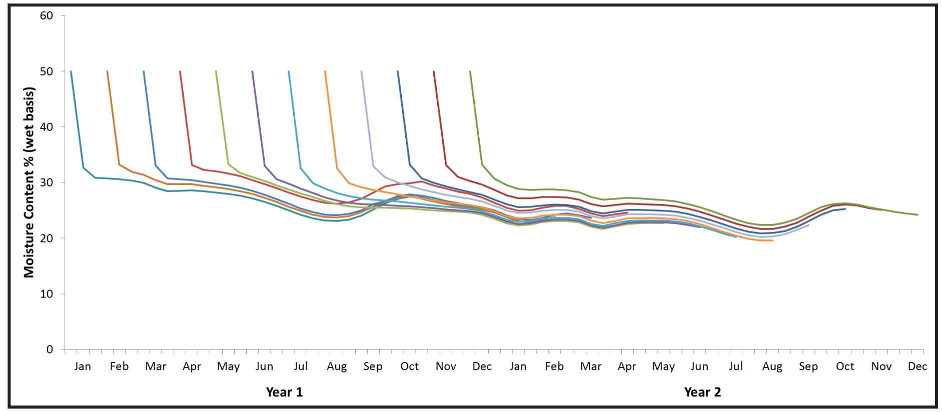

Figure FL-2.31. Drying curves for Douglas-fir piled residue based on modeling of Valley East Douglas-fir empirical data.

4.6. Results

4.6.1. Baseline Scenario

After economic optimization of the problem, the result indicates that all the residues from the previous year are used to help supply the power plant during the first four monthly periods (January to April of year 1). Then, the excess residue produced in May and June is left to dry to supply the deficit in August and September (Figure FL-2.32). A total of 75% of the available harvest residue is processed and delivered to the cogeneration plant in Lyons, Oregon. The average round-trip distance for the cable logging units is 72 km and 32 km for ground-based units.

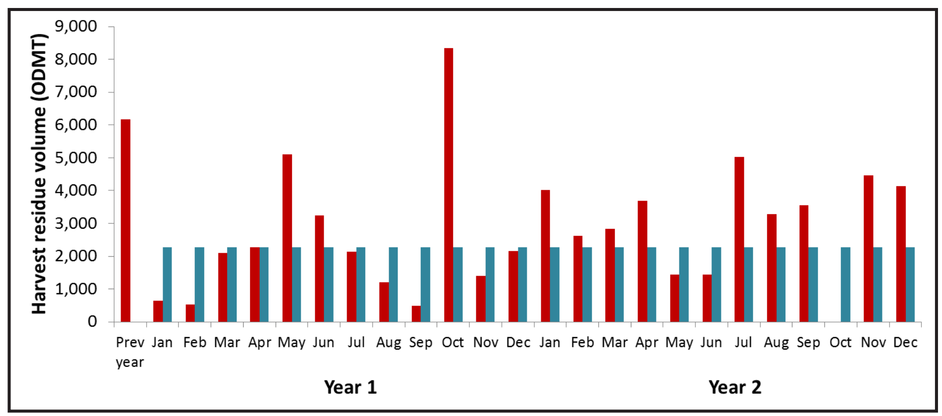

Figure FL-2.32. Harvest residue volume distribution over the two year period.

In the baseline scenario, using a 13.7 m trailer and 160 kg/m^3 material bulk density, 98% of the volume harvested by cable system is processed and delivered to the plant, and only 56% of the volume harvested with a ground-based system is delivered to the plant (Figure FL-2.33). The average round trip distance of the material left in the harvest units is 87 km.

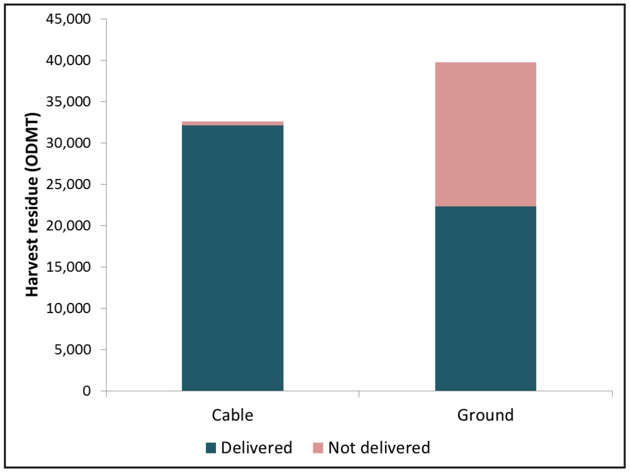

Figure FL-2.33. Delivered residue volume by harvest system.

The average moisture content (wet basis) of the residue for both cable and ground-based harvest systems for the two year period is 34%. And the majority of the residue is left to dry for one month, especially the material harvested with a cable system. Very little volume is left to dry for more than four months (Figure FL-2.34). Probably because the single trailer becomes volume limited and there is not an advantage to let the material dry for much longer. Additionally, material is needed to cover volume gaps in preceding periods.

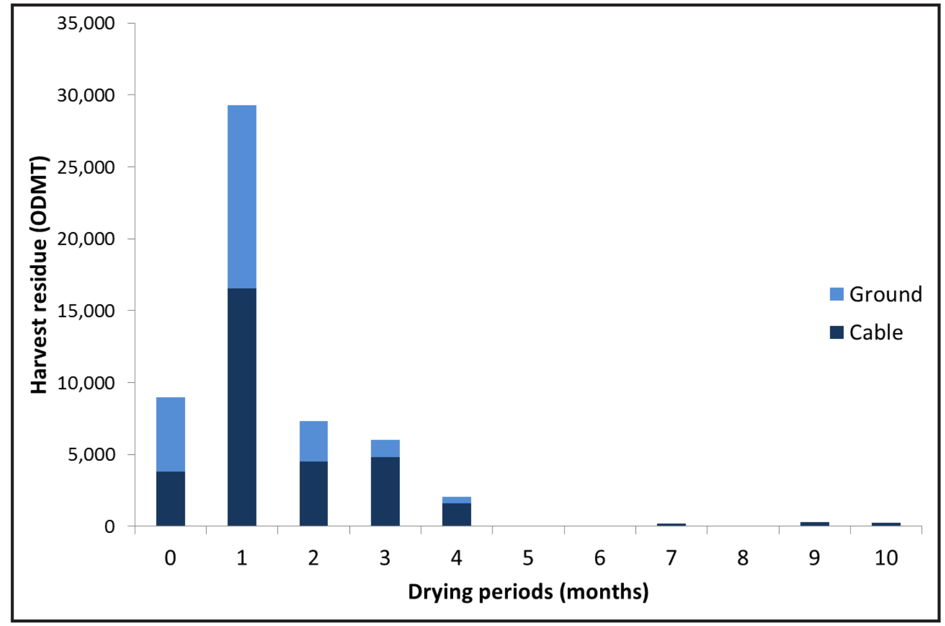

Figure FL-2.34. Number of dying periods for delivered harvest residue volume by harvesting system.

4.6.2. Energy-based Scenario

After implementing the harvest residue demand depending on its energy content, the total amount of volume delivered to the plant is reduced by 16% (8 874 ODMT in the two-year period) without affecting the energy needs to keep the plant generating electricity at the same level as the baseline scenario. In terms of harvest systems, the ground-based system volume delivered to the plant is reduced by 32% and the cable system by 5% (Figure FL-2.35).

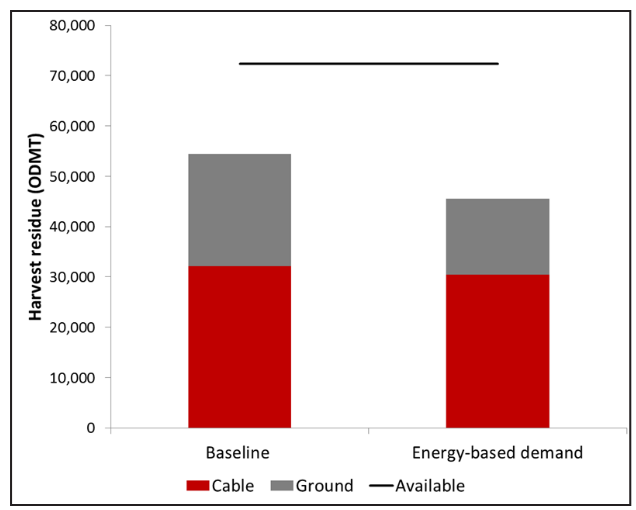

Figure FL-2.33. Delivered residue volume by harvest system.

The amount of volume delivered to the plant is not only reduced when the demand for harvest residues is based on energy content. It also changes the number of drying periods of the residues in the field, shifting towards longer drying times. There is a minimal amount of residues processed and transported immediately after harvesting, and residue volume is shifted towards 2, 3 and up to 6 drying periods compared to the baseline scenario (Figure FL-2.36).

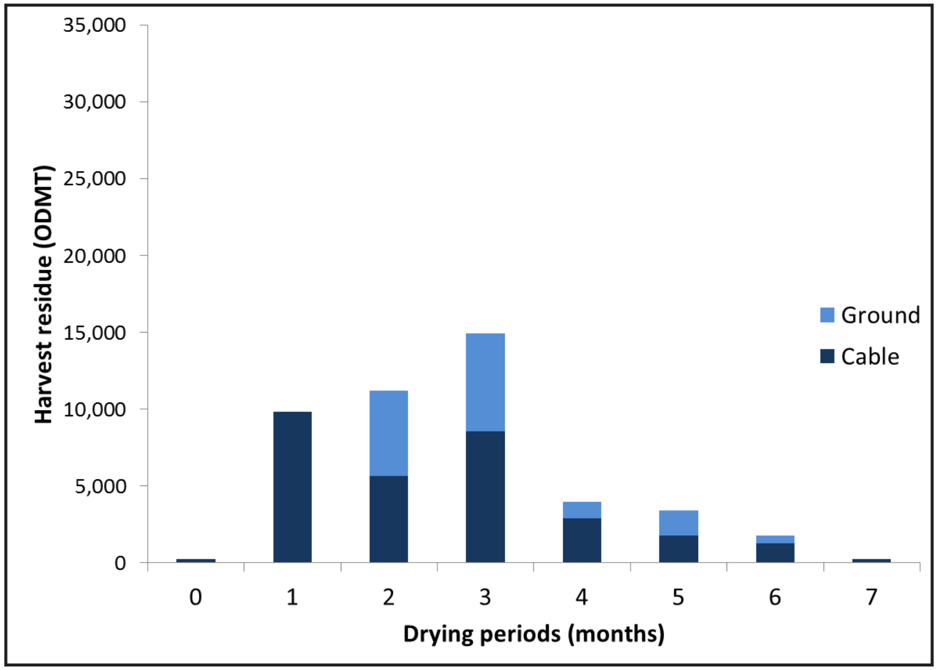

Figure FL-2.36. Number of dying periods for delivered harvest residue volume by harvest system.

By recognizing the value of drier material the problem shifts towards delivering material with lower moisture content. In the first two periods, the average moisture content is the same for both cases, probably because there is a smaller pool of harvest units to choose from. However, as more harvest units become available, the average moisture content starts decreasing, especially in the last two warmer months. During fall season, the average moisture content of delivered residues drops down even by 30% (Figure FL-2.37).

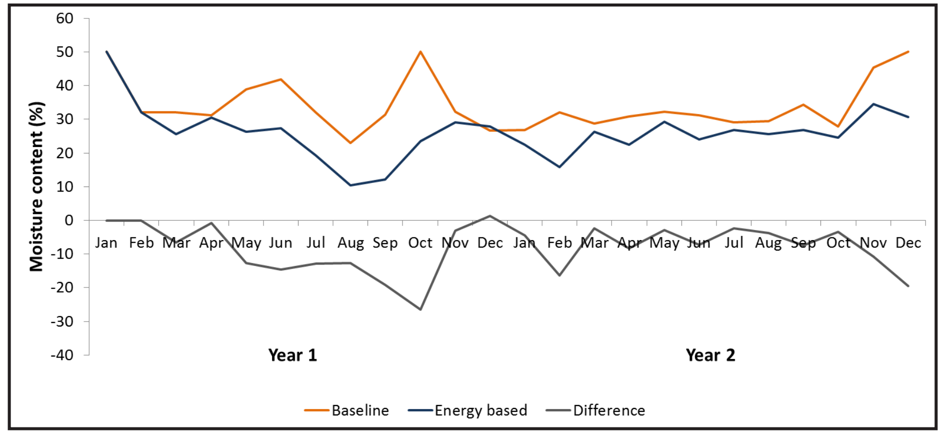

Figure FL-2.37. Average moisture content (wet basis) of delivered harvest residue per period

4.7. Cost Analysis

4.7.1. Baseline

At the ground-based units, the largest proportion of the variable cost is collection (24.3 US$/ODMT) which can be avoided in a cable unit because the material is already at the landing (Figure FL-2.38). Even when the average truck transportation cost for the cable system is 17.8 US$/ODMT and ground-based harvesting system is 11.3 US$/ODMT, the higher residue drying rates achieved on a ground-based system are not enough to offset the transportation cost. The difference between both systems is 17.7 US$/ODMT.

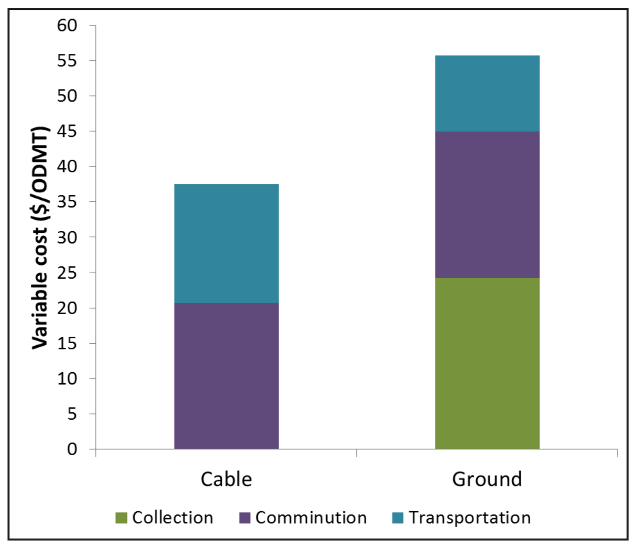

Figure FL-2.38. Variable cost by logging system.

The total cost for the operation is US$2,700,326 (50 US$/ODMT) over the two -year period. This is the objective function value with 0.7% gap, meaning the total cost of the optimal solution cannot be lower than 99.3% of this (integer) solution.

4.7.2. Energy-based Demand

Since collection and comminution costs are assumed constant, only the amount of residue volume and harvest units chosen in the energy-based scenario differ from the baseline scenario resulting in a transportation cost is on average 0.7 US$/ODMT lower. When the cost is separated by harvesting system, the cost is 1.0 US$/ODMT lower for the cable system and 0.5 US$/ODMT lower on the ground-based system (Figure FL-2.39).

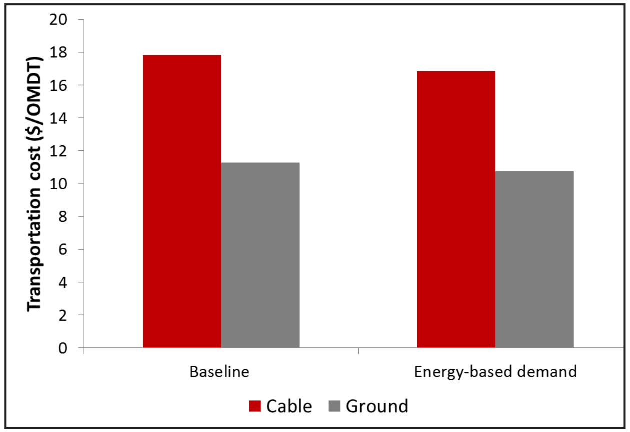

Figure FL-2.39. Transportation cost by logging system for the two scenarios.

When compared with the baseline scenario, the total cost of the operation during the 24 periods is 20.4% lower (US$550,947 lower). The average cost for the operation is 47 US$/ODMT.

4.8. Discussion

Drying rates for piled and scattered residues are quite different. Scattered residue is more sensitive to changes in the environment than residue stored in piles. It will reach lower moisture content, dry faster during the summer months and will get wetter during the rainy season. So if residue is to be stored in the field, it is best to store scattered residue over the summer and process it before it gets wet. But if the residue is piled, it will get less wet over the rainy season when compared with scattered residue. That is, if residue needs to be processed in the wet season, it is better to do so with material that has been previously piled.

The amount of forest residue available for this case study is enough to supply 63% of feedstock for a 6 MW-hr cogeneration plant in Lyons, OR. The majority of the residue coming from a cable system operation is delivered to the plant (98%), even when the cable units are further from the plant and have a lower drying rate. The ground system units are closer to the plant, but the collection cost is too high to have those units be more cost effective than the cable units.

For both cases, piled and scattered residue, moisture decreases rapidly during the first month. For that reason, most of the residue is left to dry for the first month for the baseline scenario. This result is different from what Acuna et al. (2012) found. Their results indicated that they should have left the residues to dry for 7 to 8 months. However, they had multiple types of feedstocks to supply the plant such as whole trees and delimbed stems with higher storage costs than harvest residues. Currently, since harvest residues are usually left to dry for burning in the fall, storage cost was not considered in our case study.

In terms of variable cost, the ground-based units are 46-48% higher compared to units harvested with a cable system. The main reason for this difference is the collection cost that needs to be incurred when the residue is scattered over the unit. This makes the overall cost in the ground-based units too high, even when these units have an advantage in terms of material moisture (drier than cable) and distance to the plant (lower transportation cost).

When the plant demand is based on the residue moisture content and its effect on the plant energy recovery, the amount of material needed to obtain the same output of energy is reduced by 16%. This is caused by energy losses due to the vaporization of water contained in the wood during the combustion process (Bowyer et al. 2003). For that reason, drier residues make energy production more efficient. Most of this reduction occurred in the ground-based units (32% reduction), mainly because of the collection cost. As expected, when drier material becomes more attractive from the demand point of view, there is an additional incentive to let material dry in the field for longer time. Almost no fresh material is taken to the plant in the energy-based demand scenario (Figure FL-2.36). This material is left to dry for at least one period, and as more harvest units become available, material starts shifting towards more drying periods. Since there is no cost to let the material dry, this presents an added benefit to the value of drier material.

The changes in moisture content, quantity, and origin of the harvest residues delivered to the plant result in a lowered transportation cost that averages 0.7 US$/ODMT compared to the baseline scenario. This cost could be further reduced if a double trailer was to be used for harvest units further from the plant. Double trailers present an advantage compared with single trailers since they have larger volumetric capacity (Zamora-Cristales and Sessions 2015). The total cost of the operation during the 24 periods is 20.4% lower than when energy recovery in the plant is not considered. This is a result of having the plant demand being driven by the harvest residue energy content as a function of its moisture content instead of assuming a fixed 0.91 ODMT/MW-hr at 50% moisture content.

4.9. Conclusions and Future Work
In this case study, it is more cost effective to process and transport forest harvest residues from cable logging units rather than ground-based logging units. This was true despite the greater average distance from those units to the plant (30% greater) compared to the ground-based system. In all the scenarios evaluated in this study, 98% of the harvest residue originated by a cable logging system is processed and delivered to the plant.

For the baseline scenario (24 periods), the longest residue storage period in the harvest units was seven months. Most of the material is stored for one month followed by two months. Under the circumstances of this study, letting the material dry for a longer time does not seem beneficial.

Since fuel value is inversely related to moisture content, grindings with lower moisture content are more valuable at the plant. In our case study, 16% fewer ODMT of residues are required to generate a fixed power output. This approach incentivizes longer drying times in the field and can result in a more accurate estimate of operation cost (20.4% lower) than the baseline scenario of 0.91 tonnes/MW-hr.

The conclusions are limited to a specific area. However, drying rate schedules can be derived for other climate regions in the Pacific Northwest and can be used to investigate the effects of forest residue. We assumed that all cable harvest units required use of the more expensive self-steering trailer. Not all cable units will require self-steering trailers and 6 x 6 truck tractors. However, as cable harvest units were chosen over ground-based units, using less expensive trucks on some cable units probably would not have affected the biomass utilization schedule for this example. Lastly, the effect of feedstock moisture content will be affected by the efficiency of the specific plant (US DOE, 2011). Specific design features may favor operation in specific moisture content ranges to achieve complete combustion.

5. Implications of Fresh Versus Aged Residues for Liquid Biofuel Production

High moisture content in forest harvest residues can increase the costs of processing and transportation and may be associated with a reduction in the content of polysaccharides for liquid fuels production as well as reduce the combustion efficiency in boilers for power generation. Different moisture management strategies can be implemented in the field to reduce the water content prior to grinding and transport but the value gain of these practices along the supply chain has not been clearly understood. By knowing the value gains, landowners, forest managers, contractors and other participants in the supply chain could benefit by drying the material in the woods. In this study we developed a cost framework to evaluate the economic trade-offs between grinding, transporting and pretreating fresh residue (immediately after harvesting), versus aged residue. In Douglas-fir, fresh harvest residues needles are often still attached to the branches and could represent an important part of the grinding mix if processed a short time after harvest. Aged residue, on the other hand, usually contains a smaller proportion of needles and bark depending on drying time and weather conditions on the site. These differences in proportion of tree components may affect polysaccharides content because each tree component has a different amount of them. Whether to process and transport fresh or aged residues is a decision that depends on the interests of the supply chain stakeholders. For landowners, the removal of harvest residues after timber harvesting may be a priority to prepare the area prior to planting. For contractors and bioenergy industries, it may be more profitable to process and transport residues when aged to maximize their benefit. In any case, as renewable energy markets emerge, it is important to recognize that proper economic incentives must exist for landowners to ensure the supply of high quality biomass to bioenergy conversion facilities. One first step is to evaluate the effects of grinding and transporting fresh versus aged residues in the supply chain to estimate the opportunity cost that may benefit landowners by giving them incentive to develop moisture management strategies.

The effect of moisture content on the quality of feedstocks and moisture management strategies for biofuel and energy production have been documented in the literature. FAO (1990), discussed how moisture content affects the combustion efficiency of boilers for power generation. By reducing moisture content via air drying it could help to improve combustion and reduce humidity fluctuations in the boiler that can negatively affect the power generation. Roser et al. (2010) studied different methods to reduce moisture content and improve the quality of feedstocks for power generation. Ghaffariyan et al. (2013) developed an optimization model to optimize storage time and minimize total forest residue supply cost to a bioenergy facility. Nilsson et al. (2015) studied the effects of moisture content and storage time on forest harvest residues with emphasis on needle retention. Nilsson et al. (2015) cited previous studies in Sweden that found that the composition of Norway spruce forest harvest residues was approximately 33-50% wood, 10-20% bark, 5-15% branches, 20-30% needles, and 5-10% fines. After letting forest harvest residues sit in piles over one summer, Nilsson et al. (2015) concluded that about 1/3 of the needles were found in the field between harvester piles, 1/3 of the needles had fallen to the bottom of harvester piles (12-15% of clearcut area), and 1/3 arrived at the plant. Others have found forest harvest residue storage to be similar or even more effective in promoting needle loss. Nurmi and Hillebrand (2001), also in Norway spruce, found fresh forest harvest residues contained 19% needles. Seasoning the residues from 4-8 weeks lowered the percentage to 2% on the clearcut area and to 4.0% on the landing piles. Ash content fell from 2.1% residue content to 1.5% during the first month of storage.

Research has addressed moisture content in the forest biomass supply chain (Acuna et al., 2012), however many field drying cost estimation and optimization models are based on assumptions rather than actual data from controlled tests that could bring an operational perspective and solution to the problem. By analyzing the operational impact of moisture content in the supply chain it could be possible to identify benefits that could be accrued to a number of the participants in the chain.

This analysis could help to quantify the value gains of implementing moisture management strategies by estimating the economic effects in grinding and transportation as well as the potential pretreatment polysaccharides yields (for biochemical pathway conversions) of fresh versus aged harvest residues. We focus on harvest residues comminuted in the field using grinders and loaded and transported in chip vans. Specifically, we discuss differences in grinder fuel consumption, bulk density, bark and needles content, and polysaccharides yield. We quantified each of these variables and analyzed their effect on the supply chain costs. This study is part of a series of studies to understand the effect of feedstock characteristics on the economics of the renewable aviation biofuel supply chain from forest harvest residues (Zamora-Cristales et al., 2015 and 2016). The initial study reported on the effect of different grinder bit types and screen sizes on fuel consumption and bulk density in aged residue (Zamora-Cristales et al., 2015). In this study, we focused on the effect of fresh versus aged residue on fuel consumption and bulk density, and polysaccharides content to analyze the economics of the supply chain.

5.1. Materials and Methods
We processed 40 tonnes of fresh and 40 tonnes of aged forest harvest residues from two managed 45 year-old Douglas-fir (*Pseudotsuga menziesii*) stands. Aged residues were collected from a harvest unit located 25 km north of Springfield, Oregon, USA (44°11’21”N, 122°59’15’’W). Residues were produced during timber harvesting in late winter and were left in piles for approximately five months. Fresh residues were collected in January following timber harvesting from a harvest unit located 28 km southeast of Springfield, Oregon, USA (43°53’57”N, 122°47’10’’W). Both fresh and aged residues were transported to a centralized yard where residues were processed. During the following summer season, aged residues were placed in windrows in the centralized yard for two weeks to facilitate additional drying prior to grinding. Moisture content of aged residues, when ground, was measured at 15% (wet basis). Fresh residues when ground had an average moisture content of 60% (wet basis). Both types of residues consisted mainly of branches and tops with diameter averaging less than 10 cm and an average length of 1 m. Fresh residues were not only wet, but fresh in the sense that residue was processed just four weeks after harvesting.

5.2. Grinding and Fuel Consumption
Residues were processed using a Peterson 4710B (570 kW) horizontal grinder in roughly 1.3 tonne trials. Both fresh and aged residues were ground with the same machine, screen size combination and bit type. Twenty-four trials for each residue type were performed. After grinding, material was loaded into a small bin truck where it was weighed at a truck scale. Fuel consumption was measured by using a 19 liter container to provide fuel to the grinder. Before each trial the tank was filled with diesel to a known level. After each 1.3 tonne trial the tank was refilled and the quantity added was measured with a graduated cylinder (Zamora-Cristales et al., 2015).

5.3. Bulk Density and Moisture Content
After each trial we collected a 20 kg sample of ground residues for laboratory testing. Bulk density was measured following ISO method 15103, 2011-10-12. Moisture content of ground material was estimated by adapting ASTM standard E871-82 for moisture analysis in particulate wood fuels.

5.4. Bark and Needles Content
A five liter sample was taken to estimate the proportion of non-wood by total weight. The proportion of bark and needles was measured by manual separation from the wood in the test samples. Soil particles were also separated from woody pieces.

5.5. Polysaccharides Content
To produce high quality biofuels and co-products, a pretreatment process is needed to break up the wood components. Samples of aged and fresh residues (40kg per trial) were evaluated at the Weyerhaeuser Technology Center where the polysaccharides content was measured by adapting the National Renewable Energy Laboratory protocol for biomass compositional analysis (NREL, 2015). In this method a 500 g analytical sample for each trial was taken and reduced to less than 1 mm particle size using a Wiley mill. Once the material is resized, an analytical two step acid hydrolysis procedure is performed to obtain the proportion of polysaccharides, lignin, acid insoluble (Klason), and total extractives. Ash content was calculated by dry oxidation at 575 degrees Celsius. After hydrolyzing the polysaccharides the resulting sugar monomers content is measured by High-Performance Anion Exchange Chromotography with Pulsed Amperometric Detector (HPAEC-PAD) (Figure FL-2.40).

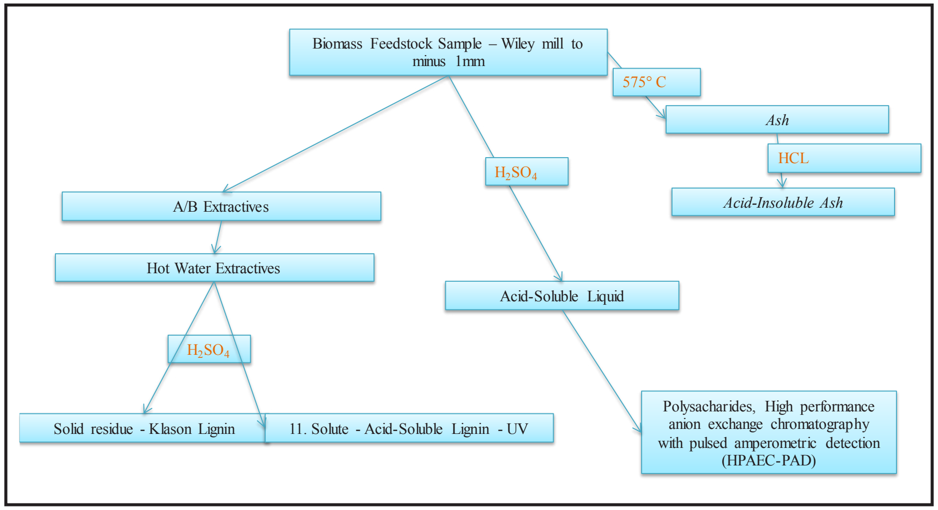

Figure FL-2.40. Analytical pretreatment process to estimate polysaccharides content.

When such a feedstock is treated via a biofuels production simulation using the Mild Bisulfite pretreatment process (Zhu et. al., 2015), about 89.2% of the polysaccharides are converted to sugar monomers and thus nominally accessible to subsequent conversion steps (e.g, fermentation to alcohols). The actual weight of monomers is 1.11 times the polymer weights.

5.6. Statistical Analysis

To estimate statistical differences in the variables under study (grinder fuel consumption, polysaccharides content, bulk density and bark and needle content) by type of residue, we ran statistical tests to check normality, and equal variance assumptions. We also performed a t-test to identify statistical differences between the two types of residues. We assumed that p-values below 0.05 indicate strong evidence of a difference between the two elements compared.

5.7. Economics of Collection, Grinding, and Transportation

In gentle terrain, residues may need to be piled and transported to the most cost-effective landing for grinding. Collection cost in this study was assumed to be 22.00 $/oven-dry tonne based on previous study (Zamora-Cristales and Sessions, 2016). Since residues are usually collected and transported fresh to the landing we assumed no cost difference in both residue types. Independent from the moisture content, residue during collection, is usually volume rather than weight limited. The cost of grinding residues was calculated based on the use of a Peterson 4710B (540 kW) horizontal grinder to process the residues. We derived theoretical grinder productivity values from the fuel consumption data and assumed the grinder was operating at 75% of maximum power, () with an engine theoretical consumption, (), of 0.213 kg kW^{-1} h^{-1} and a diesel weight (), of 0.84 kg l^{-1}. Since the grinder productivity is also dependent on operational factors such as site accessibility, number of trucks and truck capacity, we simulated a grinding operation using the model by Zamora-Cristales et al. (2015). As inputs, the simulation uses the theoretical productivity and the capacity of the truck at each moisture content and provides as output the utilization rate of the grinder along with other important operational variables such as truck travel and idling time. The model simulates trucks arriving to the grinding site empty to be loaded and then returns to the bioenergy conversion facility. The model finds the number of trucks for a specific grinding location that minimizes the grinding and transportation cost. Other inputs for the simulation model were the distance on gravel and paved roads. For illustration purposes we used 80 km travel on paved roads (from the forest unit entrance to the bioenergy facility) and 10 km on gravel roads (from the forest unit entrance to the grinding location) (Eq. 19).

$$GTprod_i = \frac{GrinderPower\left(\frac{EngineFc}{DieselWg}\right)wl}{FC_i\, MC\%} \qquad \text{(Eq. 19)}$$

Where

$GTprod_i$: Grinder theoretical productivity of residue type i, in oven-dry t h^{-1}
$Grinderpower$: Maximum rated grinder power, assumed kW
$EngineFc$: Engine theoretical consumption, kg kW^{-1} h^{-1}
$DieselW_g$: Weight of a liter of diesel, kg
wl : Grinder workload processing residue type *i*, %
FC_i : Fuel consumption of residue type *i* at its specific moisture content, t h^{-1}
$MC\%_i$: Moisture content, wet basis, of residue type *i*, %

Grinder operational productivity was estimated as the product between the theoretical productivity and the machine utilization rate from the simulation model (Eq. 20).

$$GOprod_i = GTprod_i * UT\% \qquad \text{(Eq. 20)}$$

Where

$GTprod_i$: Grinder operational productivity of residue type *i*, in oven-dry t h^{-1}
$UT\%_i$: Grinder utilization rate processing residue *i* %

The grinder costs were estimated from previous studies and compared to similar operations reported in the literature (Zamora et al., 2015; Anderson et al., 2013). Costs were divided into an operating cost to represent the cost when the grinder is processing the material and grinder idling cost to represent the cost when the machine is idling waiting for trucks. This costing framework was introduced by Matthews (1942) and has been used by others such as FAO (1976). Operating costs were divided in two categories: (1) ownership (depreciation, interest, taxes), and (2) variable (repair and maintenance, labor, support equipment, overhead and loader). An excavator-loader was included in the cost to load the residue into the grinder when processing. The following formula was used to calculate the grinding cost:

$$Gcost_i = \frac{(GLfuel+HFC_i(GTProd_i)Gprice(1+lubs\%))*UT\%+GIdle*(1-UT\%)}{GOprod_i} \qquad \text{(Eq. 21)}$$

Where

GCost$_i$: grinding cost of residue type i USD per oven-dry tonne
GIdle : Grinder idling cost, USD h-1
GLfuel : Hourly grinder cost without fuel, USD h-1
HFC$_i$: Hourly fuel consumption for residue type i, l t-1
Gprice : Diesel cost per liter, USD l-1
lubs% : Lubricants cost as a percentage of fuel cost, %

To understand the effect of residue type on the economics of transportation, it was assumed that a 13.7 m long trailer (100 m^3 of volumetric capacity), pulled by a 6x4 truck-tractor was used to transport the ground residues from the forest to a conversion facility. This configuration is commonly used in biomass operations in the Pacific Northwest Region, USA, and it is potentially the longest trailer that can reliably access most forest roads. Longer trailers are available in the market, however the steep terrain conditions of many operations in western Oregon and Washington, USA make it infeasible to use them. Additionally, chip vans have several engineering limitations compared to log trucks when driving on steep roads (Sessions et al., 2010). A typical 13.7 m long trailer can carry approximately 21.4 tonnes of material due to legal road limitations in the USA that are based on the number and spacing between axles (Sessions and Balcom, 1989). Figure FL-2.41 shows the dimensions of the truck-trailer that was used to estimate the economics.

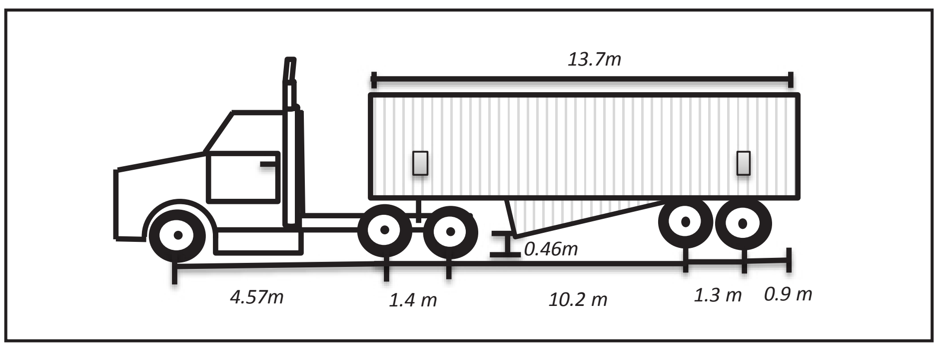

Figure FL-2.41. Truck-trailer configuration (100 m3 of volumetric capacity) used to estimate the economics of transportation.

To calculate transportation cost, USD per dry tonne, we assumed an average travel speed on paved roads (loaded and unloaded) of 70 km h^{-1} and an average speed of 15 km h^{-1} on gravel roads. A loading time was adjusted depending on the productivity on fresh and aged residue and an unloading time at the conversion facility of 0.58 h. was used. Truck capacity was estimated by using the bulk density values and calculating the amount of residue that could achieve the volumetric capacity of the truck. In high moisture content material the volumetric capacity of the truck may not be reached due to the maximum allowable legal weight regulations (Sessions and Balcom, 1989). Transportation cost, USD per oven-dry tonne, is estimated as follows:

$$TCost_i \frac{2Tpavedcost_s(TPtime_d)+TICost(Utime+Ltime)+2Tgravelcost_s(TGtime_{dg})}{Tcap\ (1-MC\%_i/100)} \qquad \text{(Eq. 22)}$$

$$Tcap = \begin{cases} 21.4\ t, & (Bulk_i(TVol)/1000) > 21.4\ t \\ Bulk_i(TVol)/1000), & (Bulk_i(TVol)/1000) < 21.4\ t \end{cases} \qquad \text{(Eq. 23)}$$

Where

TCost$_i$: Transportation cost of residue type i, USD per oven-dry tonne
TpavedCost$_s$: Hourly transportation cost when traveling on paved roads in state $_s$ (empty or loaded), USD h^{-1}
TICost: Hourly transportation cost when idling, USD h^{-1}
TPtime: One way average traveling time on paved roads, h
Utime: Unloading time as a function of the travel speed and distance on paved roads *d*, h
Ltime: Loading time as a function of the travel speed and distance on gravel roads *dg*, h
Tgravelcost$_s$: Hourly transportation cost on gravel roads in state s (empty or loaded), USD h^{-1}
TGtime: One-way travel time on gravel roads, h
Bulki: Bulk density of residue type *i* (fresh or aged), kg m^{-3}
TGtime: One-way travel time on gravel roads, h
TCap: Trailer capacity, t

The total delivery cost at different distances from the forest to the bioenergy facility can be expressed as (Eq. 24):

$$FDC_i = Col + Gcost_i + TCost_i \qquad \text{(Eq. 24)}$$

5.8. Cost of Feedstock for Biochemical Sugar Production
To analyze the impact on feedstock value of biochemical sugar production in fresh and aged material, the cost of sugar monomers per kilogram in each feedstock type was measured and compared. The delivered cost of feedstock to the biomass conversion facility is the sum of the collection, grinding and transportation (as a function of the distance) per oven-dry tonne. The cost difference was calculated as follows:

$$Spoly_i = (0.892\ Pw_i) \quad \text{(Eq. 25)}$$

$$Smono_i = \frac{Spoly_i}{1.11} \quad \text{(Eq. 26)}$$

$$XtraDel = \frac{Smono_{fresh} - Smono_{aged}}{Smono_{fresh}} \quad \text{(Eq. 27)}$$

$$Cdiff = FDC_{fresh}(1 + XtraDel) - FDC_{aged} \quad \text{(Eq. 28)}$$

Where

FDC_i : feedstock cost delivered at the bioenergy conversion facility of residue type *i*, USD t^{-1}
Pw_i : Polysaccharides as percentage of dry weight, %
$Spoly_i$: sugars as polysaccharides tonne per tonne of feed of residue type *i*
$Smono_i$: sugars as monomers, tonne per tonne of feed of residue type *i, kg*
XtraDel : Additional fresh residues to deliver the same amount of sugars from aged material, %
Cdiff : cost difference of fresh over aged residues, USD per oven-dry tonne

The cost difference, *Cdiff*, can be interpreted as the maximum cost per oven-dry tonne that could be expended on a management program to deliver aged residues rather than fresh residues to the conversion facility.

5.9. Results

For fuel consumption, a statistical difference was found between aged and fresh residue (p-value <0.001 from a t-test). Grinder fuel consumption per tonne of aged material is more than double that in fresh material (Table FL-2.18).

Table FL-2.18. Fuel consumption for fresh versus aged residue at their specific moisture contents.

Type of residue	Fuel Consumption l t^{-1}	Moisture content (%)
Aged	2.2 (σ=0.49)	15.3 (σ=3.2)
Fresh	1.0 ((σ=0.25)	60.0 (σ=1.8)
Difference	1.2 ± 0.3	44.7 ± 1.6
p-value	<0.00001	<0.0001

For bulk density, significant differences were found (p-value <0.00001 from a t test) in aged residue compared to fresh residue (Table FL-2.19). Bulk density of fresh residue is 2.1 times the bulk density of aged residue.

Table FL-2.19. Bulk density of aged and fresh residues.

Type of residue	Wet bulk density kg m^{-3}
Aged	184.2 (σ=16.8)
Fresh	388.1 ((σ=17.9)
Difference	203.9 ± 10.1
p-value	<0.00001

The bark and needle content of the aged biomass (Table FL-2.20), as a percentage of the dry mass, was about 0.58 of the amount in the fresh residues (p-value <0.0001). Fresh residue contained greater amounts of needles and soil particles trapped by the high moisture of the material thus increasing the percentage of these components in each sample.

Table FL-2.20. Bark and needles content as a percentage of the dry mass.

Type of residue	Bark and needle content (%)
Aged	8.6 (σ=6.25)
Fresh	14.7 (σ=4.65)
Difference	6.1 ± 3.2
p-value	<0.0001

Bark and needle content are difficult to estimate and vary considerably among the relatively small test samples. A second test at the analytical laboratory yielded bark at 6.2% for aged and 16.7% for fresh material. The polysaccharides content for the aged residue was about 1.26 times the amount for the fresh residue, as a percentage of the dry matter. Other components such as lignin, extractives and ash are also shown (Figure FL-2.42). In general terms ash content in fresh residues in approximately 10 percent higher than in aged residues.

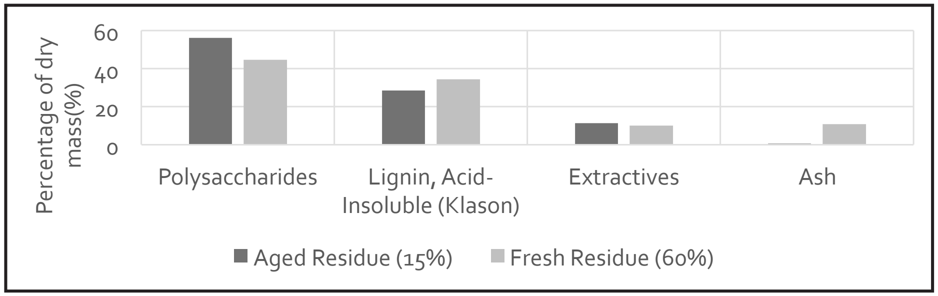

Figure FL-2.42. Polysaccharides content as a percentage of the dry mass from the analytical test.

5.10. Economic Implications

5.10.1. Grinding

Costs for grinding are shown in Table FL-2.21. Fuel cost is a function of fuel consumption that is dependent on the residue type (either fresh or aged).

Table FL-2.21. Grinder 4710B operating and idling cost and productivity.

Cost category	Operating cost	Idling Cost
Hourly ownership cost, USD h^{-1}	95.4	35.0
Variable costs USD h^{-1}		
Labor	33.8	33.8
Grinder bits	18.7	
Repair and maintenance	27.5	
Loader cost	102.9	11.62
Support equipment	14.8	14.8
Overhead cost	21.1	21.1
Hourly variable costs, USD h^{-1}	218.7	81.3
Total Cost without fuel, USD h^{-1}	314.1	116.3
Total cost with fuel fresh residue, USD h^{-1}	357.2	
Total cost with fuel aged residue USD h^{-1}	405.6	
Hourly theoretical productivity fresh oven-dry t h^{-1}	41.7	
Hourly Theoretical Productivity aged oven-dry t h^{-1}	41.2	
Maximum grinder utilization rate processing fresh residue (simulation results)	66%	
Maximum grinder utilization rate processing aged residue (simulation results)	80%	
Hourly Operational productivity of fresh residue in oven-dry t h^{-1}	27.6	
Hourly productivity of aged residue in oven-dry t h^{-1}	32.9	

There were no significant differences in the costs of grinding aged versus fresh per oven-dry tonne of material. As shown on Table FL-2.18, fuel consumption (FC_i) of aged residue was 2.1 l t^{-1} compared to 1.0 l t^{-1} in fresh residue. Assuming a current fuel price of USD 0.92 l^{-1}, and using the hourly theoretical productivity from Table FL-2.21 (41.7 and 41.2 t h^{-1} for fresh and aged residue respectively) and a lubricant cost equal to 10% of the fuel cost, the hourly fuel consumption cost was USD 91.5 h^{-1} for aged residue and USD 43.1 h^{-1} for fresh residue. Adding the fuel cost to the other grinding cost, the total hourly cost was USD 405.6 h^{-1} for grinding aged residue compared to USD 357.2 h^{-1} for grinding fresh residue. Using grinder hourly operational productivity, the cost per oven dry tonne was calculated. The cost of the fresh residue per dry tonne is USD 10.0 and the cost per dry tonne of the aged residue is USD 10.6.

5.10.2. Transportation

Transportation costs vary depending on the travel time which is usually a function of the travel distance. Hourly cost as a function of the truck state (idling, traveling loaded, and traveling unloaded) was estimated based on actual rates in the region. Cost on each road surface differs due to rolling resistance changes and travel speed. Cost loaded and unloaded are different due to changes in weight that affect the power required to overcome air and rolling resistance (Table FL-2.22).

Table FL-2.22. Transportation cost by state (loaded, unloaded, idling) and road surface.

Road Surface	Loaded USD h^{-1}	Unloaded USD h^{-1}	Idling USD h^{-1}
Gravel	86.3	77.6	50.0
Paved	118.4	100.0	50.0

Figure FL-2.43 shows the transportation cost changes from 20 to 160 km one-way distance from the forest to the biomass conversion facility. For each case, 10 km of the one-way trip was gravel roads (driving speed of 25 km h^{-1}) and the remainder on paved roads. Fresh residue was USD 14.5 to 44.9 per oven-dry tonne more expensive than transporting aged residue. These costs do not consider potential savings from backhauling, e.g. trucks were assumed empty on return. Trailer capacity for aged residue was limited by the volume of the trailer. The payload of 18.4 t (volume limited) when transporting aged residue compared to 21.4 t (weight limited) when transporting fresh residue.

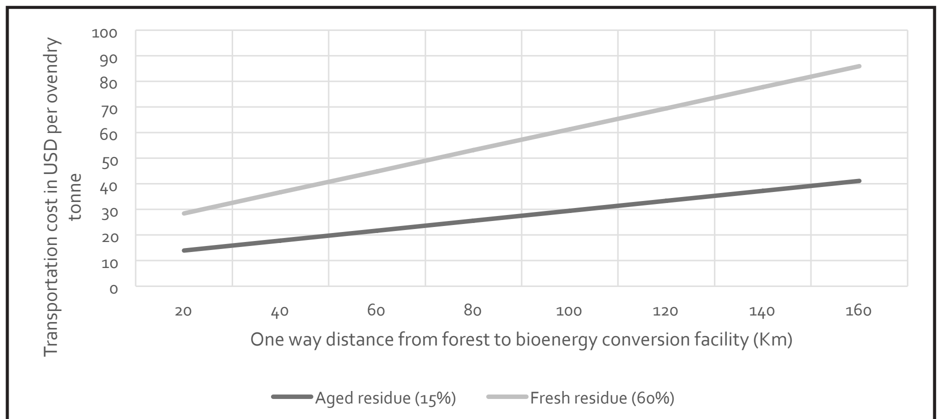

Figure FL-2.43. Transportation cost in USD per oven-dry tonne for aged and fresh residue.

5.11. Value Differences in Terms of Polysaccharides

The amount of fresh residues needed to deliver the same amount of material per dry tonne from aged residues was calculated based on hydrolysis yield (Table FL-2.23). This indicated that 26% more fresh material would be needed to supply the same amount of sugars as from aged material.

Table FL-2.23. Yield differences by feedstock type as a function of the sugar content.

Residue Type	Fresh	Aged
Total polysaccharides, weight percentage on feedstock	44.6%	56.3%
Hydrolysis yield, as polysaccharides on feed polysaccharides	89.2%	89.2%
Sugars as polysaccharides, oven-dry tonne per oven-dry tonne feed	39.8%	50.2%
Sugars as monomers, oven-dry tonne/oven-dry tonne , %	35.8%	45.2%
Additional fresh residues to obtain the same amount of sugars	26%	

Adding all the variables under study we estimated the differences in cost across the supply chain (Table FL-2.24). The potential value increase of letting residues age before delivery is equal to the difference in cost between fresh and aged residues to deliver an equal volume of sugar. At a distance of 20 km from the forest to the bioenergy facility the potential value was estimated at USD 29.6 t^{-1} for letting the material dry to a moisture content of 15% or below. The USD 29.6 t^{-1} difference in value included transportation cost savings of USD 14.5 plus USD 15.7 t^{-1} at the mill site minus the small difference in grinding of USD 0.6 t^{-1}. This difference in value increases as distance from the forest to the bioenergy conversion facility increases. Differences in value per kg of sugar ranged from USD 0.066 at 20 km to USD .167 at 160 km.

Table FL-2.24. Cost differences by feedstock type as a function transportation cost and sugar content. The sugar penalty reflects the 26% additional fresh material that must be delivered to create the same amount of sugar per ODT of aged material.

One-Way	Collect	Grind	Grind	Transport	Transport	Cost to Mill		Sugar	Difference	Sugar Cost	
km	Both	Aged	Fresh	Aged	Fresh	Aged	Fresh	Penalty		Aged	Fresh
	USD t^{-1}	USD t^{-1}	USD t^{-1}	USD t^{-1}	USD t^{-1}	USD t^{-1}	USD t^{-1}	USD t^{-1}	USD t^{-1}	USD kg^{-1}	USD kg^{-1}
20	22.00	10.60	10.00	13.95	28.44	46.55	60.44	15.71	29.60	0.103	0.169
40	22.00	10.60	10.00	17.83	36.15	50.43	68.15	17.72	35.44	0.112	0.190
60	22.00	10.60	10.00	21.72	44.88	54.32	76.88	19.99	42.55	0.120	0.215
80	22.00	10.60	10.00	25.10	53.10	57.70	85.10	22.13	49.53	0.128	0.238
100	22.00	10.60	10.00	29.48	61.32	62.08	93.32	24.26	55.50	0.137	0.261
120	22.00	10.60	10.00	33.36	69.54	65.96	101.54	26.40	61.98	0.146	0.284
140	22.00	10.60	10.00	37.24	77.76	69.84	109.76	28.54	68.46	0.155	0.307
160	22.00	10.60	10.00	41.12	85.98	73.72	117.98	30.67	74.93	0.163	0.330

5.12. Discussion of Aged Versus Dry Residues

Fuel consumption per wet tonne in grinding aged material was higher than in fresh material due to the differences in moisture content and also possibly due to the increase in friction when residue is aged. Green needles present in fresh material are more flexible and do not provide significant resistance to the grinder cutting rotor when passing through the screens.

In this study the grinding hourly cost only varied by fuel consumption, but other operational factors that may affect productivity such as equipment balancing (availability of trucks) and bit replacement were not considered. However, if truck availability is a factor, fresh residues would be penalized more than aged residues, because more trucks are required per dry tonne. In forest operations, road access restrictions are a function of the site and not dependent of whether the residue is fresh or aged. Increasing downtimes when comminuting aged material is common in chippers where knives are used. However, in grinders, carbide hammer bits are used and are less sensitive to changes in feedstock moisture content.

Wet bulk density of fresh residue was significantly higher than in aged residue causing the trailer to be weight limited. When the material is aged it was estimated that the truck would be volume limited. Alternative technologies such as the use of blowing devices when loading could be used to compact aged residues, and thus, increase the amount of residue per trailer per trip (Zamora-Cristales et al., 2015). These devices will add a comparative advantage that will increase the cost benefit of aged compared to fresh residue.

Polysaccharides content was lower in fresh versus aged materialmost logically due to the increased presence of bark and needles that contain comparatively less cellulose and hemicellulose than wood from conifers (Räisänen and Athanassiadis, 2015). The presence of bark and needles in fresh residue was 6.1% higher than in aged residue. This was because when the material is fresh, needles are still attached to the branches and become an important part of the residue mix. In contrast, when the material is aged, fewer needles are present and bark content may also be lower. Ash content was also higher in fresh compared to aged material.

From the cost analysis it is clear that processing fresh residue has many implications in the supply chain. Costs, as we discussed, will be impacted by how far the forest residues need to be transported. A difference of USD 29.6 t^{-1} represents the value difference across the supply chain of letting the material age when distance from the forest to the conversion facility is only 20 km. For longer distances, such as 160 km, the value loss could increase up to USD 74.9 t^{-1}. This cost does not include other potential losses of having lower polysaccharides yields in fresh residue. If fresh residues were to be utilized for aviation fuel it is likely that bark and needles would be screened and allocated to a lower use such as combustion. Moisture management strategies in the field would require spreading the material to facilitate the drying process, or initially piling the material in windrows. This may involve a re-handling process with an associated cost. This re-handling may also involve the transportation of the material to a storage location, such as along seasonally accessible roads, with space available, and with good access to allow trucks to transport the material.

There were no significant differences per oven dry tonne between the costs of grinding fresh versus aged residue. The grinder productivity is higher when processing fresh compared to aged residue however this increase in productivity does not necessarily translate into an increase in dry biomass delivered because of the high moisture content. More trucks are needed to deliver the same amount of dry biomass with fresh than when processing aged residue. More trucks translates into more traffic on roads thus increasing the carbon footprint of the supply chain and more road maintenance per tonne of dry biomass. Our average truck load for aged residue was about 15.6 dry tonnes (18.4 t *0.85), as compared to 12.8 dry tons (21.4 t * 0.6) of fresh residue, so the number of trailer loads to carry the same dry weight of fresh residue is about 20% higher than the number of trailer loads to carry the aged residues. The average cost of road maintenance on gravel roads, including surface replacement, is about USD 3.75 per round-trip truck km in western Oregon (Thauland and Sessions, 2013).

We based our cost on equipment currently used in the Pacific Northwest region, USA. However, the present cost framework could be adapted to any other machinery available. For transportation, the costs were based on the selected truck-trailer configuration, but others could be selected by adjusting the volumetric and weight capacity. Transportation costs assume average speeds for the truck however depending on road conditions the speed loaded and unloaded could be different. Our study did not include site productivity effects of removing fresh versus aged residues. Needles have a proportionally larger amount of important macro and micro nutrients than wood. This, when considered with their apparent smaller contribution to sugar yields, and the higher biomass cost of comminution and transportation, may suggest moisture management strategies that leave needles on site.

In conclusion drying the material in the field could be overwhelmingly positive across the supply chain. From our analysis the value gain could be in the range of USD 29.6 to USD 74.9 per oven-dry tonne.

6. General Conclusions

Forest harvest residues are a widely available renewable energy source in the Pacific Northwest. Several researchers, private and governmental entities have directed their efforts in making this product cost effective for energy production. In the presented studies, we have learned how its moisture content changes from the beginning of the drying process through storage time in the forest. It has been demonstrated that there are ways to manage these residues to improve their natural drying and increase the cost effectiveness of its processing and transport for energy production. Specifically, on each chapter, the conclusions are the following:

6.1. Seasonal Changes in Live Branch Moisture Content of 3 Species in the PNW

Seasonal branch average moisture content was determined for four major commercial forests areas in the Pacific Northwest. After data was analyzed, the main conclusions include the following:

- In the study, only ponderosa pine averaged 50 ± 1% during the winter, all other site averages are below this MC although a few individual branches exceeded 55%.

- In terms of seasonal variation, higher initial moisture content can be expected in ponderosa pine residues during the winter. MC can be from 1.6% to 9.8% higher compared with other seasons. For Douglas-fir, initial moisture content can be expected to be lowest when water supply is limited during summer drought. MC can be from 0.8% to 3.9% lower when compared with other seasons. Western hemlock and Douglas-fir growing with a secured water supply do not present significant differences in MC.

- Branch height and heartwood content have a strong correlation with branch average MC. Branch height explains up to 74% of branch moisture content by a simple regression. These equations can be used as a non-destructive method to estimate live branch moisture content. Using a sampling destructive method to measure heartwood diameter does not improve the coefficient of determination, making the branch height the simplest and most accurate predictor to estimate average branch moisture content.

6.2. Finite Element Analysis to Predict In-forest Stored Harvest Residue Moisture Content

Finite element models were developed for four sites representing the main climatic regions in Oregon and their respective commercialized forest species. These models are able to sufficiently predict piled forest residue drying rates with weather data input such as precipitation, wind, ambient temperature and relative humidity. Conclusions include:

- Piled residue moisture content responds to the environmental conditions greatly. The selection of pile shape or size can be beneficial or detrimental towards the rate of drying depending on ambient conditions, namely precipitation.

- A berm (windrow) presents the best option for expedient drying due to its large surface area. Drying is the fastest in this shape during dry summer months; however, the pile also re-wets the fastest during winter months.

- It is best to reduce pile volume if storage will occur through summer and increase size if it will occur through winter.

- Significant reduction in drying times can be achieved if the material is cut and left to dry during the dry, warm summer months. This reduction can be up to 1/3 of the time versus starting the process in the winter.

6.3. Economic Impacts of Moisture Management

For the case study evaluated for cogeneration, scheduling of harvest residue delivery was achieved in order to supply a hypothetical cogeneration plant of 6 MW-hr by 63%. A total of 75% of the available forest harvest residue is utilized to supply the plant. Analysis of the results indicate the following conclusions:

- It is more cost effective to process and transport forest harvest residues from cable logging units rather than ground-based logging units. This was true despite the greater average distance from those units to the plant (30% greater) compared to the ground-based system. In all the scenarios evaluated in this study, 98% of the harvest residue originated by a cable logging system is processed and delivered to the plant.

- With the finite element models we were successfully able to predict drying rates for piled and scattered residues being stored at different times of the year.

- For the baseline scenario (24 periods), the longest residue storage period in the units was seven months. Most of the material is stored for one month followed by two months. Under the circumstances of this study, letting the material dry for a longer time does not seem beneficial.

- Since fuel value is inversely related to moisture content, grindings with lower moisture content are more valuable at the plant. In our case study, 13.3% fewer ODMT of residues are required to generate a fixed power output. This approach incentivizes longer drying times in the field and can result in a cost reduction of 16.5% in the total cost on a 6 year planning horizon. The conclusions are limited to a specific area. However, drying rate schedules can be derived for other climate regions in the Pacific Northwest and can be used to investigate the effects of forest residue. We assumed that all cable harvest units required use of the more expensive self-steering trailer. Not all cable units will require self-steering trailers and 6 x 6 truck tractors. However, as cable harvest units were chosen over ground-based units, using less expensive trucks on some cable units probably would not have affected the biomass utilization schedule for this example.

- For liquid fuels, the sugar yields associated with dry forest residues were significantly higher than for fresh residues due to no needles, less bark, and less dirt.   Waiting for cost example for liquid fuels

The average moisture contents, models and economic analysis were made with local data and inferences are generally specific to these locations. However, the main concepts, results and sensitivity analyses still present a general understanding for drying conditions and economic advantages in many different climates and geographic locations.

7. Literature Cited

Acuna, M., Anttila, P., Sikanen, L., Prinz, R. & Asikainen, A. (2012). Predicting and controlling moisture content to optimize forest biomass logistics. *Croatian Journal of Forest Engineering*, 33(2), 225-238.

Afzal, M., Bedane, A., Sokhansanj, S. & Mahmood, W. (2010). Storage of comminuted forest biomass and uncomminuted forest biomass and its effect on fuel quality. *BioResources*, 5(1), 55-69.

Anderson, N., Chung, W., Loeffler, D. & Jones, J. G. (2012). A productivity and cost comparison of two systems for producing biomass fuel from roadside forest treatment residues. *Forest Prod. J.*, 62(3), 222–233.

ASTM international. (2006). Standard test method for moisture analysis of particulate wood fuels. E871-82. ASTM, West Conshohocken, Pennsylvania.

Baronas, R., Ivanuskas, F., Juodeikiene, I. & Kajalavicius, A. (2001). Modelling of moisture movement in wood during outdoor storage. *Nonlinear Analysis: Modelling and Control,* 6(2), 3-14.

Baxter, G. (2009). Assessing moisture content of piled woody debris: implications for burning. Wildland Fire Operations Group, FP Innovations-FERIC. 15p.

Becerra, F. (2012). Evaluation of six tools for estimating woody biomass moisture content. Oregon State University MS Thesis. 164 pp.

Beedlow, P, Tingey, D., Waschmann, R., Phillips, D. & Johnson, M. (2007). Bole water content shows little seasonal variation in century old Douglas-fir trees. *Tree Physiology*, 27, 737-747.

Belart, F. (2016). Forest Harvest Residue Moisture Management in the Pacific Northwest, USA, PhD dissertation, Oregon State University, Corvallis, OR. 126 pp.

Bhavikatti, S. 2005. Finite element analysis. New Age International. 334p.

Bowyer, J., Shmulsky, R. & Haygreen, J. (2003). Forest products and wood science. An introduction. Blackwell Publishing. Fourth Edition. 554p.

Brandt, J., Morgan, T., Dillon, T., Lettman, G., Keegan, C. & Azuma, D. (2006). Oregon's forest products industry and timber harvest, 2003. United States Department of Agriculture, Forest Service, Pacific Northwest Research Station. General Technical Report PNW-GTR-681.

Burns, R. & Honkala, B. (1990). Silvics of North America: 1.Conifers; 2. Hardwoods. Agriculture Handbook 654. U.S. Department of Agriculture, Forest Service, Washington, DC. vol.2, 877 p.

Cermák, J. & Nadezhdina, N. (1998). Sapwood as the scaling parameter-defining according to xylem water content or radial pattern of sap flow. *Annals of Forest Science*, 55, 509-521.

Cermák, J, Kuèera, J. Bauerle, W. L., Phillips, N. & Hinckley, T.M. (2007). Tree water storage and its diurnal dynamics related to sap flow and changes in stem volume in old-growth Douglas-fir trees. *Tree Physiology*, 27, 181–198.

Clark, J. & Gibbs, R. (1957). IV Further investigations of seasonal changes in moisture content of certain Canadian forest trees. Studies in tree physiology. *Canadian Journal of Botany*, 35, 219-253.

Cook, R., Malkus, D., Plesha, M. & Witt, R. (2001). Concepts and applications of finite element analysis. Fourth Ed. Wiley. 719p.

Curcio, S., Aversa, M., Calabrò, V. & Iorio, G. (2008). Simulation of food drying: FEM analysis and experimental validation. *Journal of Food Engineering*, 87, 541-553.

DNR State of Washington Department of Natural Resources. (2014). 2014 Washington timber harvest report. 32 p.

Dobbs, R. & Scott, D. (1971). Distribution of diurnal fluctuations in stem circumference of Douglas-fir. *Canadian Journal of Forest Resources,* 1, 80-83.

El Gamal, R., Ronsse, F. & Pieters, J.G. (2013). Modeling deep-bed grain drying using Comsol Multiphysics. *Comsol Conference Proceedings*. Rotterdam, Netherlands.

eXtension (2011). Energy unit conversion factors [website]. Last accessed September 24, 2016 at http://articles.extension.org/pages/55842/energy-unit-conversion-factors

Fagan, M.J. (1992). Finite element analysis, Theory and practice. Longman Scientific & Technical. 315p.

FAO (1976). Harvesting man-made forests in developing countries. FAO, Rome. 185 pp.

FAO (1990). Energy conservation in the mechanical forest industries. FAO Forestry Paper 93.

Ferguson, W.J. & Turner, I.W. (1996). A control volume finite element numerical simulation of the drying of spruce. *Journal of Computational Physics*, 125, 59-70.

Gautam, S., Pulkki, R., Chander, S. & Leitch, M. (2012). Fuel quality changes in full tree logging residue during storage in roadside slash piles in Northwestern Ontario. *Biomass and Bioenergy*, 42, 43-50.

Ghaffariyan, M., Acuna, M. & Brown, M. (2013). Analyzing the effect of five operational factors on forest residue supply chain costs: A case study in Western Australia. *Biomass and Bioenergy*, 59, 486-93.

Gibbs R. (1957). Patterns in the seasonal water content of trees. In: International Symposium on forest tree physiology. Harvard University, Cambridge, Mass. p. 43-69.

Gingras, J-F. & Sotomayor, J. (1992). Wood moisture variation in woodland inventory: A case study. Wood harvesting Tech. Note TN-192. Forest Engineering Res. Inst. of Canada, Point Claire, QC, Canada. 6 pp.

Gjerdrum, P. & Salin, J-G. (2009). Open air drying of scots pine transmission poles prior to creosote treatment. In: Proceedings "Wood science and engineering in the third millennium". 95-102.

Glass, S. & Zelinka, S. (2010). Wood Handbook, Wood as an Engineering Material. Chapter 04: Moisture Relations and Physical Properties of Wood. General Technical Report FPL-GTR-190. Madison, WI: U.S. Department of Agriculture, Forest Service, Forest Products Laboratory: 4-1 - 4-19. Chapter 4.

Greenidge, K. (1957). Rates and patterns of moisture movement in trees. In: International Symposium on forest tree physiology. Harvard University, Cambridge, Mass. p. 19-41.

Hakkila, P. (1989). Utilization of residual forest biomass. Springer-Verlag, New York. 568p.

Hardy, C. (1996). Guidelines for estimating volume, biomass, and smoke production for piled slash. Gen. Tech. Rep. PNW-GTR-364. Potland, OR, U.S. Department of Agriculture, Forest Service, Pacific Northwest Station. 17p.

Hozjan, T. & Svensson, S. (2011). Theoretical analysis of moisture transport in wood as an open porous hygroscopic material. *Holzforschung*, 65, 97-102.

Ince, P. (1979). How to estimate recoverable heat energy in wood or bark fuels. USDA For. Ser. Gen. Tech. Rep. FPL-29.

Irudayaraj, J., Haghighi, K. & Stroshine, R. (1992). Finite element analysis of drying with application to cereal grains. *Journal of agricultural engineering research*, 53, 209-229.

Kim, D-W. (2012). Modeling air-drying of Douglas-fir and hybrid poplar biomass in Oregon. Master of Science Thesis. Oregon State University. 56 p.

Kohnle, U., Hein, S., Sorensen, F.C. & Weiskittel, A.R. (2012). Effects of seed source origin on bark thickness of Douglas-fir (Pseudotsuga menziessi) growing in southwestern Germany. *Canadian Journal of Forest Resources*, 42, 382-399.

Kovács, A., Lakatos, E., Milics, G. & Neményi, M. (2010). Finite element modeling of coupled heat and mass transfer of a single maize kernel based on water potential using COMSOL Multiphysics simulation. *Comsol Conference Proceedings.* Paris, France.

Kuehl, R. (2000). Design of experiments: Statistical principles of research design and analysis. Second edition. Duxbury press. 666p.

Lord, R. (2009). The Economics of Biomass Utilization: Will I come out ahead? Managing Forestlands for Biomass Utilization. Western Forestry and Conservation Association. December 10, 2009. Springfield, Oregon.

Loustau, D., Berbigier, P., Roumagnac, P., Arruda-Pacheeo, C., David, J.S., Ferreira, M.I., Pereira, J.S. & Tavares, R. (1996). Transpiration of a 64-year-old maritime pine stand in Portugal. *Oecologia*, 107, 33-42.

Maguire D., Johnston, S. & Cahill, J. (1999). Predicting branch diameters on second-growth Douglas-fir from tree-level descriptors. *Canadian Journal of Forest Resources*, 29, 1829-1840.

Marchant, J. (1976). The prediction of airflows in crop drying systems by the finite element method. *Journal of agricultural engineering research*, 21(4), 417-429.

Markstrom, D.C. & Hann, R.A. (1972). Seasonal variation in wood permeability and stem moisture content of three Rocky Mountain softwoods, USDA Forest Service, Rocky Mountain Forest and Range Experimental Station, CO.

Marrs, G., Mulderig, B., Davio, D. & Burt, M. (2015). *Feedstock sourcing> NARA Years 1-3*. NARA Final Reports. Pullman, WA. Northwest Advanced Renewables Alliance (NARA).

Matthews, D. (1942). Cost control in the logging industry. McGraw-Hill. 374 p

Miles, P. & Smith, B. (2009). Specific gravity and other properties of wood and bark for 156 tree species found in North America. Res. Note NRS-38. Newtown Square, PA: U.S. Department of Agriculture, Forest Service, Northern Research Station. 35 p.

Monteith, J. & Unsworth, M. (2008). Principles of Environmental Physics. Third Edition. Academic Press. 418 p.

Murphy, G. & Pilkerton, S. 2011. Seasonal impacts on bark loss for Douglas-fir and Ponderosa

Nadler, K., Choong, E. & Wetzel, D. (1985). Mathematical modeling of the diffusion of water in wood during drying. *Wood and Fiber Science*, 17(3), 404-423.

NREL (National Renewable Energy Laboratory) (2015). Biomass Compositional Analysis Laboratory Procedures [website]. Retrieved from http://www.nrel.gov/bioenergy/biomass-compositional-analysis.html. Assessed 9/16.

Nield, D.A. & Bejan, A. (1998). Convection in porous media. Second edition. Springer. 546p.

Nilsson, B., Nilsson, D. & Thörnqvist, T. (2015). Distributions and Losses of Logging Residues at Clear-Felled Areas during Extraction for Bioenergy: Comparing Dried- and Fresh-Stacked Method. Forests 2015, 6(11), 4212-4227.

Nurmi, J. (2014). Changes in volumetric energy densities during storage of whole-tree feed stocks from silvicultural thinnings. *Biomass and Bioenergy*, 61(February 2014), 114-120.

Nurmi, J. & Hillebrand, K. (2001). Storage alternatives affect fuel wood properties of Norway spruce logging residues. *N. Z. J. For. Sci. 2001*, 31, 289–297.

Oregon Department of Forestry. (2014). Forest practice administrative rules and forest practices act. Chapter 629. 94 p.

Parker, J. (1954). Available water in stems of some Rocky Mountain conifers. *Botanical Gazette*, 115, 380-385.

Pettersson, M. & Nordfjell, T. (2007). Fuel quality changes during seasonal storage of compacted logging residues and young trees. *Biomass and Bioenergy*, 31(2007), 782-792.

Phillips, N.G., Ryan, M.G., Bond, B.J., McDowell, N.G., Hinckley, T.M. & Cermák, J. (2003). Reliance on stored water increases with tree size in three species in the Pacific Northwest. *Tree Physiology*, 23, 237–245.

Pong, W.Y., Waddell, D. & Lambert, M. (1986). Wood density - moisture profiles in Old-Growth Douglas-Fir and Western Hemlock. U.S. Department of Agriculture, Forest Service. Pacific Northwest Research Station. Research Paper PNW-347.

Räisänen, T. & Athanassiadis D. (2015). Basic chemical composition of the biomass components of pine, spruce and birch. Forest Refined. Retrieved from http://biofuelregion.se/wp-content/uploads/2017/01/1_2_IS_2013-01-31_Basic_chemical_composition.pdf

Röser, D., Erkkilä, A., Mola-Yudego, B., Sikanen, L., Prinz, R., Heikkinen, A., Kaipainen, H., Oravainen, H., Hillebrand, K., Emer, B. & Väätäinen, K. (2010). *Natural drying methods to promote fuel quality enhancement of small energywood stems*. Joensuu, Finland, Finnish Forest Research Institute, Working Papers of the Finnish Forest Research Institute, 186. Available from http://www.metla.fi/julkaisut/workingpapers/2010/mwp186.pdf [Accessed December 4, 2015].

Routa, J., Kolström, M., Ruotsalainen, J. & Sikanen, L. (2015). Precision measurement of forest harvest residue moisture change and dry matter losses by constant weight monitoring. *International Journal of Forest Engineering*, 26(1), 71-83.

Sandoval-Torres, S., Jomaa, W., Puiggali, J-P. & Avramidis, S. (2011). Multiphysics modeling of vacuum drying of wood. *Applied Mathematical Modeling*, 35, 5006-5016.

Savoie, P. & Beauregard, S. (1990). Predicting the effects of hay swath manipulation on field drying. *Transactions of the ASAE*, 33(6), 1790-1794.

Sessions, J., Wimer, J. Costales, F. & Wing, M. (2010). Engineering considerations in road assessment for biomass operations in steep terrain. *Western Journal of Applied Forestry,* 25(3), 144-153.

Sessions, J., Tuers, K., Boston, K., Zamora, R. & Anderson, R. (2013). Pricing forest biomass for power generation. *Western Journal of Applied Forestry*, 28(2), 51-56.

Sessions, J. & Balcom, J. (1989). Determining maximum allowable weights for highway vehicles. *Forest Products Journal*, 39(2), 49-52.

Sessions, J., Tuers, K., Boston, K., Zamora, R. & Anderson, R. (2013). Pricing forest biomass for power generation. *Western Journal of Applied Forestry,* 28(2), 51-56.

Shelly, J. (2010). Biomass conversion to electricity [Powerpoint presentation]. Woody Biomass Workshop, Ukiah California, UC Cooperative Extension. Last accessed on September 24, 2016 at http://ucanr.edu/sites/WoodyBiomass/files/79012.pdf

Sikanen. L., Röser, D., Anttila, P. & Prinz, R. (2012). Forecasting algorithm for natural drying of energy wood in forest storages. *Forest energy observer*. Study report 27. Finnish Forest Research Institute. 7p.

Simpson, W. & TenWolde, A. (1999). Physical properties and moisture relations of wood. Wood handbook : wood as an engineering material. Madison, WI : USDA Forest Service, Forest Products Laboratory. General technical report FPL ; GTR-113: Pages 3.1-3.24.

Simpson, W.T. (1973). Predicting equilibrium moisture content of wood by mathematical models. *Wood and fiber*, 5(1), 41-49.

Simpson, W.T. & Wang, X. (2003). Estimating air drying times of small-diameter ponderosa pine and Douglas-fir logs. Res. Pap. FPL.RP.613. Madison (WI): USDA Forest Service, Forest Products Laboratory.

Smith, E., Duncan, E., McGechan, M. & Haughey, D. (1988). A model for the field drying of grass in windrows. *Journal of Agricultural Engineering Research*, 41(4), 251-274.

Temesgen, H., Monleon, V., Weiskittel, A. & Wilson, D. (2011). Sampling strategies for efficient estimation of tree foliage biomass. *Forest Science*, 57(2), 153-163.

TenWolde, A., McNatt, J.D. & Krahn, L. (1988). Thermal properties of wood and wood panel products for use in buildings. Report ORNL\USDA-21697/1. 43p.

Thauland, B. & Sessions, J. (2013). Road maintenance fee allocation model, BLM Rroad Maintenance Working Group. Updated June 27, 2013. On file with Bureau of Land Management, Portland, OR.

Thompson, N. (1981). Modelling the field drying of hay. *Journal of Agricultural Science,* 97(2), 241-260.

US DOE (2011). Biomass for electricity generation [website]. Last accessed on September 24, 2016 at https://www.wbdg.org/resources/biomass-electricity-generation

Waring, R. & Running, S. (1978). Sapwood water storage: its contribution to transpiration and effect upon water conductance through the stems of old growth Douglas-fir. *Plant, Cell and Environment,* 1, 131 -140.

Welty, J., Wicks, C., Wilson, R. & Rorrer, G. (2008). Fundamentals of momentum, heat, and mass transfer. Fifth Edition. Wiley. 711p.

Youngblood, A., Max, T. & Coe, K. (2004). Stand structure in eastside old-growth ponderosa pine forests of Oregon and Northern California. *Forest Ecology and Management,* 199, 191-217.

Zamora-Cristales, R., Sessions, J., Murphy, G. & Boston, K. (2013). Economic impact of truck-machine interference in forest biomass recovery operations on steep terrain. *Forest Products Journal,* 63(56), 162-173.

Zamora-Cristales, R, Sessions, J. Boston, K. & Murphy, G. (2015). Economic optimization of forest biomass processing and transport in the Pacific Northwest USA. *Forest Science*, 61(2), 220-234.

Zamora-Cristales, R. & Sessions, J. (2015). Are double trailers cost effective for transporting forest biomass on steep terrain? *California Agriculture*, 69(3), 177-183.

Zamora-Cristales, R. & Sessions, J. (2016). Modeling harvest residue collection for bioenergy production. *Croatian Journal of Forest Engineering,* 37(2), 287-296.

Zhu, J.Y., Chandra, M. S., Gleisner, R., Gilles, W., Gao, J., Marrs, G., Anderson, D. & Sessions, J. (2015). Case studies on sugar production from underutilized woody biomass using sulfite chemistry. *Tappi Journal*, 14(9), 577-583

8. Appendices

Appendix A: Regression output and ANOVA to predict sample moisture content by its heartwood diameter

```
Call:
lm(formula = Sam_MC ~ poly(Heart_Sam, 2, raw = TRUE))
Residuals:
    Min       1Q   Median       3Q      Max
-1.64825 -1.23514 -0.00006  0.78452  2.85806

Coefficients:
                          Estimate Std. Error t value Pr(>|t|)
(Intercept)               44.154777   1.483284  29.768 1.94e-15 ***
poly(Heart_Sam, 2, raw = TRUE)1 -0.178920   0.114750  -1.559    0.139
poly(Heart_Sam, 2, raw = TRUE)2 -0.001732   0.001921  -0.902    0.381

---

Signif. codes:  0 '***' 0.001 '**' 0.01 '*' 0.05 '.' 0.1 ' ' 1

Residual standard error: 1.444 on 16 degrees of freedom
Multiple R-squared:  0.8969,    Adjusted R-squared:  0.884
F-statistic: 69.61 on 2 and 16 DF,  p-value: 1.274e-08
```

Appendix B: Regression output and ANOVA to predict branch average moisture content by its first sample heartwood diameter

```
Call:
lm(formula = Branch_MC ~ Heart_1st)
Residuals:
    Min      1Q  Median      3Q     Max
-1.8990 -0.6696 -0.2897  0.5887  3.1350

Coefficients:
             Estimate Std. Error t value Pr(>|t|)
(Intercept) 48.57535    0.62846  77.292  < 2e-16 ***
Heart_1st   -0.12928    0.01751  -7.385 5.38e-07 ***

---

Signif. codes:  0 '***' 0.001 '**' 0.01 '*' 0.05 '.' 0.1 ' ' 1

Residual standard error: 1.288 on 19 degrees of freedom
Multiple R-squared:  0.7416,    Adjusted R-squared:  0.728
F-statistic: 54.54 on 1 and 19 DF,  p-value: 5.382e-07

Analysis of Variance Table

Response: Branch_MC
          Df Sum Sq Mean Sq F value    Pr(>F)
Heart_1st  1 90.423  90.423   54.54 5.382e-07 ***
Residuals 19 31.500   1.658

---

Signif. codes:  0 '***' 0.001 '**' 0.01 '*' 0.05 '.' 0.1 ' ' 1
```

Appendix C: Statistical tests

<u>VDL, Valley Douglas-fir</u>

```
Wilcoxon signed rank test
data:  A$Model and A$Samples
V = 23, p-value = 0.1272

alternative hypothesis: true location shift is not equal to 0

    Spearman's rank correlation rho
data:  A$Model and A$Samples
S = 6, p-value < 2.2e-16
alternative hypothesis: true rho is not equal to 0
sample estimates: rho  0.9835165

    Kendall's rank correlation tau
data:  A$Model and A$Samples
T = 75, p-value = 1.416e-07
alternative hypothesis: true tau is not equal to 0
sample estimates: tau  0.9230769
```

<u>CWH Coast Western hemlock</u>

```
    Wilcoxon signed rank test
data:  A$Model and A$Samples
V = 13, p-value = 0.02148
alternative hypothesis: true location shift is not equal to 0
```

Spearman's rank correlation rho
data: A$Model and A$Samples
S = 36, p-value < 2.2e-16
alternative hypothesis: true rho is not equal to 0
sample estimates: rho 0.9010989

Kendall's rank correlation tau
data: A$Model and A$Samples
T = 69, p-value = 7.03e-05
alternative hypothesis: true tau is not equal to 0
sample estimates: tau 0.7692308

<u>VDH, Valley-East Douglas-fir</u>

Wilcoxon signed rank test
data: A$Model and A$Samples
V = 33, p-value = 0.4143
alternative hypothesis: true location shift is not equal to 0

Spearman's rank correlation rho
data: A$Model and A$Samples
S = 98, p-value = 0.006323
alternative hypothesis: true rho is not equal to 0
sample estimates: rho 0.7307692

Kendall's rank correlation tau
data: A$Model and A$Samples
T = 61, p-value = 0.006677
alternative hypothesis: true tau is not equal to 0
sample estimates: tau 0.5641026

<u>EPP, East Ponderosa pine</u>

Wilcoxon signed rank test
data: A$Model and A$Samples
V = 2, p-value = 0.0007324
alternative hypothesis: true location shift is not equal to 0

Spearman's rank correlation rho
data: A$Model and A$Samples
S = 16, p-value < 2.2e-16
alternative hypothesis: true rho is not equal to 0
sample estimates: rho 0.956044

Kendall's rank correlation tau
data: A$Model and A$Samples
T = 73, p-value = 1.808e-06
alternative hypothesis: true tau is not equal to 0
sample estimates: tau 0.8717949